THE DISTRIBUTION OF CONCRETE STRESS IN PRE-STRESSED AND REINFORCED CONCRETE BEAMS SUBJECTED TO PURE FLEXURE

A thesis submitted to the University of London for the degree of Doctor of Philosophy

by

James Martin PRENTIS, M.Sc.(Eng.)

- 1954 -

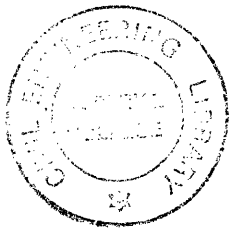

ABSTRACT

The object of this thesis is to consider the problem of determining the distribution of compressive stress in a reinforced or pre-stressed concrete beam subjected to a pure bending moment at loads approaching the ultimate.

The attainment of this object is desirable because the full development of an ultimate load theory for pre-stressed concrete appears to depend upon it. It is pointed out in the concluding chapter that this reason is debatable and indeed that the ultimate load theories themselves are at present the subject of controversy. These matters are deemed to be outside the scope of this thesis which concerns itself solely with the object stated above.

The thesis starts with a study of the normal assumptions of concrete design. It then goes on to survey the possible methods of measuring directly the stresses in a concrete beam particularly under plastic conditions. A method developed by the author for determining these stresses indirectly is then introduced. After careful study of the validity of this method it is applied to results of tests on a number of beams.

Return is then made to one of the basic assumptions of ordinary ('elastic') concrete design. An analysis is made/

made of the effect of finite spacing of tensile cracks on the distribution of compressive stress (normally it is assumed to have no effect).

An investigation is also made of the effect of end friction on the stress distribution in a cube. The object of this study is to see whether stress-strain readings taken in such a test have any significance for the same concrete used in a beam.

ACKNOWLEDGMENTS

The author wishes to thank Professor A.L.L. Baker for permission to use experimental data obtained by the D.S.I.R. group under his direction; Mr. D.N. de G. Allen for helpful advice on the use of relaxation methods; and Professor J. Allen who read the manuscript and suggested a number of improvements in the presentation.

CONTENTS

PART I INTRODUCTION

Chapter 1 THE OBJECT AND SCOPE OF THIS THESIS.

The object of this thesis is to consider the problem of determining the distribution of compressive stress in a reinforced or pre-stressed concrete beam subjected to a pure bending moment at loads approaching the ultimate.

The attainment of this object is desirable because the full development of an ultimate load theory for pre-stressed concrete appears to depend upon it. It is pointed out in the concluding chapter that this reason is debatable and indeed that the ultimate load theories themselves are at present the subject of controversy. These matters are deemed to be outside the scope of this thesis which concerns itself solely with the object stated above. Emphasis is laid on the determination of the stress distribution under plastic conditions, but first it is desirable to give close study to the normal assumptions of concrete design. The latter half of this section (Part I) is devoted to this.

Part II starts by considering various possible ways of measuring directly the compressive stresses in concrete beams. A method of determining these stresses indirectly is then introduced. After careful study of the validity of this method it is applied to results of tests on a number of beams.

In Part III return is made to one of the basic assumptions of ordinary ('elastic') concrete design. An analysis is made of the effect of finite spacing of tensile cracks on the distribution of compressive stress (normally it is assumed to have no effect).

Part IV gives an investigation of the effect of end friction on the stress distribution in a cube. The object of this study is to see whether stress-strain readings taken in such a test have any significance for the same concrete used in a beam.

I Chapter 2. GENERAL ANALYSIS OF REINFORCED AND PRESTRESSED CONCRETE BEAMS.

The following assumptions are generally made:-

(a) The concrete stress is considered to be uniquely defined by the strain.

(b) It is assumed that the concrete below the neutral axis (i.e. the axis on which the longitudinal stress is zero) has no stiffness and carries no stress.

(c) Plane sections are assumed to remain plane.

Under elastic conditions (a) is simplified by taking the stress to be directly proportional to the strain.

As the detailed analysis of reinforced and pre-stressed concrete beams under elastic conditions is given elsewhere (1, 2)* only the general principles will be given.

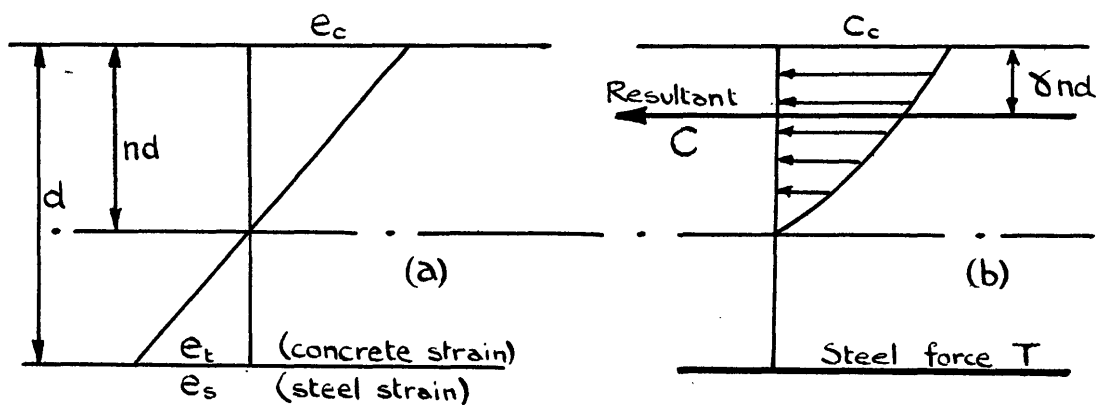

Figure 1.1

* Numbers refer to references listed in the bibliography at the end of the Thesis.

Three requirements have to be met:-

(i) there must be compatability of strains in steel and concrete,

(ii) the elements of the body must be in equilibrium under the stresses acting upon them,

(iii) these two taken together must satisfy the stress-strain relationships,

Since plane sections remain plane the strain distribution is as in figure 1.1 (a)

so that $$e_c/e_t = n(1 - n) \qquad (1.1)$$

With perfect bond (i) above requires

$$e_t = e_s \qquad (1.2)$$

where e_s is the increase in steel strain from the stage at which e_t is zero. In the case of ordinary reinforced beams $e_s = 0$ when $e_t = 0$ whilst in pre-stressed beams e_s has a stated value when e_t is zero.

If the bond is imperfect then it is necessary to introduce a factor F (3) so that

$$e_s = F \times e_t \qquad (1.2a)$$

(ii) requires equilibrium of the forces and moments acting on any vertical section of the beam so that

$$C = T \qquad (1.3)$$

and $$M = T.d(1 - \gamma n) \qquad (1.4)$$

where M is the external bending moment acting.

In order that equations (1.3) and (1.4) should be soluble for C and T use must be made of the stress-strain relationships of both the steel and the concrete. Use must also be made of the equations (1.1) and (1.2) and of the fact that the strain variation is linear down the beam.

Taken together these relationships enable c_c and T to be calculated for all values of M.

The general method given above is applicable to both reinforced and pre-stressed concrete beams at all stages of loading.

RECONSIDERATION OF THE ASSUMPTIONS.

Having given, very breifly, the outline of the main features of the theory of bending for concrete members the basic assumptions given above will now be studied in more detail. The assumption that the concrete stress is a unique function of the strain is not strictly justifiable because it takes no notice of creep phenomena. As, however, very little is known about creep at high stresses it is not feasible, as yet, to make any allowance for it. At working stresses an allowance can be made and this is done in practice although it is in fact of consequence only in pre-stressed concrete (2).

The assumption of a unique stress-strain relationship implies that the concrete is homogeneous; otherwise the relationship would vary from point to point in the medium. In fact the elastic and plastic properties of concrete do vary in this manner. Variations in the properties will occur due to different curing of various sections of the concrete. For instance the outer layers of a concrete body dry out more rapidly than the inner parts, giving rise to variation in the properties of the material. Once more little is known about such phenomena and it is not practicable to make allowance for them. A more obvious violation of the homogeneity assumption lies in the variations in physical structure from point to point in the material which consists of a matrix of mortar in which are embedded individual particles of aggregate. Such lack of homogeneity is not peculiar to concrete as many materials are made up of analogous constituents although the scale on which the structural variations may be observed is generally very much smaller. However, provided that the elementary particles of the material are small compared with a'significant dimension' of the body which it makes up lack of homogeneity is of little consequence. In the case of concrete it is necessary that the significant dimensions should be large compared with the aggregate size.

The term 'significant dimension' is best explained by means of suitable examples:- if, for instance, one wished to determine the density of concrete by casting a prism of known dimensions and weighing it, then the 'significant dimensions' are the lengths of the edges of the prism which should be long in comparison with the aggregate size in order to obtain a fair sample. The measurement of strains in concrete provides an example which is more relevant to the work in hand. Such strains must be measured by using an instrument with a gauge length long in comparison with the aggregate size. In the experimental work on which the writer has been engaged under Professor A.L.L. Baker at Imperial College an 8 inch gauge length has been used on concrete made with $\frac{3}{8}$ inch aggregate. In this case the ratio of gauge length to particle size is 21:1. Results obtained using such a gauge are quite satisfactory and measurements on beams subjected to circular bending where the strain distribution is known to be linear deviations from linearity are generally less than the 'reading error' of the gauge. Assumption (a) pre-supposes that a stress-strain relationship exists. It also implies that the form of the relationship is known or that it can be determined, otherwise the equations (I.1) to (I.4) can have no practical application.

In fact it is difficult to obtain the stress-strain relationship for concrete once the limit of proportionality has been passed. One of the main aims of this thesis is to consider this problem. A review of the difficulties of the problem and the various ways in which it may be tackled are given below.

Assumption (b) that the concrete below the neutral axis has no stiffness and carries no stress will now be considered. The assumption that concrete has no tensile strength is admittedly false but in practice it is justified because value is small compared with the compressive strength. It is generally considered that under elastic conditions the concrete stress is triangular as indicated in figure 1.2. This would be true if the concrete below the neutral axis disintegrated but in fact there is a finite distance between the vertical cracks. The blocks of concrete between those cracks have stiffness tending to retard the deformation of the concrete above the neutral axis. This action results in a stress distribution different from that indicated in the figure. The actual distribution to be expected under elastic conditions is derived in Part III.

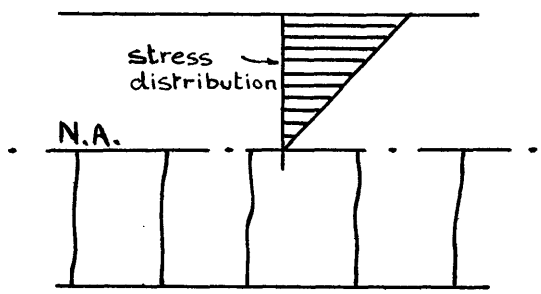

Figure 1.2.

If pure flexure is postulated then the assumption that plane sections remain plane is redundant for this can be shown to be a fact as a result of the postulate. A proof of this is given in Appendix 1.1.

In practice concrete beams are not subject to pure flexure since this implies zero shear. As the self weight of the beam is distributed this condition is obtained only at specific sections along the length of a beam. In this thesis we shall mainly be concerned with the analysis of results obtained from test beams which are, in general, light compared with the loads they carry so that for all practical purposes pure flexure will be attained. Even under these conditions there will be distortion of the planes in the immediate neighbourhood of the loading points. In bending tests pure flexure is obtained by means of four-point loading (figure 2.10). It is noticeable that compressio failure rarely occurs under one of the loads and that the crushed zone is generally a little way away from the loading plate. This may be ascribed to friction effects between the loading plate and the top of the beams which in preventing lateral expansion inhibit failure, the effect being similar to that operative between the ends of a cube and the loading plates of a crushing machine.

APPENDIX. 1.1

THEOREM. In a uniform beam subject to a pure bending moment plane sections remain plane.

Consider a uniform weightless beam so loaded that over a section PQ (figure I.3) there is no resultant shear

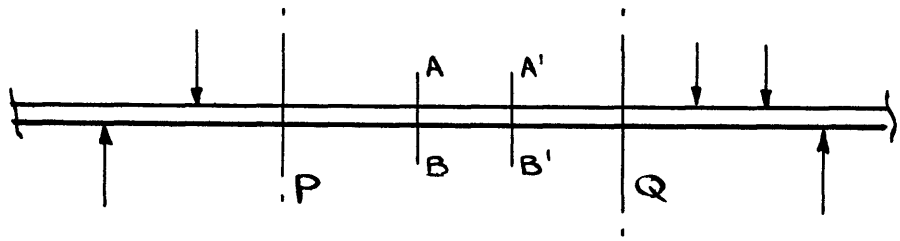

Figure 1.3

force (i.e. the bending moment is constant). If P and Q are sufficiently far removed from the loads then by St. Venant's principle, the mode of application of these loads is of no consequence. Thus the actual loading system may be replaced by another system, exterior to PQ, so that PQ is subject to the same bending moment with no change in the behaviour. Make this second system symmetrical about section AB situated mid-way between P and Q.

Since AB is in a plane of symmetry it must remain plane. Consider now any other section A'B'. As this section is subjected to precisely the same loading as AB it will distort in the same manner. But section AB remains plane therefore A'B', and all similar sections, also remain plane.

Thus under the action of a pure bending moment plane sections sufficiently far removed from the points of application of loads, remain plane.

PART II. EXPERIMENTAL DETERMINATION OF THE STRESS DISTRIBUTION IN CONCRETE BEAMS IN CIRCULAR BENDING

Chapter 1 REVIEW OF THE POSSIBLE METHODS.

The distribution of stresses in a concrete beam subjected to a bending moment can in theory be determined in a number of ways:-

(a) By obtaining the stress-strain curve for concrete tested in direct compression (e.g. in the form of a cube or cylinder) and assuming that the properties of the concrete in the beam and the specimen are the same.

(b) By embedding 'stress' gauges in a beam.

(c) Another approach is being made by Herr and Vandegrift at the Ohio State University who remove a section of the concrete in a beam and replace it by glass (3). The faces of the glass plate are then subjected to the stress distribution in the concrete when the beam is loaded. The distribution of stress in the glass is determined by photo-elastic methods.

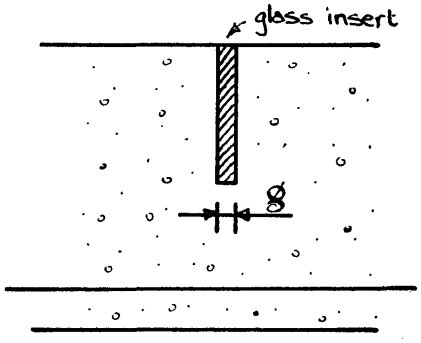

Fig. 2.1.

(d) By taking a short length of beam, applying compression to the concrete above the neutral axis by means of a number of jacks, tensioning the reinforcement by external means, and adjusting all the forces until a linear strain distribution is obtained in the concrete. The stress distribution is then given directly by the applied loads. This method has been suggested by Baker who has constructed a special machine, the bending simulation machine, for this purpose (4).

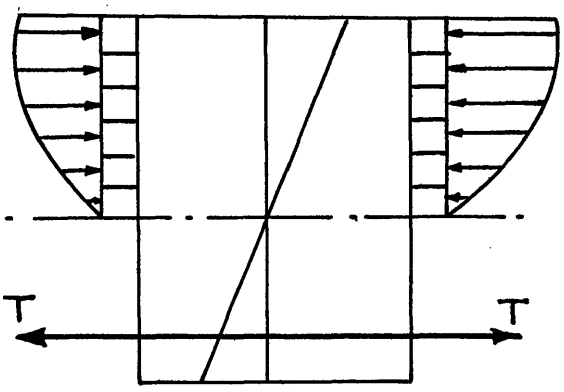

Fig. 2.2.

(e) On the basis of the assumptions on page 4 the author has evolved a method of deducing the stress distribution from a straightforward bending test on a beam. The method is given in detail on page 20 et seq.

The difficulties and drawbacks of these methods will now be dealt with in turn.

Critisism of each of the above methods.

(a) In any compression test in which the specimen is loaded between parallel plates lateral expansion of/

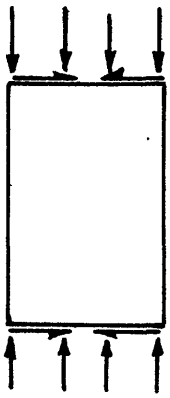

Fig. 2.3

of the concrete is restricted by friction between the specimen and the plates. In the case of concrete the effect is shown in the differences in strength obtained in comparative tests on 6" concrete cubes and 12" x 6" diam. cylinders. Concrete in cube form always has an higher apparent strength than that in the 12" x 6" cylinder. This is due to the stress distribution in the specimens being complex instead uniaxial compression. Thus any attempt to relate the overall load to strains measured on the surface of the concrete must give false result. This problem is considered in part IV of this thesis where an analysis of the stress conditions is made.

(b) Any attempt to embed stress gauges in a material to determine the stresses therein is fundamentally wrong unless the deformation characteristics of the gauge are the same as those of the body in which they are embedded for the presence of such foreign bodies disturbs the very quantity which is being measured. It follows therefore that such a gauge cannot be used in order to determine the elasticity of a material for in order to construct the gauge with properties such that it does not upset

the/

stress distribution it is necessary to know beforehand the quantity which is to be determined. Nevertheless stress gauges have been made and the errors involved by the use of gauges possessing different strain characteristics from the material in which they are embedded have been assessed (5). It has been shown that the errors are least if the gauge modulus is greater than the modulus of the material in which it is embedded and for a modular ratio of 4 the error is of the order of 10%. This accuracy is not unreasonable but at high stresses the change in stress per unit strain for concrete becomes zero and according to Whitney (6) becomes negative. It seems probable that under these conditions readings from the stress gauge will be of little value.

A further difficulty in the use of such gauges is that they should be large compared with the aggregate of the concrete in accordance with the argument advanced on page 7. This means that in order to place a reasonable number of gauges in a beam the latter will have to be rather large. While this presents no fundamental difficulty it can give rise to severe practical difficulties in testing.

(c) The method of Herr and Vandefrift suffers from the same/

same setback as the stress gauge method in that a foreign body is introduced which will upset the stress distribution. The disturbance is reduced by making the insert as thin as possible. Even so difficulties have been encountered in reconciling the total tensile force determined from strain gauge movements on the steel with the total compressive force measured photoelastically. This has been ascribed to the 'Poisson's-ratio effect'. Under plastic conditions it seems likely that the glass will inhibit the lateral expansion of the concrete considerably. Various types of coating on the faces of the glass in contact with the concrete have been tried in an attempt to eliminate this difficulty. It does appear, however, that the method holds considerable promise. The published paper is in the nature of a preliminary report and a fuller account will presumably appear in due course.

(d) The bending simulation machine provides a fundamentally sounder method of determining the stress distribution in that it makes a direct measurement of the stress distribution without the introduction of disturbing elements. The method does, however, present some difficulties. Unfortunately the two main drawbacks require opposing remedies for their eradication.

The specimen is compressed between plates in a manner similar to that described in reference to cubes and cylinders above, i.e. lateral expansion is prevented by friction between the plates and the specimen. In a beam no such restraint is present. The obvious remedy of this defect lies in the use of long specimens. Such a solution is not, however, practical as it gives rise to a further more serious difficulty found in a test on a specimen as indicated in the figure that a linear strain distribution is given by gauges B independently of the load distribution applied at the ends. Thus as far as this gauge length is concerned the object of the test which is, to vary the load distribution until one is found to give a linear strain distribution, is defeated because an infinity of solutions is possible. This demonstration of St. Venant's principle means that strain measurements must be confined to gauge lengths A and C. If this is done the method is feasible but it does mean that the strains are measured on that portion of the concrete where the stress distribution is disturbed/

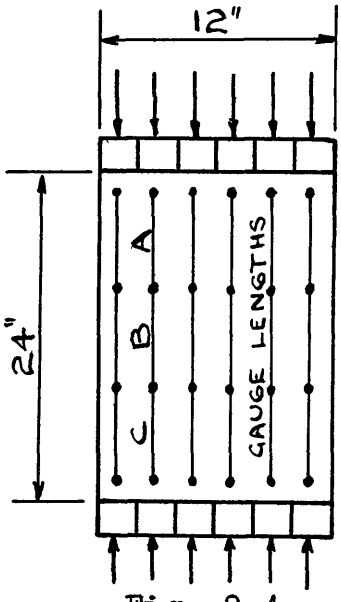

Fig. 2.4

disturbed by friction between the ends of the specimen and the plates through which the loads are applied.

The preceding remarks on methods (a) to (d) are not intended as purely destructive critism. Each method considered is quite sound apart from the sources of error which have been pointed out and it may be that some of these will be of little significance in practice. The defects which have been noted are fundamental to the methods and it must be demonstrated that the errors introduced are negligible before any reliance can be placed on the results of such experiments. Basically all these methods have to modify the quantities which they seek so measure in order that they may be measured. It is in this respect that the 'direct measurement' methods are to be contrasted with the author's method (e) which, on the basis of specified assumptions, deduces the stress distribution from simple data obtained from bending tests on beams. Simple experimental errors aside the validity of the results obtained by this method depends solely whether or not the assumptions are justified. Such an approach to the problem has the advantage that should the results of tests prove unsatisfactory attention is focused immediately on the possible deficiencies of the method. The author's analysis is given in full in the following pages consideration of its difficulties are given later.

AUTHOR'S METHOD.

The author's method of analysing beam test data to find the distribution of concrete stress has been published (7) and is given below. (A slight difference in nomenclature occurs from that used previously as in the printed paper d refers to the overall depth of the beam whilst d' is the effective depth. Generally in this thesis, d is used for the effective depth).

Taken from Magazine of Concrete Research, January, 1951

UNIVERSITY OF LONDON: CITY AND GUILDS COLLEGE

The distribution of concrete stress in reinforced and prestressed concrete beams when tested to destruction by a pure bending moment

by J. M. Prentis, M.Sc.(Eng.)

SUMMARY:

A method is given for utilizing experimental data derived from bending tests on reinforced and prestressed concrete beams to determine the stress-strain relationship for concrete. No initial assumption is made as to the shape of this curve, and the result obtained is unique for the given test data, so that the factors which govern the validity of the final result are simply the basic assumptions of the method of analysis.

Introduction

A number of papers has been published in recent years giving theories of failure for reinforced concrete beams. The basic differences between each of the proposed methods lie in the varied assumptions made as to the shape of the stress-strain curve for concrete. The general method has been to assume a reasonable shape for this curve and then deduce an expression for the ultimate bending moment.

Consider a beam subjected to a bending moment which is increased until failure takes place by crushing of the concrete. The stress-strain conditions immediately prior to the failure are as indicated in Figure 1. The moment is resisted by a tensile force T in the reinforcement and a compressive force C in the concrete equal in magnitude to T. The moment is given by this force multiplied by the lever-arm, j. Tensile stresses in the concrete are insignificant.

Among the suggestions made as to the distribution of concrete stress which gives rise to the force C we have that of C. S. Whitney* who makes direct use of the stress-strain curve obtained by measurements on a 12 in. by 6 in. cylinder. Other distributions suggested include various conic sections and the cubic and fifth parabolas. Any one of these distributions can be made to fit a given case, since the problem is indeterminate if conditions at the ultimate load alone are considered.

It is, however, possible to arrive at a unique solution if the stress history is traced at all stages up to the ultimate.

The action of a uniform rectangular beam subjected to combined bending moment and end load

If a rectangular section of breadth b is subjected to forces as shown in Figure 2, then the extreme fibre stresses are given by the following equations :

$$f_c = \frac{1}{bd^2}\left[\frac{1}{(e_c-e_t)}\frac{d}{de_c}\left\{\Big(M+P\,(d-d')\Big)(e_c-e_t)^2\right\} + Pd\frac{de_t}{de_c}\right] \quad . . (1)$$

$$f_t = \frac{1}{bd^2}\left[\frac{1}{(e_c-e_t)}\frac{d}{de_t}\left\{(M-Pd')\,(e_c-e_t)^2\right\} + Pd\frac{de_c}{de_t}\right] \quad . . . . . (2)$$

These relationships are deduced in Appendix 1. Clearly it is of no consequence whether the force P is applied by an internal bar or wire, as in the cases of

* WHITNEY, C. S. Plastic theory of reinforced concrete design. *Proceedings of the American Society of Civil Engineers.* 1940. Vol. 66. No. 10. pp. 1749-1780.

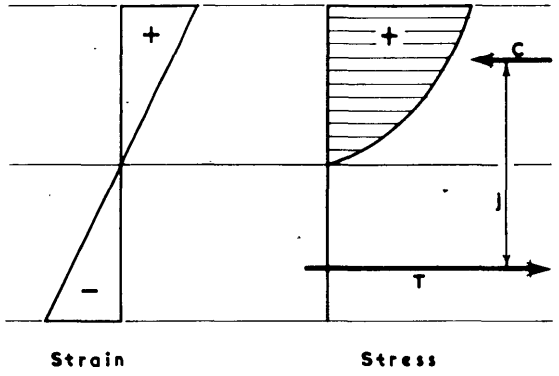

Figure 1.

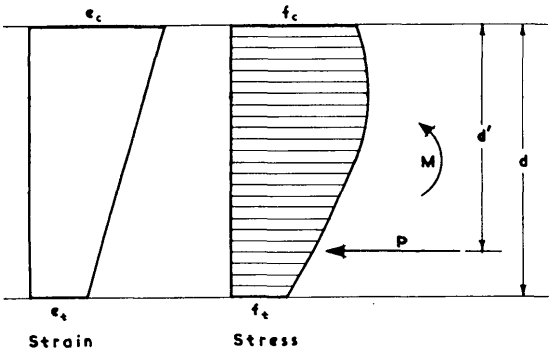

Figure 2.

reinforced and bonded prestressed beams, or whether it is applied externally as in an end-anchored prestressed beam or eccentrically loaded column.

To apply equations 1 and 2 it is necessary to measure the strains on the top and bottom of a beam, the force P, and the moment M at a series of loading stages. The values of f_c and f_t can then be calculated for each load stage, and since the corresponding strains have been measured the stress-strain curve for the concrete may be plotted for the whole range of the test.

Evaluation of equations 1 and 2 necessitates graphical differentiation. The author has found that the above form is somewhat inconvenient as the slopes to be measured increase very rapidly. This operation is rendered simpler by the use of the extended forms :

$$f_c bd^2 = (e_c - e_t)\frac{d}{de_c}\left\{M + P(d-d')\right\} + 2\left\{M + P(d-d')\right\}\left(1 - \frac{de_t}{de_c}\right) + Pd\frac{de_t}{de_c}$$

$$f_t bd^2 = (e_c - e_t)\frac{d}{de_t}\left\{M - Pd'\right\} - 2\left\{M - Pd'\right\}\left(1 - \frac{de_c}{de_t}\right) + Pd\frac{de_c}{de_t}$$

When prestressed concrete beams are considered the value of f_t is initially the prestress value. With the application of load this stress falls while f_c increases. If both equations 1 and 2 are plotted against strain it will be found that the rising f_c curve coincides with the falling f_t curve. With further increases of bending moment f_t falls to zero and becomes negative. It increases negatively until the concrete cracks, when it falls once more to zero. A check on the work is provided by the fact that the value of f_t given by equation 2 should be zero for all stages beyond the cracking moment.

When an ordinary reinforced concrete beam is loaded the cracking stage is reached very quickly, and since the cracking moment is a small percentage of the ultimate moment it is reasonable to assume, as in normal design, that f_t is zero at all loads. Equating f_t to zero and eliminating M from equation 1 we obtain :

$$f_c bd^2 = \frac{d}{de_c}\left\{P(e_c - e_t)\right\} \quad \ldots\ldots\ldots\ldots (3)$$

Basic assumptions

The basic assumptions upon which the analysis is based are given in Appendix 1 as they are applied, but it is desirable that they should be stressed here.

(*a*) It is assumed that plane sections remain plane where the bending moment is unaccompanied by shearing forces. There appears to be some controversy on this point, but there is much experimental data to support the assumption.

(*b*) It is assumed that no straining takes place without an increase in stress, that is, that there is no creep of the concrete during the period of the test. This is a somewhat severe approximation, as concrete creeps at all stresses, and as failure becomes imminent the creep rate is very high. However, the author's experience leads him to believe that little error is introduced, except at very high loads, if the test is carried out speedily. It should be borne in mind that, although the rapid creep which occurs at say 95 per cent of the ultimate load renders the analysis somewhat dubious for higher loads, the stress-strain diagram which has already been deduced prior to that loading stage is quite valid.

(*c*) Lastly, it is assumed that a given strain may be identified with a specific stress irrespective of the position and history of the element considered.

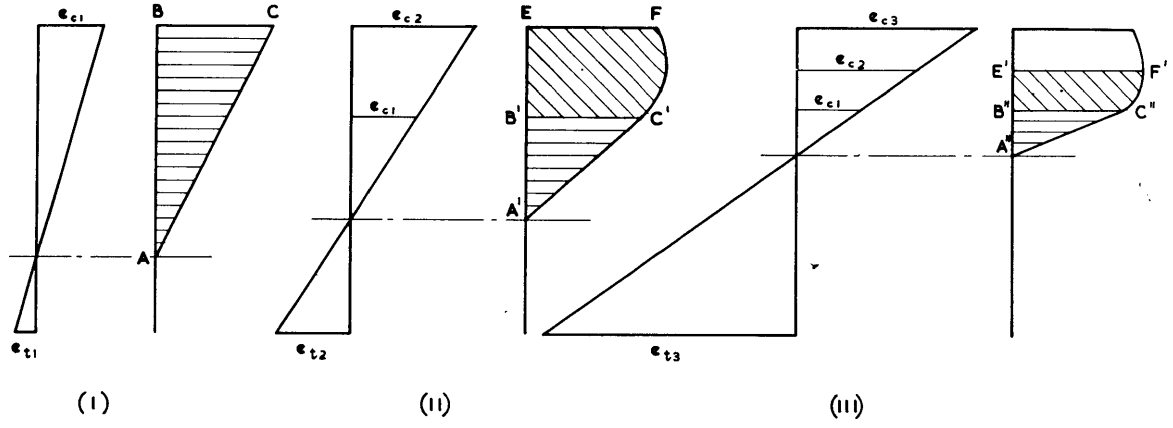

Figure 3.

The particular significance of assumptions (*b*) and (*c*) in this problem may be illustrated with reference to Figure 3. If at stage I we have a stress BC corresponding to strain e_{c1} and at stage II an increase of moment increases the top fibre strain to e_{c2}, the above assumptions state that the stress in the fibres where the measured strain is now e_c is B′C′ = BC. The stress triangle ABC is reduced in the vertical direction in the ratio $\frac{A'B'}{AB} = \frac{e_{c1}}{e_{c2}}$. Similarly at stage III, B″C″ = B′C′ = BC, and E′F′ = EF.

Conclusion

Thus within the framework of the above assumptions the analysis leads to a stress-strain curve which may be utilized to determine the stress distribution in a beam at all stages of load. By examining test data from a series of beam tests it should be possible to determine the influence, if any, of various factors such as age, mix, etc., upon the shape of this curve.

The basic differences between the various plastic theories of failure for reinforced concrete beams result mainly from differences of opinion as to the form of this curve, and it is hoped that application of the above analysis will help to resolve the problem.

APPENDIX 1

The derivation of equations 1 and 2

The quantities to be measured during the test are those given in Figure 4. The force P may be measured directly in the case of end-anchored prestressed concrete beams, but in other cases it must be deduced from the strains measured on the concrete or from strain gauge measurements on the reinforcement.

In the present analysis it is assumed that no creep takes place during the test, so that the stress-strain relationship may be represented by :

$$f = \varphi(e)$$

Equating horizontal forces,

$$P = b\int_o^d f\,dx = b\int_o^d \varphi(e)\,dx \quad \ldots\ldots(5)$$

where x is measured positive upwards from the bottom of the section. Assuming that plane sections remain plane we obtain by geometry,

$$e = e_t + \frac{x}{d}(e_c - e_t) \quad \ldots\ldots(6)$$

Substituting from equation 6 in equation 5, and changing the variable,

$$P = \frac{bd}{(e_c - e_t)}\int_{e_t}^{e_c} \varphi(e)\,de \quad \ldots\ldots(7)$$

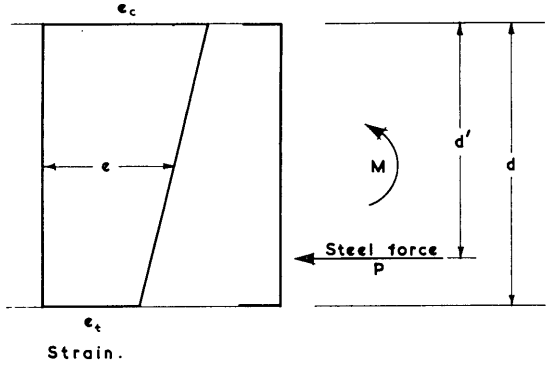

Figure 4.

Taking moments about the origin and equating internal and external moments we obtain

$$M+P(d-d') = b\int_o^d x\ f\ dx$$

$$= \frac{bd^2}{(e_c-e_t)^2} \int_{e_t}^{e_c} (e-e_t)\ \varphi\ (e)\ de$$

or

$$\frac{1}{bd^2}\left\{M+P(d-d')\right\}(e_c-e_t)^2 = \int_{e_t}^{e_c} (e-e_t)\ \varphi\ (e)\ de$$

Differentiation with respect to e_c gives

$$\frac{1}{bd^2}\frac{d}{de_c}\left[\left\{M+P(d-d')\right\}(e_c-e_t)^2\right]$$

$$= (e_c-e_t)\ \varphi\ (e_c) - \frac{de_t}{de_c}\int_{e_t}^{e_c} \varphi\ (e)\ de$$

Substituting from equation 7 and re-arranging, we find

$$f_c bd^2 = \frac{1}{(e_c-e_t)}\frac{d}{de_c}\left[\left\{M+P(d-d')\right\}(e_c-e_t)^2\right] + Pd\frac{de_t}{de_c} \quad .(1)$$

Similarly, it may be shown that

$$f_t bd^2 = \frac{1}{(e_c-e_t)}\frac{d}{de_t}\left[\left\{M-Pd'\right\}(e_c-e_t)^2\right] + Pd\frac{de_c}{de_t}$$

(equation 2)

NOTE

If P is made zero in equations 1 and 2, we get

$$f_c bd^2 = \frac{1}{(e_c-e_t)}\frac{d}{de_c}\left[M\ (e_c-e_t)^2\right] \quad \ldots\ldots\ldots (1a)$$

$$f_t bd^2 = \frac{1}{(e_c-e_t)}\frac{d}{de_t}\left[M\ (e_c-e_t)^2\right] \quad \ldots\ldots\ldots (2a)$$

These equations, which may be utilized to deduce the stress-strain relationship for a material in the form of a rectangular homogeneous bar, may be re-arranged to give an equation published by Nadai.*

APPENDIX 2

Worked example

The data chosen to illustrate this method were obtained from test results on an end-anchored prestressed concrete beam tested recently in the Concrete Technology Department of the Imperial College, London, on behalf of the D.S.I.R. and under the supervision of Professor A. L. L. Baker. The beam section, detailed in Figure 5, was prestressed by four cables, each consisting of eight 2 mm diameter high-tensile steel wires. The cable loads were measured by using electrical strain gauges, and the strain distribution in the concrete was measured by means of a mechanical strain gauge.

The entire calculation is set out in Table 1, where the bending moment and the steel force have been divided by bd^2 and bd respectively to reduce them to the dimensions of stress. It may be noted also that m, p and e_t have been tabulated for regular intervals of e_c. These values were obtained from the mean curves obtained by plotting experimental results. The full stress-strain curve which was obtained is given in Figure 6.

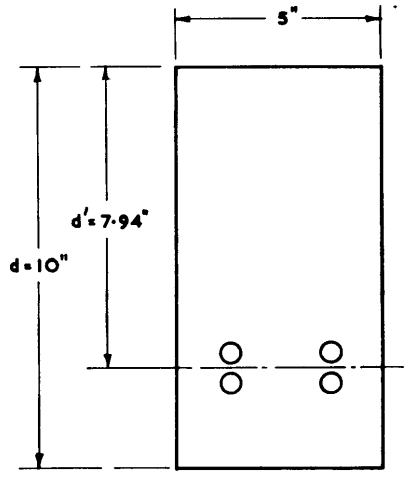

Figure 5.

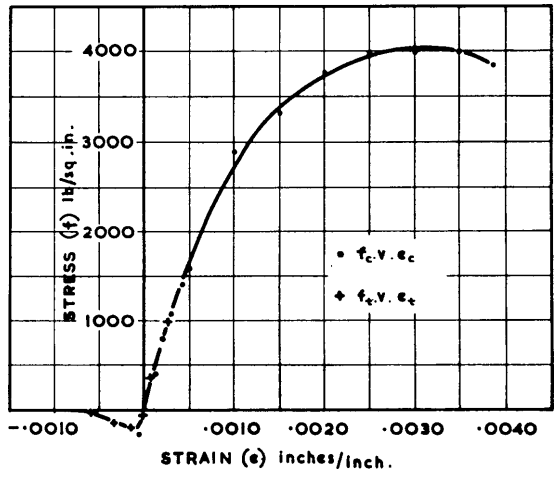

Figure 6.

* NADAI A. Plasticity. 6th. impression. New York and London. *McGraw-Hill Book Company Inc.* 1931. Chapter 23. pp. 164-167.

Stresses in beams subjected to pure bending moment

TABLE 1.

$m=M/bd^2$		0	38	106	173	220	242	253	273	297	323	345	363	376	382
$p=P/bd$		343	344	345	347	351	355	359	384	417	445	474	496	512	522
$m+p\ (1-d'/d)$		71	109	177	244	292	315	327	352	383	415	443	465	482	489
$m-pd'/d$		−272	−235	−168	−103	−53	−40	−32	−32	−34	−30	−31	−31	−30	−33
e_c	in./inch $\times 10^{-4}$	**−0.6**	**0**	**+1.0**	**2.0**	**3.0**	**4.0**	**5.0**	**10**	**15**	**20**	**25**	**30**	**35**	**38.3**
e_t	in./inch $\times 10^{-4}$	**+2.5**	**+1.9**	**+0.8**	**−0.2**	**−1.4**	**−3.3**	**−6.0**	**−30**	**−60**	**−92**	**−121**	**−149**	**−176**	**−194**
e_c-e_t	in./inch $\times 10^{-4}$	−3.1	−1.9	+0.2	2.2	4.4	7.3	11.0	40	75	112	146	179	211	232
de_t/de_c		−1.07	−1.07	−1.07	−1.07	−1.43	−2.30	−3.00	−6.06	−6.06	−6.06	−5.77	−5.45	−5.40	−5.40
de_c/de_t		−0.935	−0.935	−0.935	−0.935	−0.700	−0.435	−0.333	−0.165	−0.165	−0.165	−0.173	−0.184	−0.185	−0.185
$1-de_t/de_c$		2.07	2.07	2.07	2.07	2.43	3.30	4.00	7.06	7.06	7.06	6.77	6.45	6.40	6.40
$1-de_c\ de_t$		1.935	1.935	1.935	1.935	1.700	1.435	1.333	1.165	1.165	1.165	1.173	1.184	1.185	1.185
$d/de_c\{m+p(1-d'/d)\}$		66.6	66.6	66.6	66.6	34.1	17.5	8.34	6.33	6.33	6.00	5.00	3.90	2.78	1.66
do.	$\times(e_c-e_t)$	−206	−126	+13	147	150	128	92	260	470	610	730	700	590	390
$2\{m+p(1-d'/d)\}$															
	$\times(1-de_t/de_c)$	294	451	732	1010	1420	2080	2620	4970	5400	5860	6000	6000	6170	6260
$p\ de_t/de_c$		−367	−368	−369	−371	−502	−820	−1078	−2330	−2530	−2700	−2740	−2700	−2760	−2820
f_c	lb per sq. in.	**−279**	**−43**	**+376**	**786**	**1070**	**1390**	**1630**	**2900**	**3340**	**3770**	**3990**	**4000**	**4000**	**3830**
$d/de_t\{m-bd'/d\}$		−63.0	−63.0	−63.0	−63.0	−18.2	−5.13	−1.33	—	—	—	—	—	—	—
do.	$\times(e_c-e_t)$	195	120	−13	−139	−80	−37	−15	—	—	—	—	—	—	—
$-2\{m-pd'/d\}$															
	$\times(1-de_c/de_t)$	1052	910	650	399	180	115	85	75	79	70	73	73	71	78
$p\ de_c/de_t$		−320	−322	−323	−324	−246	−154	−120	−63	−69	−73	−82	−91	−95	−97
f_t	lb per sq. in.	**927**	**708**	**314**	**−64**	**−146**	**−76**	**−50**	**+12**	**+10**	**−3**	**−9**	**−18**	**−24**	**−19**

CRITISISM OF THE AUTHOR'S METHOD.

The most obvious defect of the above method is that the author neglects the creep component of the overall strains from which the stress distribution in the beam is deduced. This means that, on theoretical grounds alone, the method cannot be used to derive the true distribution because it deliberately neglects a factor known to exist, unless, of course, the rate of loading is infinite. This defect is in direct contrast to the drawbacks of methods (a) to (d) which present practical problems making it difficult to attain the theoretically possible, and correct, end.

Before dealing with this point in detail it must be pointed out that the author's method does entail certain experimental difficulties. These do not come in the same category as those inherent in methods (a) to (d) since the sources of error are not characteristic of the method and their eradication is simply a matter of experimental technique. The technique of testing concrete beams has been studied by the author and a description of this work with particular reference to the difficulties hinted at above will be given in chapter 3 of this section.

Chapter 2. THE INFLUENCE OF CREEP ON STRESS DISTRIBUTION.

The physical nature of creep in various materials has received much attention and many publications have appeared on the subject. However, there appears to be little evidence of the emergence of a general theory for the behaviour of bodies under complex stress when the material of which they are made is subject to creep phenomena. That such a study of the phenomenological aspects of creep presents considerable difficulties is shown by the fact that little progress appears to have been made since a classic paper on the subject by Boltzman in 1876 (8). This particular contribution will be referred to later.

It would appear fortunate that, from the point of view of the subject studied in this thesis, complex stress systems need not be considered. This is indeed so, but even when attention is confined to the case of material subjected to a uni-axial stress, (i.e. as in the case of simple bending) difficulties still arise.

Consideration will now be given to the quantitative aspect of creep in order to define the difficulties mentioned above and to see if it is possible to assess the effect, if any, on the stress distribution in concrete beams.

The following work will be restricted to a study of the simple case of uni-axial stress.

THE GENERAL CREEP EQUATION AT CONSTANT STRESS.

The creep equation is generally given in the form:-

$$c = f.\theta(t) \qquad (2.1)$$

c being the creep strain, f the stress and $\theta(t)$ a time function. A variety of forms have been suggested for $\theta(t)$ but these are of no concern for the moment. Equation (2.1) will be referred to as the 'general creep equation'. This equation is strictly applicable only when the stress f is constant. It is thus of limited value since in general, the stress varies with time.

CREEP UNDER VARYING STRESS.

This problem has been dealt with in a variety of ways:-

(a) by the use of an effective modulus. The concrete Young's modulus is replaced by $E_e = E/(1 + E.\theta(t))$ (2.2) and this value is used in the normal equations of reinforced concrete. Basically the use of this method assumes that all the creep has taken place at the final concrete stress i.e. $c_T = f_T.\theta(T)$.

(b) by assuming that the rate of creep is given by

$$\frac{\partial c}{\partial t} = f \frac{d}{dt}\theta(t) \qquad (2.3)$$

The author has argued elsewhere (9) that for a continuously increasing stress assumptions

assumptions (a) and (b) give upper and lower bounds respectively for the total creep.

(c) by using a principle of superposition. The suggestion that such a principle may be applied to creep is due to Boltzman (8). The application of the method to concrete has been shown to be admissible by McHenry (10) who expresses it mathematically in the form

$$c_T = \int_{\tau}^{T} \theta(t, T-t) \frac{df}{dt} dt. \qquad (2.4)$$

where τ is the age at loading.

The effective modulus method is certainly the simplest to apply and according to McHenry it is sufficiently accurate for a large class of problems. The method is fundamentally unsound in that it does not give a true picture of the behaviour and if applied indiscriminately it might lead to erroneous results. It gives most accurate results if the variation in f is small over the period of time considered. Method (b) does lead to results which are more satisfying from the descriptive viewpoint but which are unsound because the basic assumption presumes that the rate of creep is independent of the stress history of the material. McHenry's method takes into account the whole stress history and is in consequence far superior although mathematical difficulties are met in its application.

It will be seen from the foregoing remarks that creep problems can be divided broadly into two classes. In the first class we have those systems in which the stress variation is small, thus allowing the use of the effective modulus. Secondly we have systems in which the variation of stress is large and consequently require the application of equation (2.4) for their solution. Fortunately the majority of cases met in normal practice fall into the first class. The second case arises in testing where the concrete stress ranges from zero up to the crushing value. These two cases will be considered with particular reference to concrete beams.

CREEP IN ORDINARY REINFORCED CONCRETE BEAMS WITH SMALL VARIATIONS IN STRESS.

The effect of creep in the concrete and steel upon the stress distribution in pre-stressed concrete beams has been dealt with by Magnel (2).

The case of the redistribution of stress in ordinary reinforced concrete beams due to creep will now be studied. Before any analysis can be undertaken the assumptions upon which it is to be based must be specified. It will be assumed -

(a) that the concrete stress is uniquely defined by the instantaneous strain,

(b) that the concrete below the neutral axis has no stiffness and carries no stress.

These are the assumptions specified on page 1 except that (a) has been modified to exclude creep strains. It is now necessary to make a further assumption defining the method by which the creep strains are to be assessed:-

(c) It will be assumed that creep may be allowed for by the use of an 'effective modulus' (p.27).

The use of the effective modulus is known to be reasonable provided that the stress variations are not large. If, as a result of the analysis, it were shown that the changes in stress are large then the result would be incompatible with the assumption showing the latter to be untenable.

Consider a rectangular reinforced concrete section of breadth b and effective depth d having an area of reinforcement A_s. The strain distribution with bending moment M applied will be as in the diagram the geometry of which gives

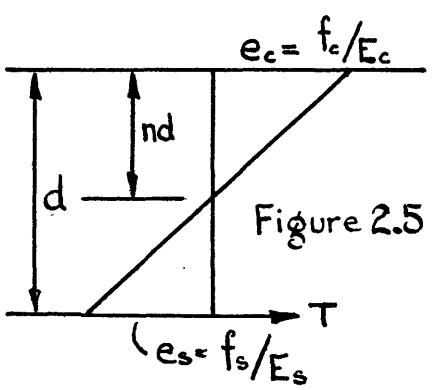

Figure 2.5

$$\frac{n}{1-n} = \frac{f_c}{f_s} \cdot \frac{E_s}{E_c} \qquad (2.5)$$

Equating horizontal forces

$$f_c = \frac{2}{n} \times f_s \times A_s/bd \qquad (2.6)$$

Equating moments

$$M/bd^2 = \tfrac{1}{2} f_c n(1 - n/3) \qquad (2.7)$$

From (2.5) and (2.6) we obtain

$$\frac{n^2}{1-n} = 2\frac{A_s}{bd} \cdot \frac{E_s}{E_c} \qquad (2.8)$$

If in this equation E_c is replaced by the effective modulus the variation of n with time is obtained. Substitution of this relationship in equation (2.7) gives the variation in concrete stress.

The variations in f_c and n with modular ratio are plotted in Fig. 2.6. The range of modular ratio given is extreme as the lower limit of 4 would only be obtained with very rapid loading of concrete having a cube strength of about 8000 lb. per sq. inch, whilst 64 is attained only as limiting value ($t \to \infty$) for very low strength concrete (c_u = 2000 lb. per sq. inch). Nevertheless, the changes in concrete stress and neutral axis position due to creep appear to be substantial. The variations in the steel stress are, on the otherhand, negligible.

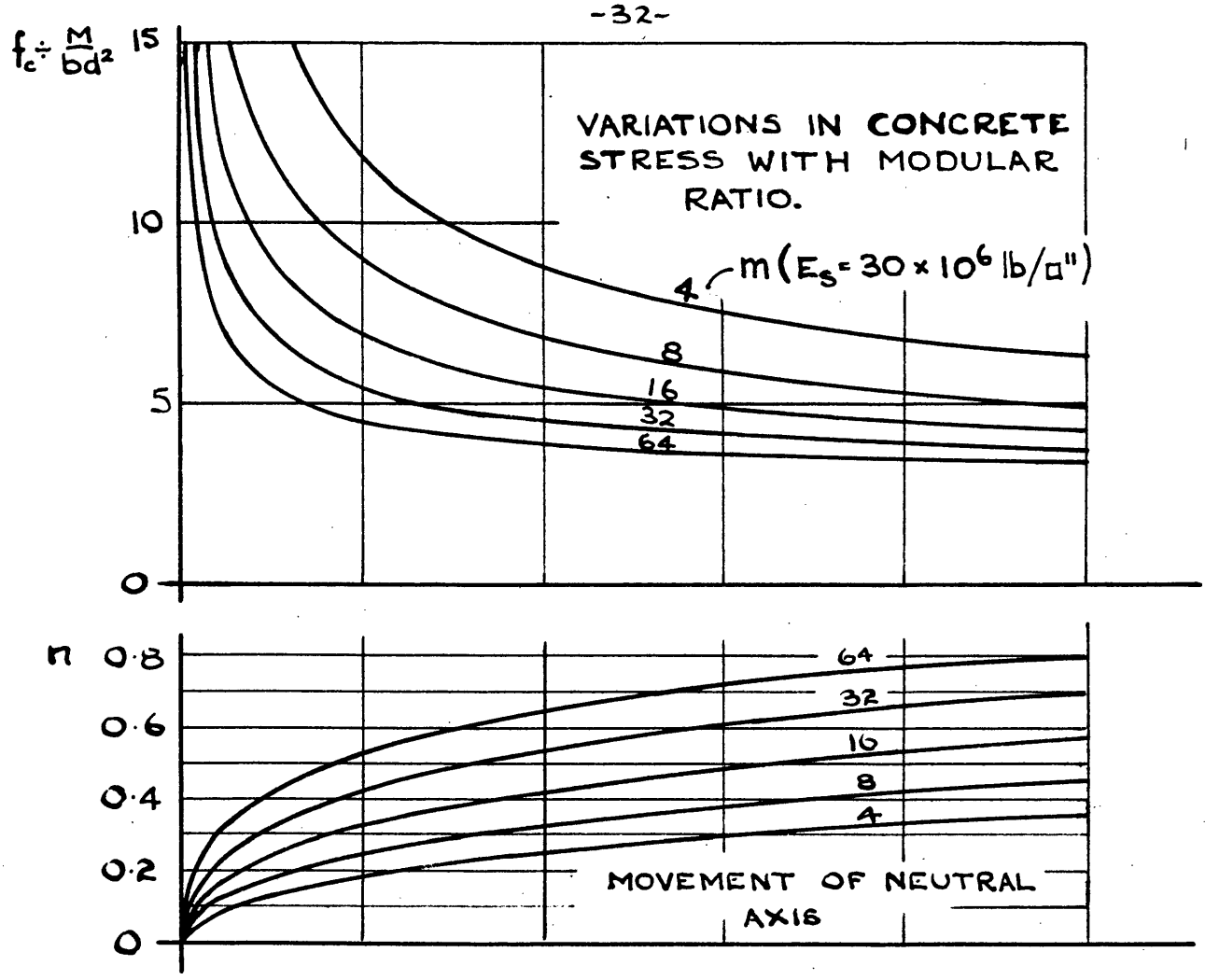
$f_c \div \frac{M}{bd^2}$
15
10
5
0
VARIATIONS IN CONCRETE STRESS WITH MODULAR RATIO.
m ($E_s = 30 \times 10^6$ lb/□")
4
8
16
32
64
n
0·8
0·6
0·4
0·2
0
64
32
16
8
4
MOVEMENT OF NEUTRAL AXIS

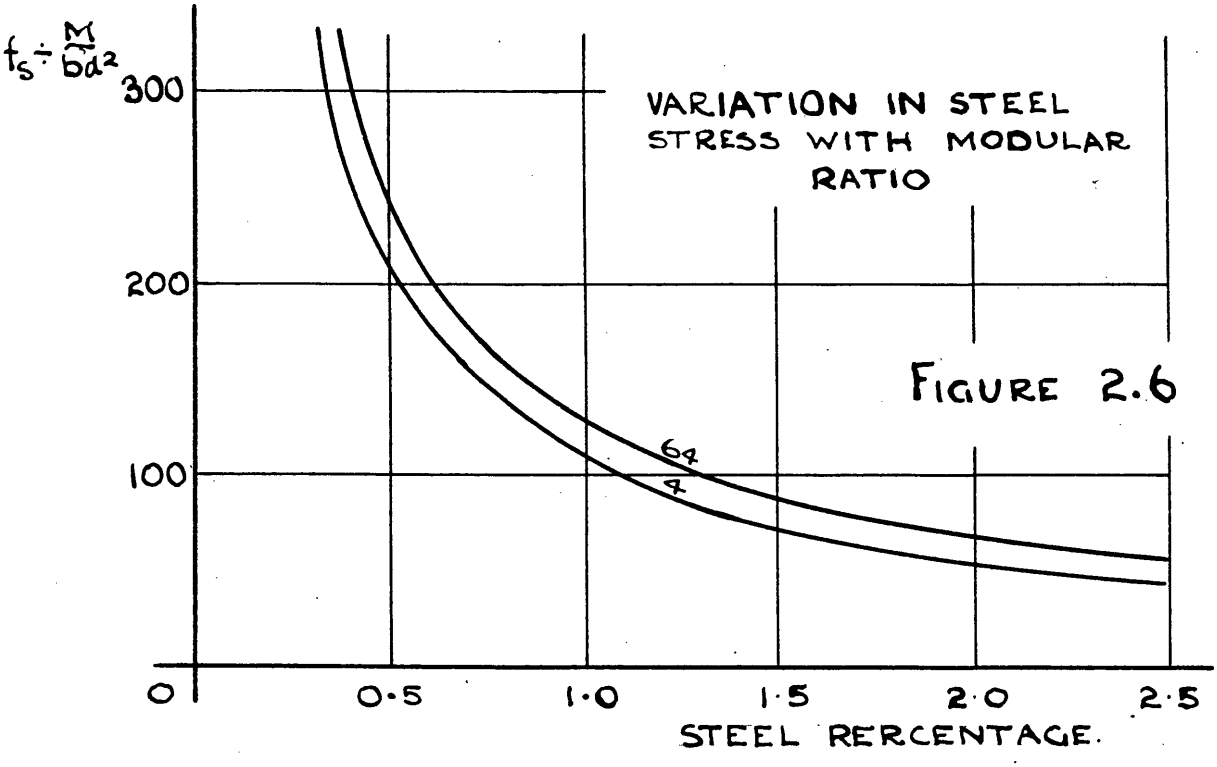
$f_s \div \frac{M}{bd^2}$
300
200
100
0
VARIATION IN STEEL STRESS WITH MODULAR RATIO
64
4
0·5
1·0
1·5
2·0
2·5
STEEL RERCENTAGE.

FIGURE 2.6

The curves indicate the concrete stress to be 20% to 30% below the calculated value based on the usual design assumption of a modular ratio of 15. This estimate is slightly conservative as the use of the effective modulus underestimates creep when, as in this case, the stress decreases with time. This is a corollary to the remarks in paragraph (b) on page 27. Professor A.D. Ross has presented the case for using a high modular ratio in design rather than the value of 15 (11) so that this aspect need not be pursued further here. The analysis above confirms the conclusions reached by Ross.

We must now refer back to assumption (c) on page 30 which pre-supposes small stress changes, and decide whether or not it is justified. One way to do this would be to assume that $\frac{\partial c}{\partial t} = f \frac{d}{dt} \Theta(t)$ and compare the results with those obtained on the basis of the effective modulus assumption. It is known that the true creep is intermediate between that obtained as a result of each of these methods. Unfortunately attempts to use this assumption result in unmanageable equations and a solution has not been found. As an alternative approach $\frac{\partial c}{\partial t} = f \frac{d}{dt} \Theta(t)$ will be integrated using the stress variations given in figure 2.6. The creep strains so obtained are then compared with the creep strains obtained on the basis of the effective modulus calculations.

$\frac{\partial c}{\partial t} = f \frac{d}{dt} \Theta(t)$ cannot be integrated in general terms so a specific example must be taken. In order to exaggerate the effects the case of a low percentage of reinforcement together with a low concrete strength is considered. The values of the effective modulus for concrete having a cube strength of 2000 lb. per sq. inch are given in the table below together with the variations in concrete stress obtained from figure 2.6. The integrated values on the fifth line of the table have been obtained graphically from a more detailed plot of the values involved, the actual curves are of little interest and have not been included. Apart from this the first eight lines of the table are self-explanatory.

1	Time	0	1 D	7 D	1 M	6 M	12 M
2	Effective modulus	10.0	22.0	27.5	37.5	50.0	56.5
3	$\Theta(t) \times 10^6$	0	0.40	0.58	0.92	1.33	1.55
4	$f_c \times M/bd^2$	8.2	6.2	5.9	5.1	4.8	4.7
5	$\int f_c \frac{d\Theta}{dt} dt \times (M/bd^2) \cdot 10^6$	0	2.8	3.9	6.3	8.3	9.4
6	Elastic strain $= \frac{f_c}{E_o} \times 10^6$	2.7	2.1	2.0	1.7	1.6	1.6
7	Total strain $= \frac{M}{bd^2} \times 10^6$	2.7	4.9	5.9	8.0	9.9	11.0
8	$f_c / E_o \times (M/bd^2) \cdot 10^6$	2.7	4.5	5.4	6.4	8.0	8.8
9	Modified Eff. Mod.	10.0	23.6	29.8	46.8	62.1	77.0
10	" $f_c \times \frac{M}{bd^2}$	8.2	6.0	5.6	4.7	4.5	4.3

The seventh and eighth lines enable a comparison to be made between the strains obtained by integration and those given by direct application of the effective modulus. The two methods do not, at first sight, appear to compare very well but as it is the stress distribution which concerns us the calculations are carried a little further in the last two lines. In line nine the modified effective modulus is calculated on the basis of the integrated strain (line 7) and the original f_c values. The modified effective modulus enables f_c to be recalculated from equations 2.4 to 2.6 these values are tabulated in line 10. The new $E_{eff.}$ and f_c could be taken and the integration repeated. Inspection shows that the process converges. However, comparison of the two f_c values shows good agreement indicating that little change can be expected from further interations.

The conclusion to be drawn from this is that the stress changes are 'small' thereby justifying the use of the effective modulus.

CREEP PHENOMENA IN BEAMS SUBJECTED TO LARGE VARIATIONS IN BENDING MOMENT.

It has already been remarked that the use of the effective modulus and equation (2.3) is inadmissible when the material considered is subjected to severe variations in stress.

In such cases it is necessary to use McHenry's equation:-

$$c_T = \int_{\tau}^{T} \theta(t, T - t) \frac{df}{dt}\, dt. \qquad (2.4)$$

where τ is the age at loading.

When stated in the above form the equation can be applied to allow for the effects of ageing. This property is illustrated in fig. 2.7, which is abstracted from McHenry's paper (10). It can be seen that $\theta(t)$ is dependant on the age at which the concrete is loaded.

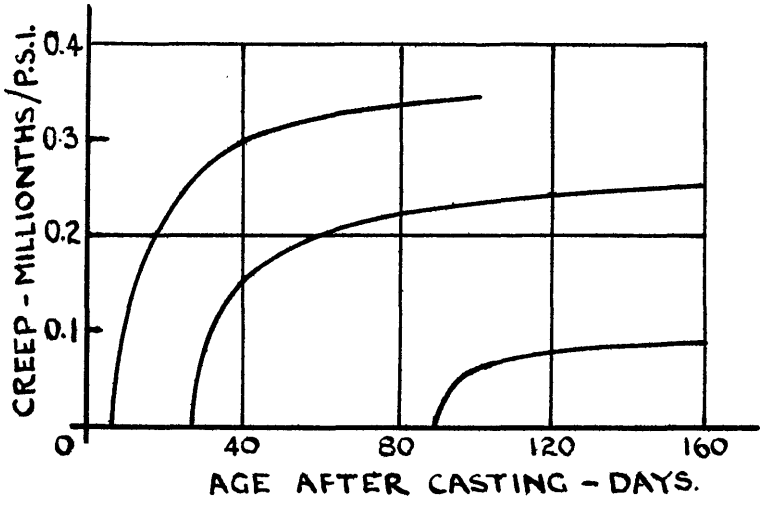

Figure 2.7

If the material is subject to severe load variations and the period of load is long then the phenomenon of ageing must be considered. The problem does not arise in testing, for in such cases the time taken to load the specimen to destruction is short so that the properties of the concrete do not change appreciably during the period of testing. In this case (2.4) can be amended to read

$$c_T = \int_{0}^{T} \theta(T - t)\, \frac{df}{dt}\, dt \qquad (2.9)$$

As it is very simple to deduce this equation from first principles its derivation is given below to illustrate the use of superposition.

DERIVATION OF EQUATION (2.9)

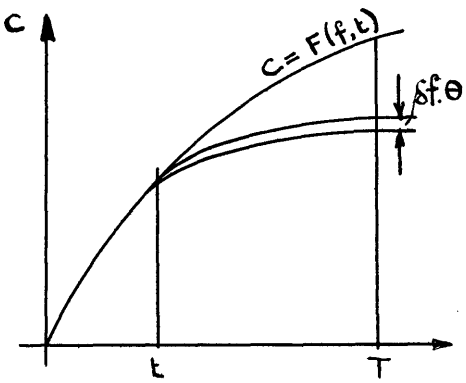

Assuming that the creep equation is $c = f.\theta(t)$, f being a constant stress, and applying the principle of superposition, the creep at time T due to an increment of stress δf applied at time t is

$$c = \delta f.\theta(T - t)$$

therefore

$$c_T = \int_{t=0}^{t=T} \theta(T - t).df$$

$$= \int_0^T \theta(T - t) \frac{df}{dt} dt.$$

CREEP AT HIGH STRESSES.

Although equation (2.9) can be used to calculate the creep in a material which is subject to severe stress variations the stresses must not approach the ultimate strength of the material. This is because equation (2.9) is based on the fundamental creep equation which assumes that at constant stress the creep is proportional to that stress. It is known that the linear relationship does not hold for high stresses for which the rate of creep is higher than that given by equation (2.1).

The creep properties of concrete at high stresses do not appear to have been studied. In a recent search through the literature the author was able to find but one publication dealing with this problem (12). This paper by Shank (published 1949) shows that the problem is being considered but that as yet very little information is available.

It would be unprofitable at this stage, to speculate upon the stress creep relationships at high stresses and attempt to build up a theory of the behavious of beams upon such a basis.

Despite this assertion the author has given the problem some consideration, but he has tackled it indirectly by assuming a simple mode of behaviour and determining the stress creep conditions which must occur to give the assumed result. As the results are of some interest the work is given below.

AUTHOR'S HYPOTHESIS FOR CREEP AT HIGH STRESSES.

It is sometimes suggested (see for example reference (11)) that as the creep rate is relatively high at large stresses there is a tendency in beams for the more highly stressed outer fibres to throw some of their stress on to the inner fibres.

Thus it is suggested that the stress distribution indicated in figure 2.8(a) degenerates as a result of creep into that indicated in (b), where a homogeneous beam is considered

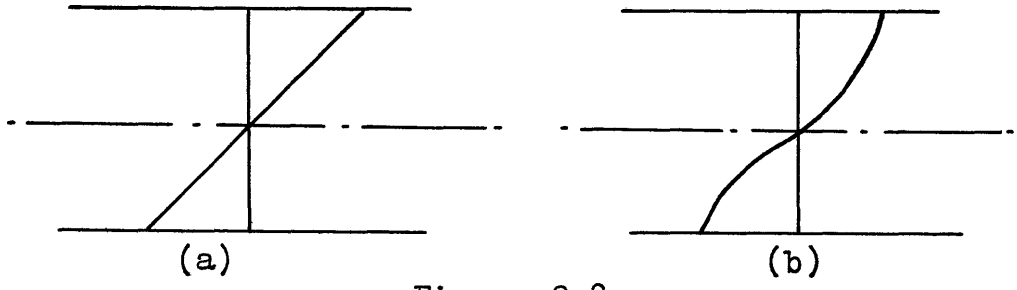

Figure 2.8

for simplicity. It is evident that in general some such action must occur but it is of interest to seek the conditions under which there is <u>no</u> re-distribution of stress.

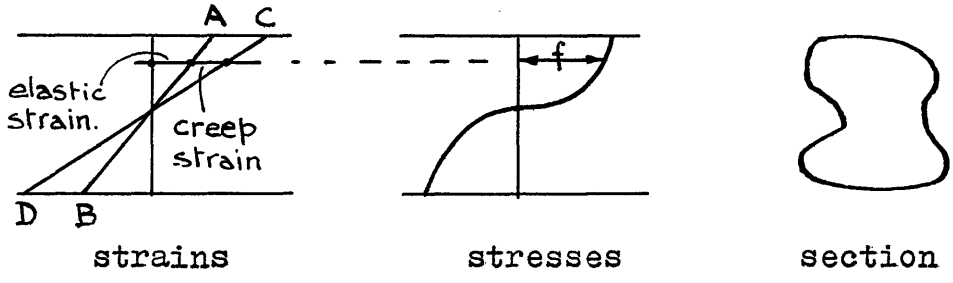

Figure 2.9

Consider a beam under a constant moment M. Assuming that the bending moment is unaccompanied by shear plane sections remain plane so that the distribution of <u>total</u> strain across the section must remain linear as indicated by CD. If the distribution of 'elastic' strain is not changed with time and is given by AB then by similar triangles we have at all positions in the depth of the beam

$$c \propto e$$

$$\text{i.e.} \qquad c = k.e.\theta(t) \tag{2.10}$$

Hence if the creep is proportional to the 'instantaneous' strain no re-distribution of stress will occur.

Note that no assumption has been made regarding the stress distribution so that the reasoning is not confined to the case of a linear stress strain relationship and is applicable to plastic conditions. If $f = \phi(e)$, equation (2.10) can be written in the form

$$c = k.\phi^{-1}(f).\theta(t) \tag{2.11}$$

under elastic conditions $\phi^{-1}(f) \equiv f/E$ and $k = E$ so that (2.11) reduces to (2.1).

If the principle of superposition is assumed in respect of strains equation (2.9) becomes

$$c_T = k \int_0^T \theta(T - t)\frac{de}{dt}\, dt \tag{2.12}$$

and it can be shown that the stress distribution is unaffected by creep for the case of a varying bending moment. As this proof is slightly more complex it will not be included in the text but is given in Appendix 2.1.

The above analysis raises the hope that the problem of creep at high stresses may yield to rational analysis. It is evident that if the stress distribution in a homogeneous structure is dependent upon creep then any resulting analysis/

analysis will be complex and probably impossible to apply reasonably to reinforced concrete. If on the other hand the desired condition of equation (2.10) is realised the problem is very much simpler.

Professor Shank's work when it is published in full will show if it is justifiable to consider the creep under constant stress as proportional to the instantaneous strain. Until some such evidence is available for consideration further study of this particular aspect is not warranted.

CONCLUSION.

The conclusions to be drawn from this chapter are:-

(i) Under normal working conditions the use of the effective modulus gives reasonable accuracy in the prediction of the redistribution of stress in reinforced concrete beams. In this instance the effective modulus underestimates the creep effect but even under very adverse conditions the error in concrete stress is unlikely to be greater than about 5% (see page 34).

(ii) If the beam is subjected to large variations in moment then McHenry's method using the principle of superposition, should be used. The method is, however, restricted in application to cases where the concrete stress does not approach its ultimate value.

(iii) The subject of creep of concrete under high stresses appears as yet to be an almost completely un-explored field and in the absence of a rational basis it is impractical to digress on the behaviour of beams at loads near failure.

It has been shown, however, that if the fundamental creep equation can be written $c = k.e.\theta(t)$ for high stresses, and if the principle of superposition can be applied to strains then the problem is very much simplified.

Before concluding this chapter we will refer once more to the author's method for determining the distribution of stress in reinforced concrete beams. This method is based on the assumption that creep is negligible. It is clear from paragraph (iii) above that, as yet, this assumption can not be replaced by a more fundamental one allowing for the effects of creep. Even if the creep data were available it would not be a simple matter to allow for it. All the work in this chapter has been devoted to evaluating creep strains under specified stresses and adding the elastic strains to obtain the total. It is very much more difficult to separate the two components when, as in the author's analysis, the total strain is given. If creep effects are to be eliminated it will be necessary to compute the creep strains, subtract them from the total and apply the analysis to the residue.

But the elastic strains must be known before the creep strains can be calculated!

The mode of attack appears to be:-

(i) Using the measured strains and knowing the creep properties, which are supposed related to the instantaneous strain, calculate the creep strains.

(ii) Subtract these values from the total strains.

(iii) Repeat step (i) using the residual strains. This will give the second approximation for the creep strains.

(iv) Continue the iterations until the convergence is satisfactory.

(v) Having subtracted the 'accepted' creep strains from the total strains apply the author's analysis to the residual strains.

NOTE, however, that the method will be valid only if the creep laws are such as to allow of the superposition of strains. Otherwise it will be found after step (ii) that plane sections are no longer plane. This is known to be physically impossible with circular bending.

The above suggestion is open to the objection that it would be necessary to obtain the creep data from uniaxial compression tests whilst this method is considered undesirable/

undesirable for the determination of the stress strain curve. The disadvantages of measuring the stress strain characteristic in a 'simple' compression test are given on page 13 paragraph (a). The same defects do not arise in creep tests because there is but little lateral creep due to a longitudinal stress so that the complications due to lateral restraint do not apply.

There is an alternative method which whilst being theoretically attractive is, in the opinion of the author, impossible practically. The method would be to make a number of identical bemas and test them at different rates of loading. All the appropriate data plotted to a base of time would then be extrapolated to give the 'zero-time' values. Employing the author's analysis on the resulting data the stress strain curve would be obtained exclusive of creep strains. A similar method has been used by Glanville to determine the 'instantaneous' stress strain curve in a uniaxial compression test. (13).

The difficulty of applying this method would lie in producing sufficiently identical beams. It seems likely that the normal variation which one would expect between the strengths of similar beams (say 10%) would mask the effects of creep to such an extent as to make the method suggested impracticable.

II Chapter 3. THE TESTING OF RECTANGULAR REINFORCED AND PRE-STRESSED CONCRETE BEAMS TO DESTRUCTION.

Whatever method is used to determine the distribution of stress in concrete beams the results must eventually be considered in the light of tests on actual beams. Although the following work is concerned with determining the data required for the method of analysis given on pages 20-24, the observations made are applicable to beam tests generally, irrespective of the way in which the derived data are applied.

Recapitulating from page 21, the experimental quantities required for the author's analysis are:-

(a) The dimensions of the section.

(b) The bending moment.

(c) The steel force.

(d) The eccentricity of the steel.

(e) The longitudinal strains.

EXPERIMENTAL TECHNIQUE

The general arrangement of the testing apparatus used for beam tests is given in figure 2.10. The determination of each of the above quantities will now be considered in detail.

(a) The dimensions of the beam section should be obtained by measurement of the actual specimen.

It is undesirable that the nominal shuttering sizes should be taken for granted as being correct. This is particularly so in the case of small beams.

(b) The dynamometers through which the load is applied to the beam can be calibrated independently and provided that care is taken in placing them in position the bending moment can be computed accurately. In the course of the series of tests quoted later two types of dynamometer were used, firstly a mercury filled diaphragm type and secondly a proving-ring. The writer considers the later to be the more suitable instrument in that its readings may be taken quickly without the element of personal error. For whereas the proving-ring gives a direct reading on a dial gauge, the diaphragm type requires the adjustment of a calibrated screw to bring the mercury to a specified level in a capilliary tube. The diaphragm type is at a further disadvantage in that changes in the room temperature can alter the zero reading of the instrument.

(c) The determination of the steel force can present difficulties. In the case of ordinary reinforced concrete beams with large diameter bars the steel strain can be measured by the attachment of electrical resistance strain gauges or, by stripping some of the cover and affixing mechanical or optical strain gauges (14).

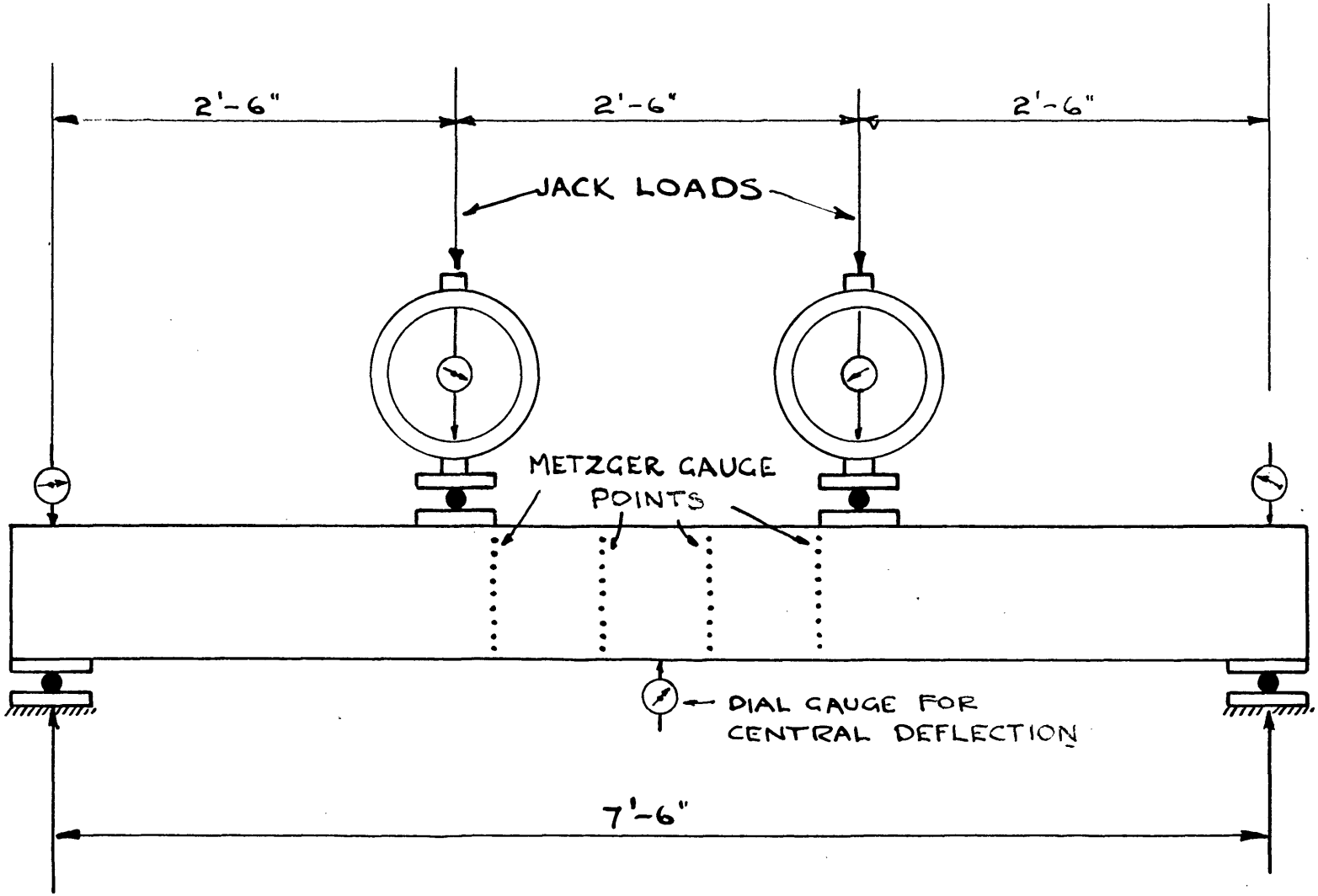
2'-6"
2'-6"
2'-6"
JACK LOADS
METZGER GAUGE POINTS
DIAL GAUGE FOR CENTRAL DEFLECTION
7'-6"

FIGURE 2.10

Similar methods can be used in testing bonded pre-stressed beams having 5mm. or 7mm. diameter wires. As the stresses are inferred from the total strain measurements, errors are introduced here if the creep is significant. In the case of bonded pre-stressed beams using 2mm. diameter wires (which are too thin to permit of the attachment of gauges) the only method of estimating the steel force appears to be by inference from the concrete strains on the assumption that there is no slip. With non-bonded wires the steel force can be obtained by the insertion of a dynamometer between the cable anchorage and the end of the beam. Two types of dynamometer, both on the same principle, have been in use in the Civil Engineering Department at Imperial College. The first was devised by Lao (15). A modified version used in the tests described here is indicated in figure 2.11. It consists of a duralumin tube with electrical resistance strain gauges stuck along two diametrically opposite generators. The two gauges, which are connected in series, give the mean strain which is independent of the eccentricity of loading. The instrument is calibrated by measuring the change in resistance due to a pre-determined load.

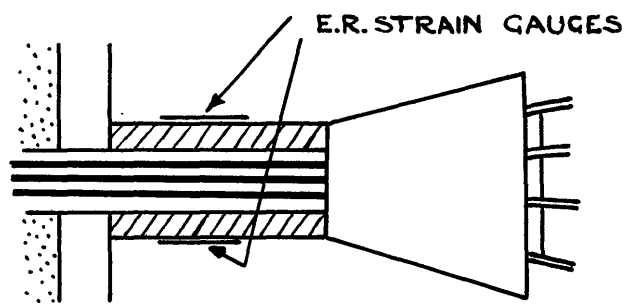

Figure 2.11

(d) The actual position of the reinforcement in the beam should be checked at the section of failure after the beam has been broken as it is easy for the reinforcement to be displaced relative to the shuttering during casting. This check is particularly desirable when beams of small section are used.

(e) In the tests with which the writer has been associated the concrete strains have been measured with a Metzger gauge (see ref. 4 for description). This gauge is not fixed in one position but is demountable and is used for measuring strains over a number of independent gauge-lengths. It is in fact used for measuring strains at all the gauge stations indicated at the centre section of the beam in figure 2.10. The demountable gauge is certainly less accurate than a fixed gauge but it has the advantage that strains can be recorded at a far greater number of gauge stations than would otherwise be possible. It is much more satisfactory to have a large number of fairly accurate readings than to rely on a few readings of supposedly high accuracy. In any case the Metzger gauge is sufficiently accurate for the measurement of bending strains since an experienced operator can guarantee that 95% of his readings will be accurate to a strain of $\pm$ 12.5 x 10^{-6} or a stress of approximately $\pm$ 50 lb. per square inch.

We have left out of account the possibility of using electrical resistance strain gauges for the measurement of the concrete strains. It is the opinion of the author that this type of gauge should, if possible, be avoided for this purpose. Not only are they far more trouble to fix than the mechanical gauge but drift phenomena are particularly troublesome when electrical resistance gauges are attached to concrete. Claims have been made that drift can be eliminated, but from his own experience and from observation of other people's work it appears to the writer that the use of resistance gauges on concrete provides a continuous source of difficulty. Their use on concrete should, therefore, be restricted to places which are inaccessible to the Metzger (or similar) gauge or where stress variations are such that the use of a long gauge-length is not permissible. Even so a very short gauge-length should not be used as strain variations due to local irregularities are recorded rather than the average strain condition (16).

Referring to figure 2.10 it will be seen that three gauge lengths are indicated in the centre span where the bending moment is nominally constant. It has been found that the provision of a single central length is inadequate as the failure is generally localised and it is necessary to provide gauges at a number of sections in order to ensure that the crushing zone is covered.

Figure 2.12 gives a typical example of the variation in strain obtained at the three sections.

THE CHECKING OF TEST DATA.

One of the major problems in testing pre-stressed concrete beams is in the making of an accurate assessment of the steel force. With grouted beams the difficulty arises because of the lapse of time which must take place between pre-stressing and testing. During this period there is a loss of steel stress due to creep and shrinkage. Electrical resistance strain gauges attached to the steel cannot give a useful estimate of this loss for two reasons: Firstly because resistance gauges are unreliable for long period tests and secondly because the strains even if accurately recorded would include the creep strains of the steel. Thus, whilst strain gauges attached to the steel may give the strain changes which take place during the course of a test the initial stress in the steel must be a doubtful quantity.

With non-bonded beams use of the Lao type dynamometer gives a fair estimate of the cable force if the cable is straight. If there are bends in the cable friction can cause the steel force at the centre of the beam to be different from that recorded at the ends.

FIGURE 2.12.

VARIATION IN STRAIN WITH GAUGE POSITION

BEAM Nº II

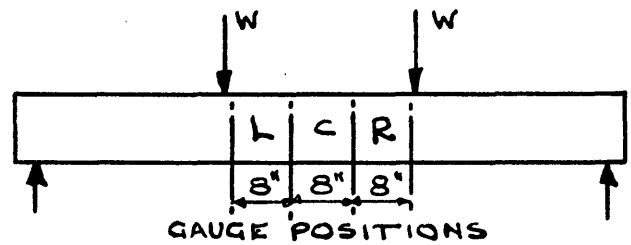

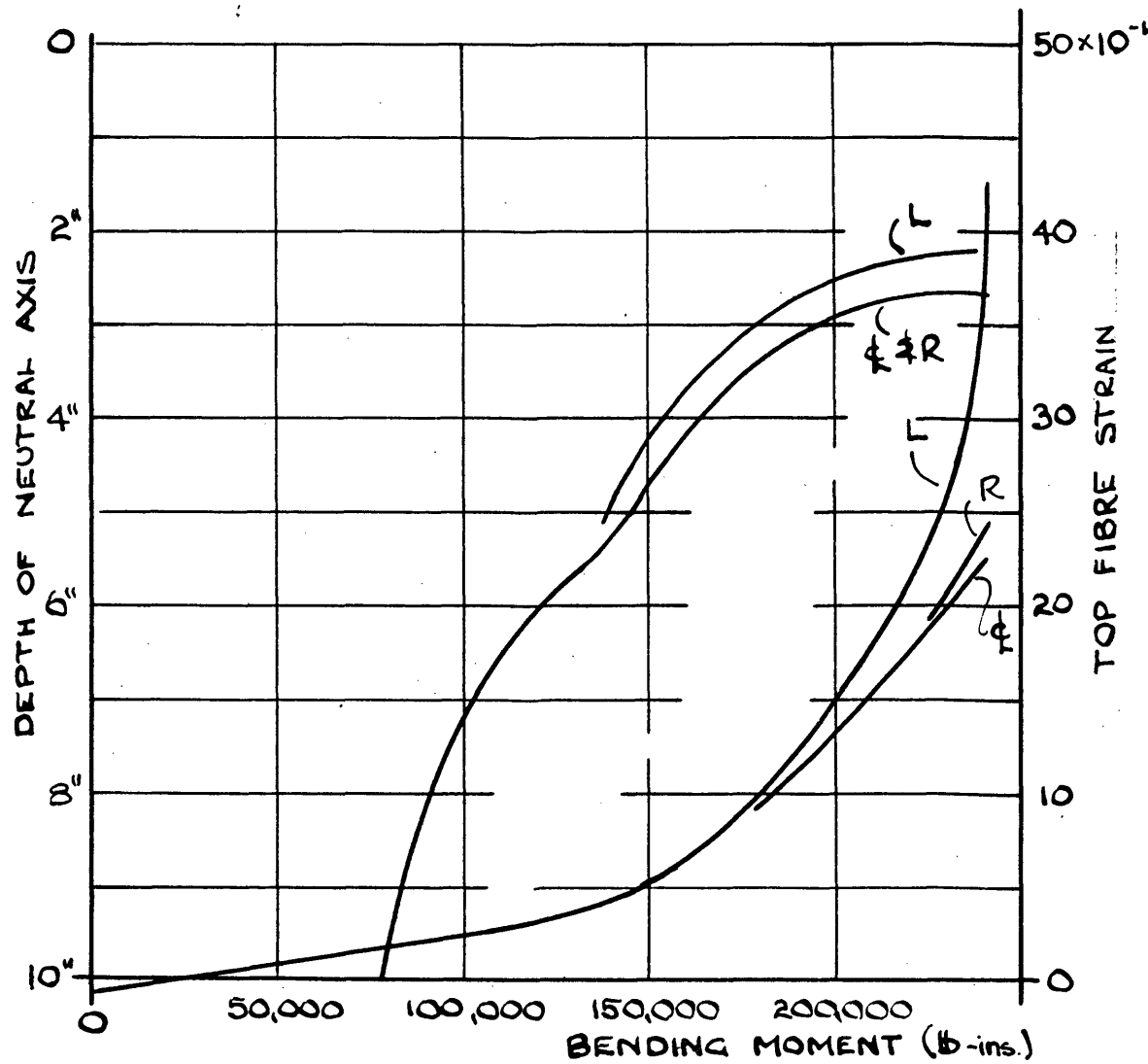

In the light of these observations the author considers that it is vital to apply a cross-check to verify the steel force. He has used two simple checks which enable this to be done.

THE ASSESSMENT OF THE STEEL FORCE IN PRE-STRESSED BEAMS.

METHOD I.

The deflection readings are used to effect this check. Such readings are taken with dial gauges situated at the ends and centre of the beam, as indicated in figure 2.10, whilst the beam load is increased until the cracking load has been passed and the presence of the tensile cracks verified. The beam is then unloaded and reloaded. The load-deflection curves obtained from such a procedure during an actual test are given in figure 2.13 to which the reader is now referred. It will be seen that the curve obtained on the second loading follows the first curve until point 'A' is reached where a discontinuity occurs in the second curve. This discontinuity is due to a change in the effective stiffness of the beam as the cracks, already formed during the previous loading, start to re-open. As the bending moment is increased the original curve is rejoined when the load reaches the maximum value attained in the previous loading.

The focus of interest is on point 'A'. At this stage when the cracks start to reopen the stress distribution can reasonably be assumed to be triangular as in figure 2.14 (Assuming that there is no plasticity, and this will be the case if the design is a practical one).

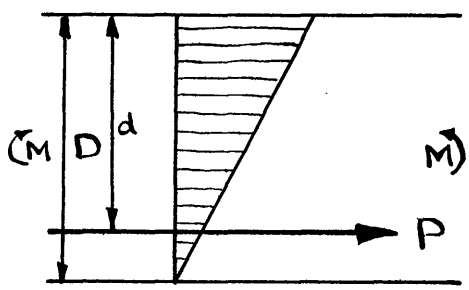

Figure 2.14

The bending moment at stage 'A' is read from figure 2.13. At This stage the centre of compression of the concrete stress is known to be D/3 from the top surface of the beam.

Equating the moments acting on the concrete we obtain,

$$P = M.(d - D/3)^{-1} \qquad (2.10)$$

Hence the steel force P is determined.

If there is a lapse of time between pre-stressing and testing the elastic strains in the concrete are unknown at zero load, due to creep, loss of pre-stress, etc., and these must be computed to enable the total strains in the concrete to be determined since strain readings will generally be taken relative to the 'zero-load' values unless the pre-stressing and testing are done on the same day. The initial concrete strains can only be calculated if the steel force and Young's modulus are known. We have seen how the steel force may be obtained. The same load-deflection curve can be used to determine the modulus of elasticity.

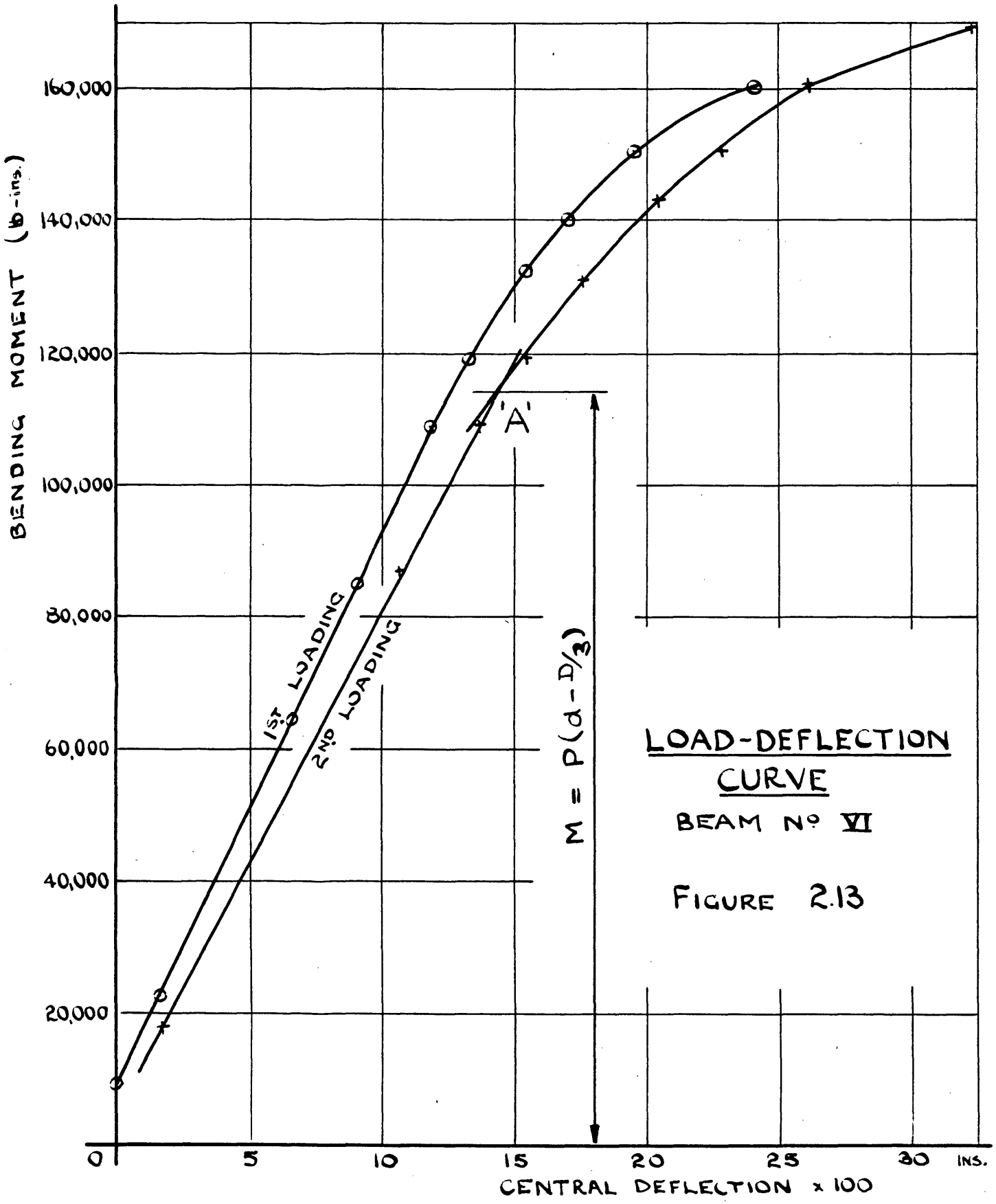

LOAD-DEFLECTION CURVE

BEAM Nº VI

FIGURE 2.13

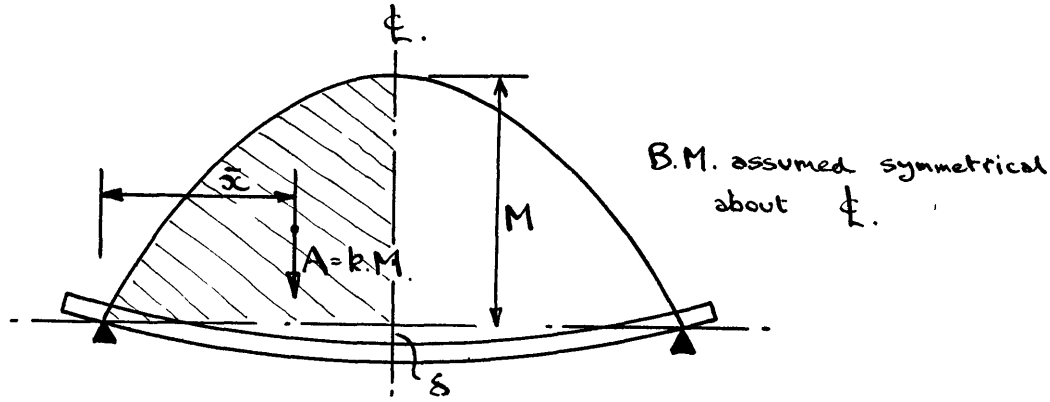

Figure 2.15

For a symmetrically loaded beam the central deflection is given by

$$\delta = \frac{1}{EI} \times k.M\bar{x}$$

thus

$$E = \frac{I}{k.\bar{x}} \quad x(\text{slope of moment deflection curve}) \qquad (2.11)$$

Knowing both P and E it is now a simple matter to compute the 'zero-load' strains due to self weight and pre-stress alone.

METHOD II.

The second method of checking the steel force is not so wide in application as the deflection method in that it can only be used if the elastic strains due to pre-stressing are known. That is to say its use is restricted to those tests in which the loading follows immediately on pre-stressing so that the concrete strains are measured relative to the unstressed state.

In fact the member is nearly always stressed due to its own weight but for the purpose of this check these strains must be excluded. The second method is given because in the case where it is applicable it provides an independent check on the Young's modulus in addition to giving the steel force.

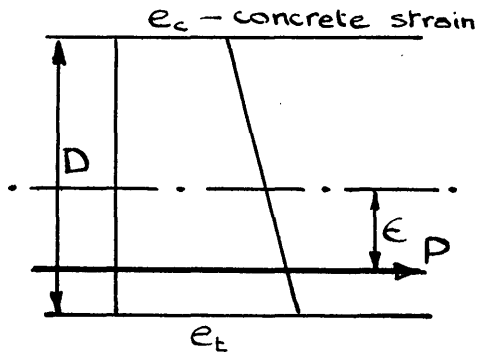

Figure 2.16

The pre-stressing force, applies a bending moment to the beam by virtue of its eccentricity. This moment curves the member.

It is fundamental to pre-stressed concrete that this curvature is counter to that produced by the loads applied to the beam. Thus if the loading is applied gradually there is a stage when the beam is once again straight, at any section chosen for consideration. At this juncture the external bending moment M must equal the pre-stress moment P.ϵ. Thus if this value of M can be determined P is immediately calculable.

It is easy to show that the radius of curvature of the beam is given by $D/(e_c - e_t)$, where e_c and e_t are the concrete strains as indicated in figure 2.16. When the beam is straight $(e_c - e_t) = 0$.

The external moment M plotted against $(e_c - e_t)$ gives a straight line provided that the moment is not large. This line cuts the moment axis such that the intercept gives the moment which is just sufficient to counteract the curvature due to pre-stressing. Hence the steel force, P, is determined. Results from an actual beam test are plotted in figure 2.17.

It is readily seen that the slope of the line, $\frac{\Delta M}{\Delta(e_c - e_t)}$, equals EI/D. This determination of E is independent of the deflection method of obtaining this quantity and it is possible that the two methods may give differing values. The reason for this, assuming that no grave error is revealed, is probably due to the deflection method giving an average value of E for the whole beam whereas the strain method derives E at a specific section.

DERIVATION OF STEEL FORCE IN A BONDED BEAM UNDER ULTIMATE CONDITIONS.

The methods given in the preceding pages provide a check on the steel force at the cracking moment. In a non-bonded beam the steel force can be kept under constant observation by means of a dynamometer is inapplicable. If the reinforcement is 5 mm. in diameter or larger electrical resistance strain gauges can be fixed to the steel before casting the beam.

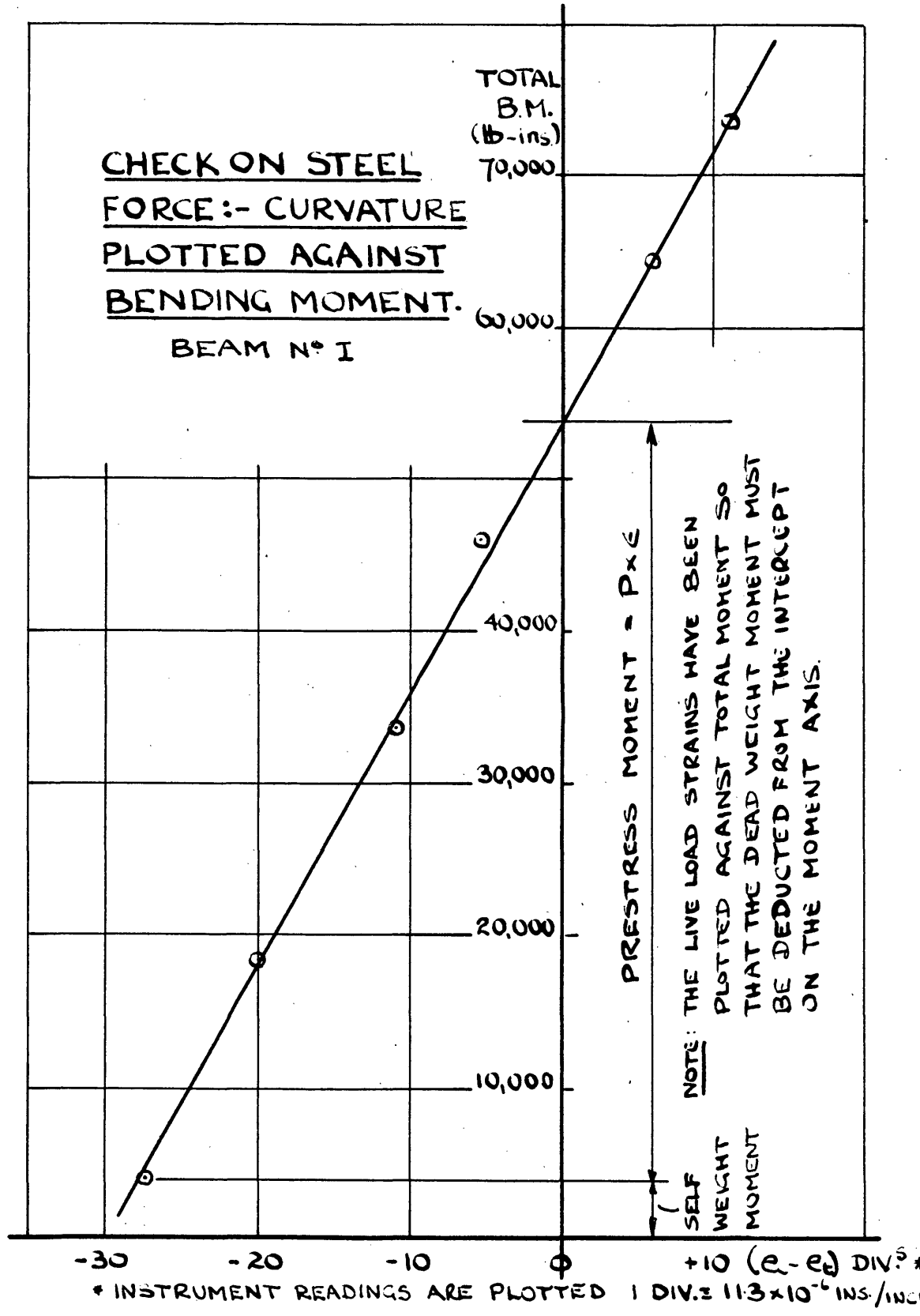
CHECK ON STEEL FORCE:- CURVATURE PLOTTED AGAINST BENDING MOMENT.
BEAM Nº I
TOTAL B.M. (lb-ins)
70,000
60,000
40,000
30,000
20,000
10,000
PRESTRESS MOMENT = P×e
SELF WEIGHT MOMENT
NOTE: THE LIVE LOAD STRAINS HAVE BEEN PLOTTED AGAINST TOTAL MOMENT SO THAT THE DEAD WEIGHT MOMENT MUST BE DEDUCTED FROM THE INTERCEPT ON THE MOMENT AXIS.
-30
-20
-10
0
+10 (e-e0) DIVS *
* INSTRUMENT READINGS ARE PLOTTED 1 DIV. = 113×10⁻⁶ INS./INCH

FIGURE 2.17

Such gauges frequently fail to operate properly and in the case of high tensile steel wire interpretation of the strains in terms of stress is difficult for it has been shown that the stress-strain curve is very much dependent on the rate of loading. It is hardly possible to stick resistance gauges to 2 mm. diameter wire.

When it is impractical to attach gauges direct to the reinforcement of a bonded beam the steel force must be estimated by inference from the concrete strains on the assumption that there is no slip between the steel and concrete. Not only is it difficult to obtain a good estimate of the stress from the strains but there is almost certainly slip between the steel and the concrete as failure becomes imminent (Baker suggests an F of 0.85 for bonded beam) and frequently slip occurs at lower loads. Thus in the case of bonded beams a correct assessment of the steel force is very difficult to obtain. Unfortunately, if the test is carried out with the object of determining the constants is, say, Baker's theory (4) the value of these constants depends almost completely on knowing the actual steel force. Using Baker's symbol's:-

$$\frac{M_u}{bd^2} = n(1-\gamma n)(\alpha c') \qquad (2.12)$$

and

$$\frac{T_u}{bd} = n.(\alpha c') \qquad (2.13)$$

where M_u and T_u are the bending moment and steel force at failure. δ and n which give the centre of compression and the position of neutral axis are as already used in figure 1.1. c' is the top fibre stress and α is a shape factor for the stress-strain curve. (α c') has the dimensions of stress and it is not necessary to separate the two components.

Assuming that the test has been carried out with the object of determining (α c') and δ it can be seen from the above equations that M_u, n and T_u are all required. For small values of n, δ can be guessed and (α c') can be calculated with fair accuracy from (2.12). If this is done (2.13) can be used to calculate T_u which can be compared with the value calculated from the strain measurements thus enabling the F factor to be computed. This process is clearly somewhat make-shift and it is far better to try to obtain the actual T_u by some other means. In any case for low position of the neutral axis i.e. large n, the value of (α c') determined from (2.12) will depend upon the guessed value of δ to a significant extent.

USE OF AUTHOR'S ANALYSIS TO DETERMINE STEEL FORCE.

The analysis given on pages 20 to 24 can be used as a check on the steel force.

The stresses in top and bottom fibres of a concrete beam are given by the two equations:-

$$f_c = \frac{1}{bd^2}\left[\frac{1}{(e_c-e_t)}\frac{d}{de_c}\left\{(M + P\overline{d-d'})(e_c-e_t)^2\right\} + P.d\,\frac{de_t}{de_c}\right]$$

$$f_t = \frac{1}{bd^2}\left[\frac{1}{(e_c-e_t)}\frac{d}{de_t}\left\{(M - Pd')(e_c-e_t)^2\right\} + P.d\,\frac{de_c}{de_c}\right]$$

It has been pointed out on p.18 that the second equation is really a check equation for once the beam has cracked f_t is obviously zero. If, as in the case of beam II, this is not the case an error is present. On the basis of the reasoning in the past few pages the steel force is the most likely source of any significant error. Provided that this is the case the above equations can be used to calculate the actual steel force.

The method is best explained with the aid of an example: On page 63 the author's analysis is applied to data obtained from a test to destruction on a pre-stressed concrete beam. The beam was made as identical as possible to that described on page 23 except that the pre-stressing cables were grouted after tensioning. 2 mm. diameter wires were used for the reinforcement so that direct measurement could be made of neither the steel force nor strain. The steel force tabulated in the second line of the table was obtained on the assumption that there was no slip between the concrete and steel.

DETERMINATION OF STRESS-STRAIN CURVE FOR BEAM NO. II

1	$M/bd^2=m$	0	40	104	168	222	275	295	363	408	440	464	479	488	489	490
2	$P/bd^2=p$	332	333	350	355	363	380	396	509	647	696	857	908	945	947	949
3	$e_c \times 10^{-4}$	-0.6	0	1.0	2.0	3.0	4.0	5.0	10	15	20	25	30	35	40	45
4	$e_t \times 10^{-4}$	2.4	1.8	0.7	-0.3	-1.7	-3.5	-6.2	-25	-47	-67	-87	-105	-124	-143	-161
5	f_c	-260	-20	+380	770	1220	1630	2210	3260	3640	3900	3880	3480	3220	2960	2930
6	f_t	860	650	320	25	-150	-220	-71	51	216	351	704	549	510	415	415
7	f_c							2730	3450	3770	3890	3680	3350	3090	2950	
8	$f_c.\delta e_c \div 1000$							13.7	17.2	18.9	19.4	18.4	16.8	15.4	15.0	
9	$\int f_c de_c \div 1000$							4.5	18.3	35.5	54.4	73.8	92.2	109	124	139
10	p'							406	526	571	624	662	682	686	680	678
11	f_c'							2210	3150	3700	3790	3830	3710	3550	3410	3400
12	p''							406	519	566	618	652	677	691	694	700
13	f_c''							2210	3160	3770	4030	4130	4100	3970	3830	3760
14	p'''							406	520	570	618	663	700	722	738	746
15	f_c'''							2210	3170	3690	3820	3880	3780	3620	3410	3310
16	p''''							406	520	568	618	657	682	698	703	703
17	f_c''''							2210	3170	3700	3820	3850	3740	3600	3470	3380
18	f_t''''								10	-26	5	9	15	11	-13	-21

It can be seen from line 6 that some considerable error must be present as the numerical value of the calculated tensile stress approaches 20% of the value of the compressive stress when in fact it is known to be zero. If f_t is assumed to be zero the first of the above equations can be reduced to

$$f_c = \frac{1}{bd}\frac{d}{de_c}\left[P(e_c - e_t)\right]$$

Integrating

$$\int_{e_t}^{e_c} f_c \, de_c = \frac{P}{bd}(e_c - e_t)$$

or

$$p = \frac{P}{bd} = \frac{1}{(e_c - e_t)}\int_{e_t}^{e_c} f \, de \quad *$$

The integral term represents the area under the stress-strain curves. Since f_c has been obtained for a succession of e_c's, $\int_{e_t}^{e_c} f \, de$ can be evaluated for the same e_c's

All quantities have been plotted for regular intervals of e_c so that it is simple to evaluate the integral in a table. This is done in lines 7-9 on page 63. p is given in line 10. If this is compared with line 2 it can be seen that there must have been a fair amount of slip, for at failure p is 678 compared with 949 calculated on the no-slip assumption.

* Note:- This expression can be derived quite simply by saying that the tensile force in the steel must equal the total compressive force in the concrete.

As P is now amended f_c must be recalculated, line 11. It is not necessary to recalculate f_t at this stage; it is simpler to evaluate the new p. This is used to obtain a further value for f_c and the process is repeated until f_c and p cease to vary with each iteration. In line 17 f_c is deemed to have reached a sufficiently stable value. As a check, f_t is now calculated and it is seen in line to be negligible.

One point requires a little elaboration: It will be noticed that the area under the stress-strain curve is evaluated between the limits e_c and e_t. This means that the whole of the shaded area given in the adjacent figure must be summed algebraically. The first calculation of the stress-strain curve leads to curve ABCOD. We know that section AB is incorrect (there can hardly be compressive stress in a region cracked in tension) so that in evaluating the intregral the curve A'BCOD is used. That means that we assume section BCO to be correct. No other course is open for the method of checking the steel force just described is only legitimate as long as the concrete is cracked.

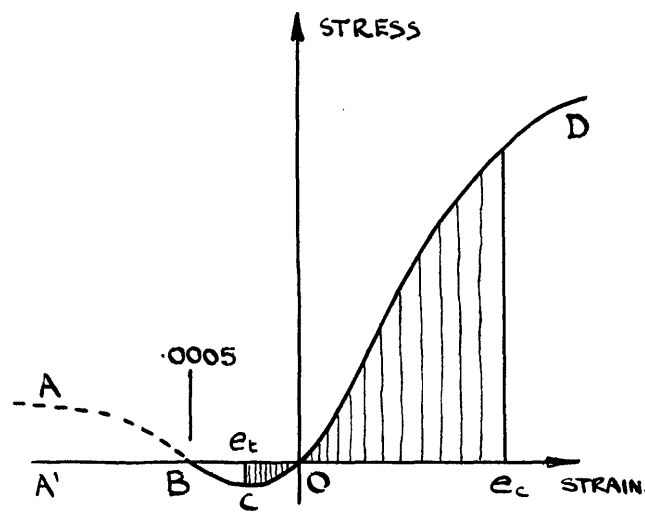

Figure 2.18

In any case the value of the steel force up to the cracking stage should be known as bond failure is hardly likely to occur before cracking. It is assumed that the checks described previously (pp. 51-58) have been used to check the steel force up to the cracking stage. If these checks fail badly the results of the test are of little value.

The resultant stress-strain curve from this test is plotted in figure 2.19 where it is compared with the original curve obtained before correction of the steel force.

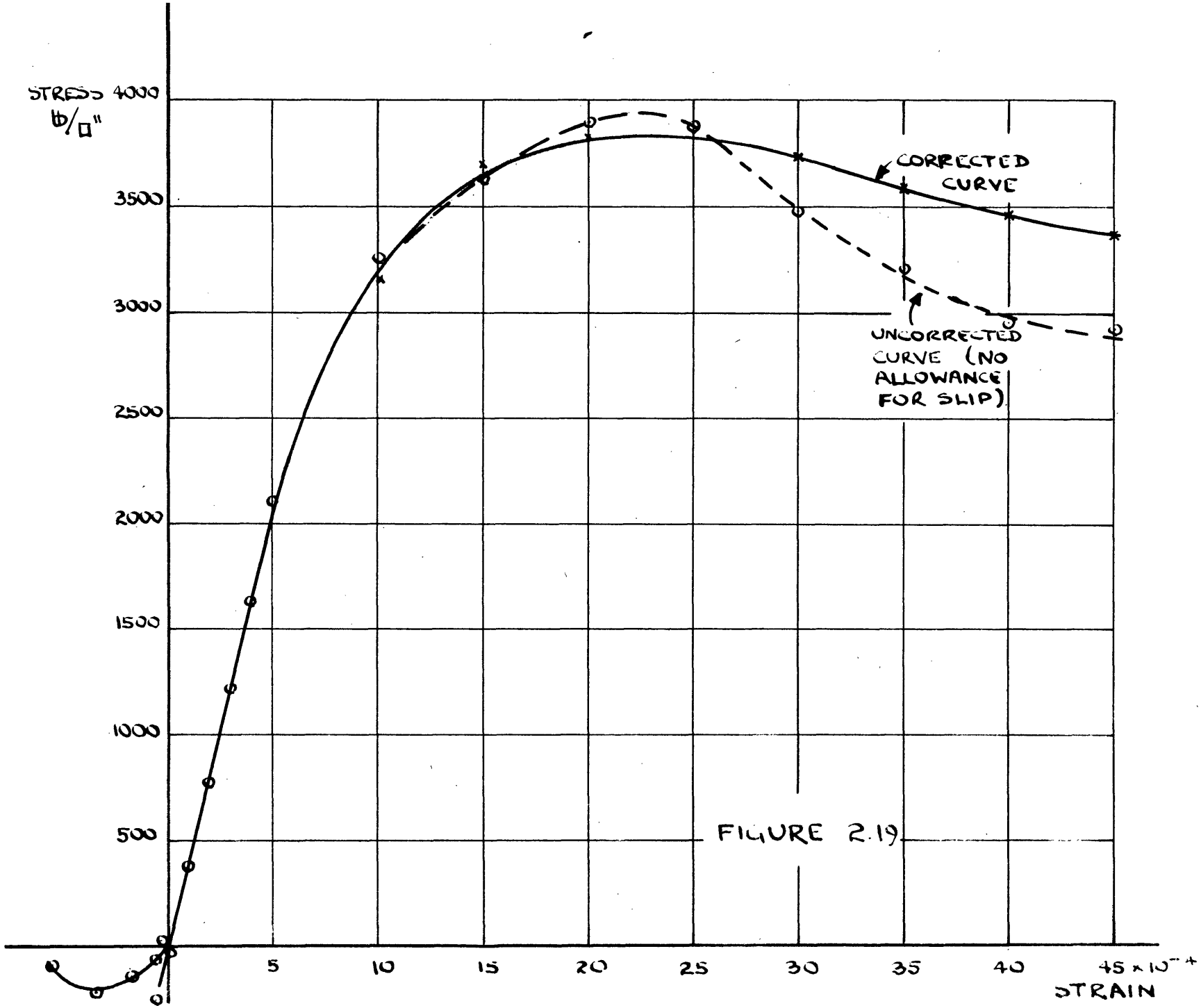
STRESS lb/□"
4000
3500
3000
2500
2000
1500
1000
500
0
5
10
15
20
25
30
35
40
45 x 10⁻⁶
STRAIN
CORRECTED CURVE
UNCORRECTED CURVE (NO ALLOWANCE FOR SLIP)

FIGURE 2.19

II Chapter 4. RESULTS OF TESTS ON A NUMBER OF PRE-STRESSED CONCRETE BEAMS.

ACKNOWLEDGMENT

The tests considered in this chapter were carried out by the D.S.I.R. group in Concrete Technology under the direction of Professor A.L.L. Baker B.Sc.(Tech.), M.I.C.E., M.I. Struct.E. at the Imperial College of Science and Technology, S. Kensington, London. The author, a member of the group when the tests were made, wishes to thank Professor Baker for permission to use the results.

GENERAL DESCRIPTION OF BEAMS TESTED

In this chapter the author uses his analysis to determine the stress strain curve for the concretes used to a series of six pre-stressed beams. The original object of the tests was to provide a direct comparison of the strength of beams having a normal, high, and very high pre-stress (in terms of concrete stress) and between those having the same pre-stress but which differ by their being either grouted or non-bonded.

Beams I - IV were all nominally 5 inches wide and 10 inches deep having an effective depth of 8 inches. Beams V and VI were 5 inches wide by 7 inches deep and had an effective depth of 5 inches. All beams had an overall length of 8 feet.

Precise details of each beam will be given as each one is considered.

All beams were cast in the same timber shuttering. Beams I-IV were hand rammed whilst beams V and VI were vibrated externally.

The beams were all post-tensioned by cables consisting of a number of 2 mm. diameter high tensile steel wires. The general disposition of the cables

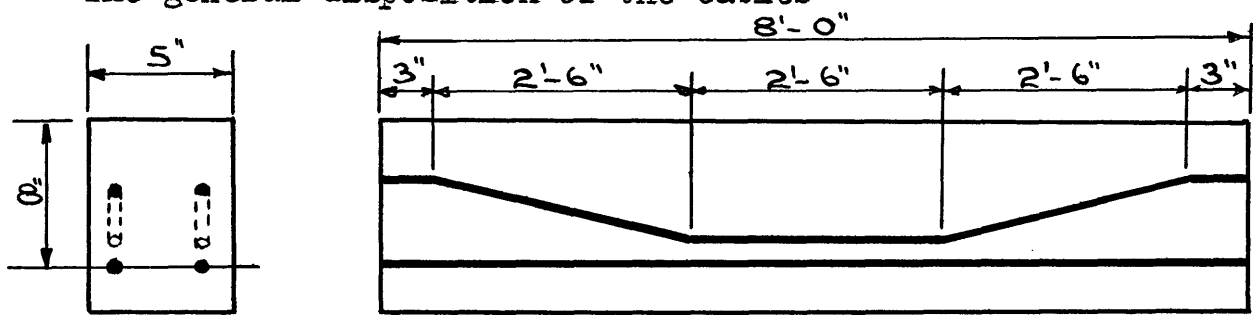

Figure 2.20

is given in figure 2.20. The holes through which the straight cables were passed were formed by means of a length of Bunsen tubing held rigid by a steel bar passing through it. With the bent-up cables it was not possible to use a steel bar so to prevent the tube being crushed a rope core was used. The tubing was held in position by binding wire.

The method of anchoring and prestressing the cables was designed by members of the D.S.I.R. group and is indicated in figure 2.21.

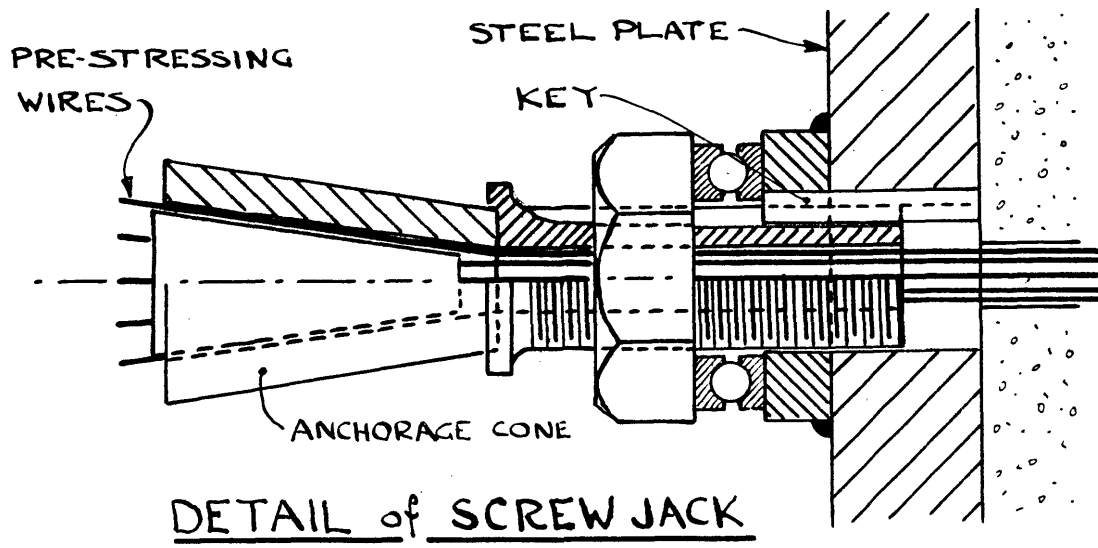

Figure 2.21

EXPERIMENTAL TECHNIQUE

As a general rule the technique and checks described in II Chapter 3 have been applied in all the tests although some of the methods were developed as the experiments progressed.

Four-point loading was used as shown in figure 2.10. In all beams strain readings were taken over the three gauge lengths indicated in the figure. In the following pages the author applies his method of analysis to each beam and where the strain distribution varies with the position, the stress-/

stress-strain curve will be determined for all three sections of each beam. Where circumstances warrant it the steel stress figures are amended in the manner suggested at the end of the last chapter. The original experimental data from which the concrete stress-strain curves have been deduced, is summarized in Appendix 2.2.

BEAM No. I.

Concrete 1:1:1½ by weight. Water cement ratio 0.4.

Average cube strength 6,900 lb/sq.in.

Reinforcement - 4 cables each consisting of 8 high tensile steel wires 2 mm. diameter. Non-bonded.

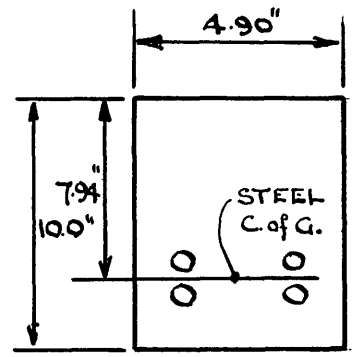

Figure 2.22

This beam has already been analysed to a certain extent on pages 17 to 22, where the stress strain curve is evaluated for the centre section.

The stress strain curves for the other two sections, L and R, are plotted with the curve obtained at the centre section in figure 2.23. In each case the f_t values for the cracked beam are 'zero' thereby verifying the steel force.

It will be seen that there is remarkable agreement between the figures obtained for the left-hand and centre sections.

Note that this is despite the fact that the strains recorded were much higher in the latter section. It appears odd that the maximum strain at the centre section should be 30% greater than that in the left-hand section when both are subjected to the same moment and when the concrete in the two sections appear to be identical in deformation properties. The reason is quite simple; the first crack opened in the centre section and the neutral axis was always higher there than in the other two sections, so that with the smaller compression zone the compressive stress, and hence strain, was also higher there.

Crushing actually occurred at the junction of the left-hand and centre sections. The stress strain curves indicate the reason for this: the concrete in the right-hand section is shown to be stronger.

BEAM No. II

Except that the cables were grouted after pre-stressing and that the cube strength was 7,300 lb/sq.in. beam II was the same as beam I.

BEAM No. I

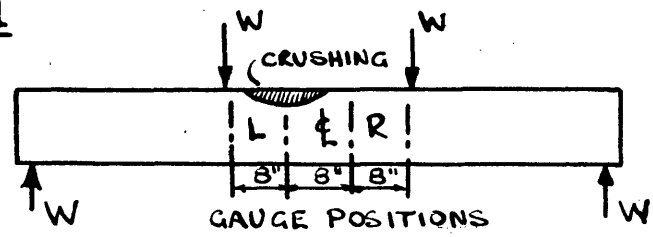

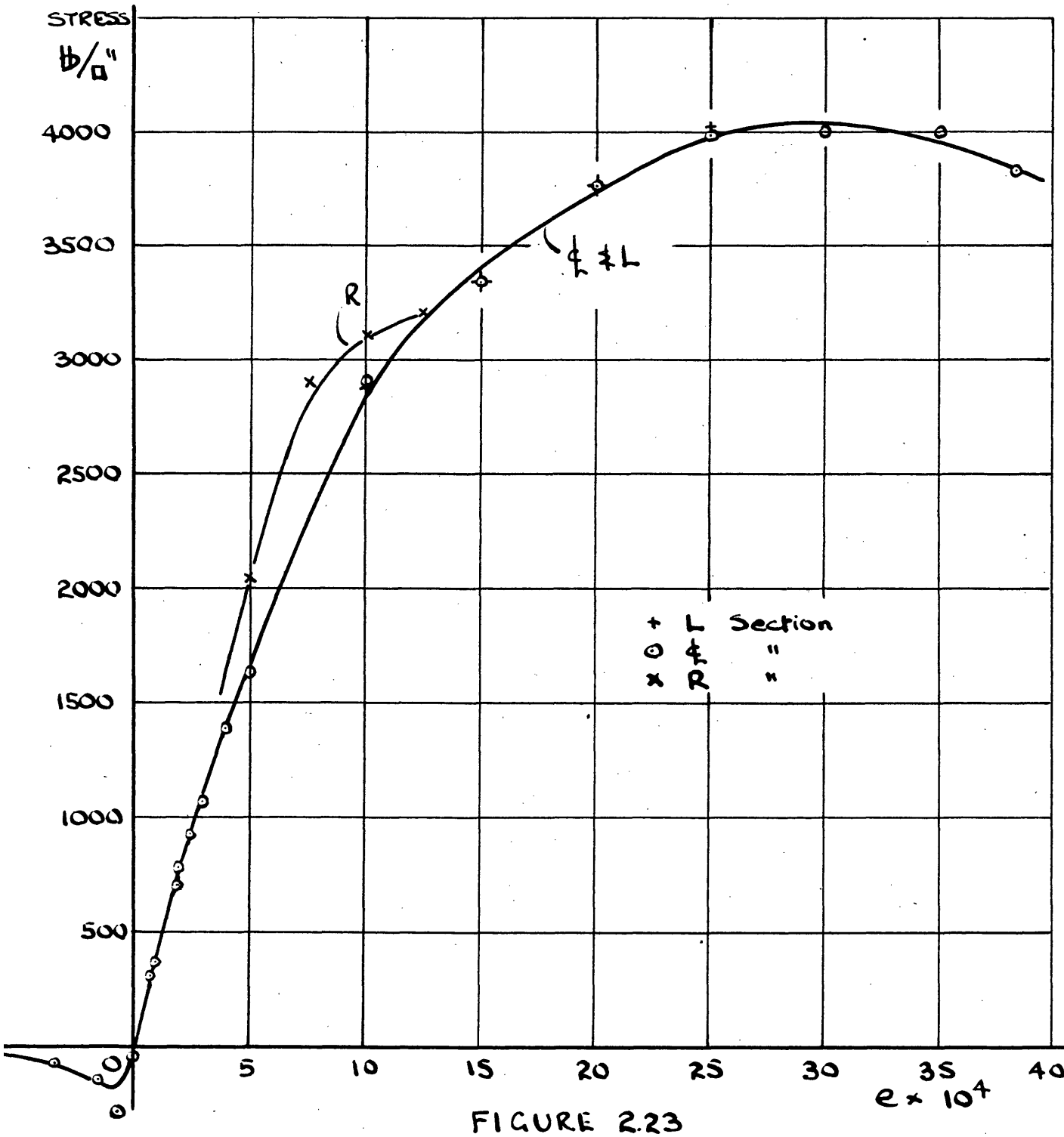

FIGURE 2.23

The difficulty of obtaining the steel force in a grouted beam has already been stressed. In analysing the results obtained from this beam it was assumed in the first instance that there was no slip between the steel and concrete and was calculated on that basis. As is shown in the table on page 63 this leads to impossible values for f_t. In the same table the method of correcting the steel force is elaborated and figure 2.19 shows the effect of steel force correction on the stress strain curve.

The same process has been effected with the data obtained from the left-hand gauge length. In figure 2.24 the corrected stress strain curves obtained from both the left-hand section and centre section are compared.

The figures for the right-hand section agree so well with those obtained from the centre section that it is impossible to distinguish the separate curves. For this reason the results from this section have been omitted.

The results are interesting because failure appears to have occurred in the region where the concrete is slightly stronger although the difference between the two curves is slight. Once again the neutral axis is higher at the section of failure and the reason appears to be that slip was slightly more severe at this section.

This can be seen from figure 2.25 where the original and corrected steel force curves are plotted. At first sight it appears strange that the corrected curve which is supposed to correct for slip should give a steel force which is initially higher than the uncorrected value. The reason for this is as follows:-

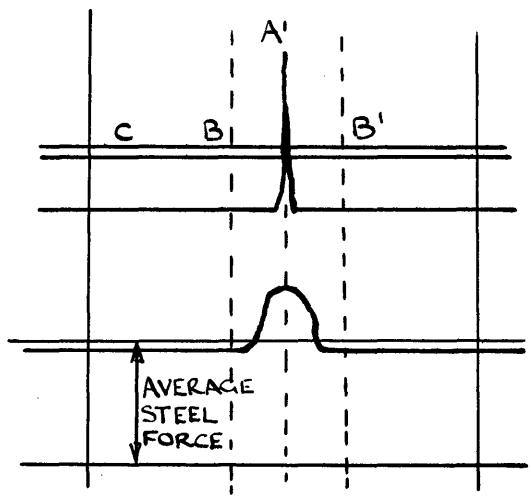

Figure 2.27.

The wire is not likely to slip throughout its length the moment that the first tensile cracks appear. Refering to figure 2.27, assume that the crack has just formed. At section A all the tensile load is correct in the steel. At section C some of the tensile load will be in the steel and some in the concrete. Thus the steel force will be higher at A than at C. This means that between A and C bond stresses must be operative. These stresses will be a maximum at the crack and will diminish towards C and provided that the ultimate bond stress is not reached slip will not occur. It is clear that a certain amount of slip must occur, (otherwise the steel in the gap would be strained infinitely) say as far as B and B'. Over the length BB' the steel force will be above the average value given by the strain measured over the whole gauge length.

BEAM No. II

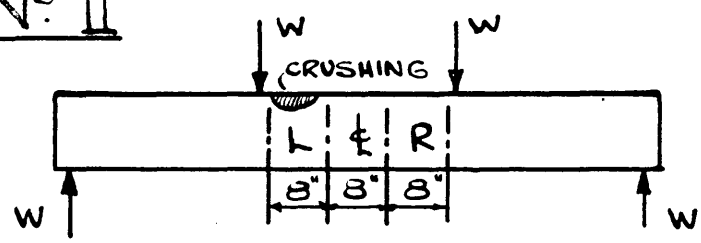

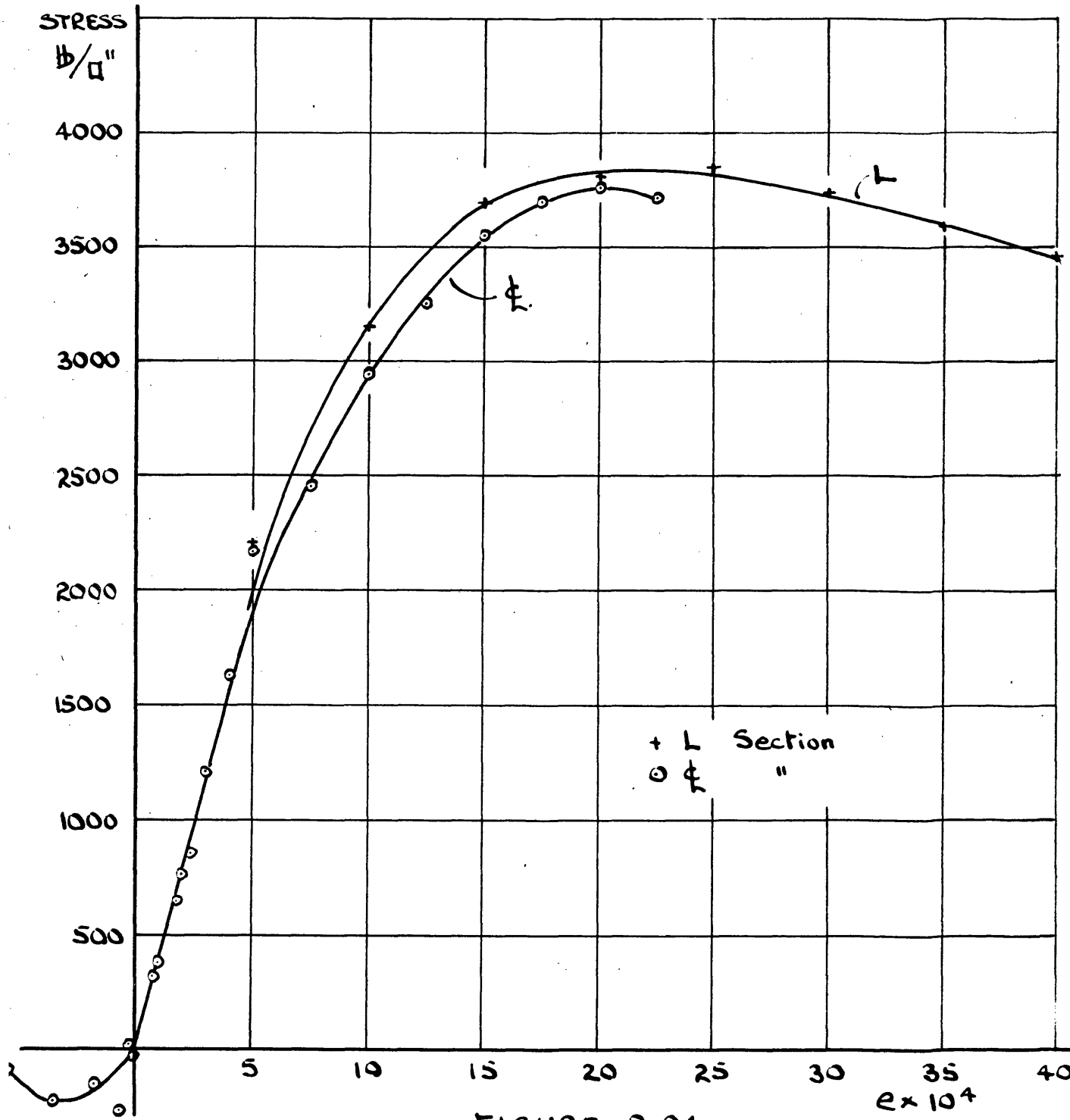

FIGURE 2.24

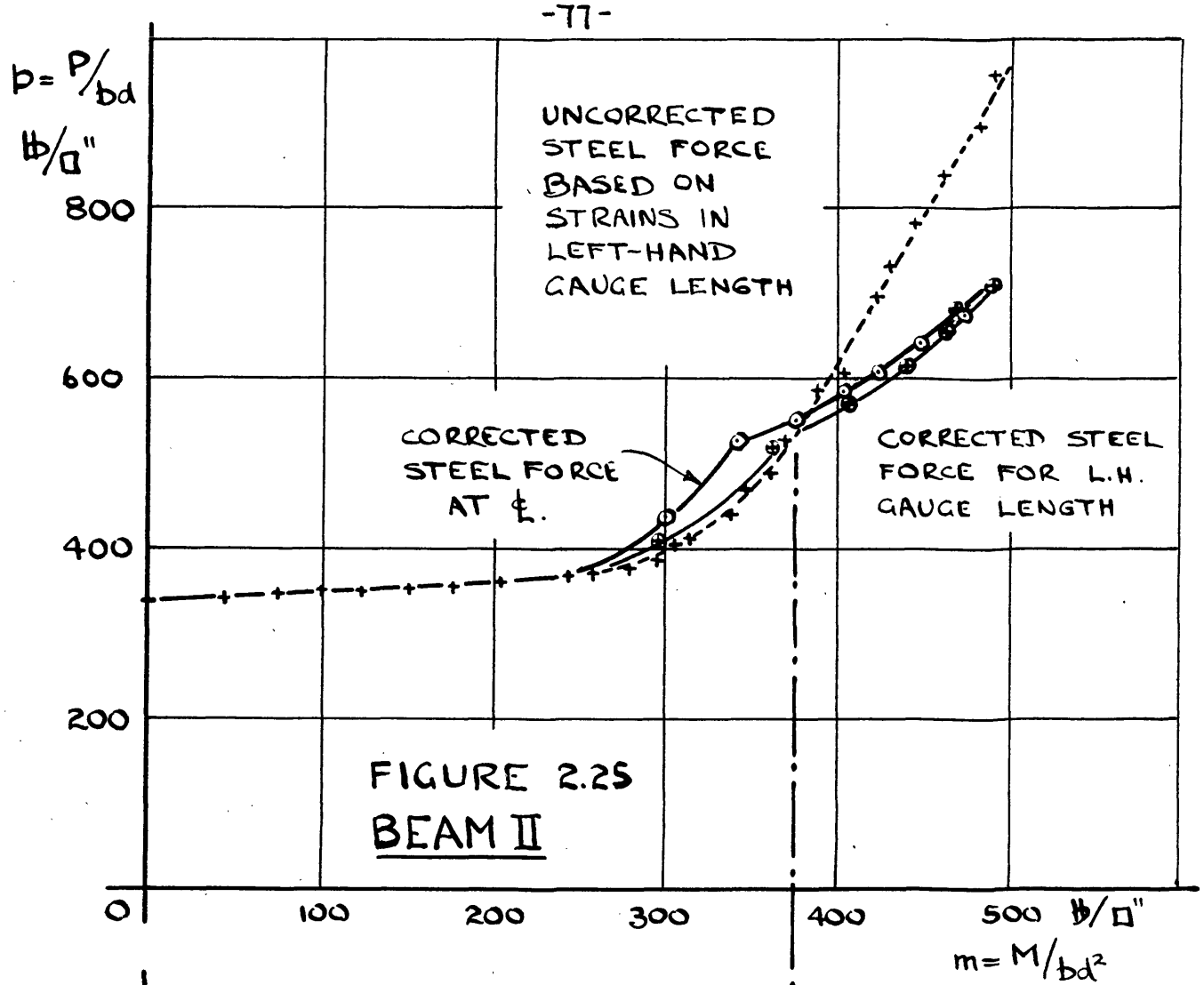

FIGURE 2.25
BEAM II

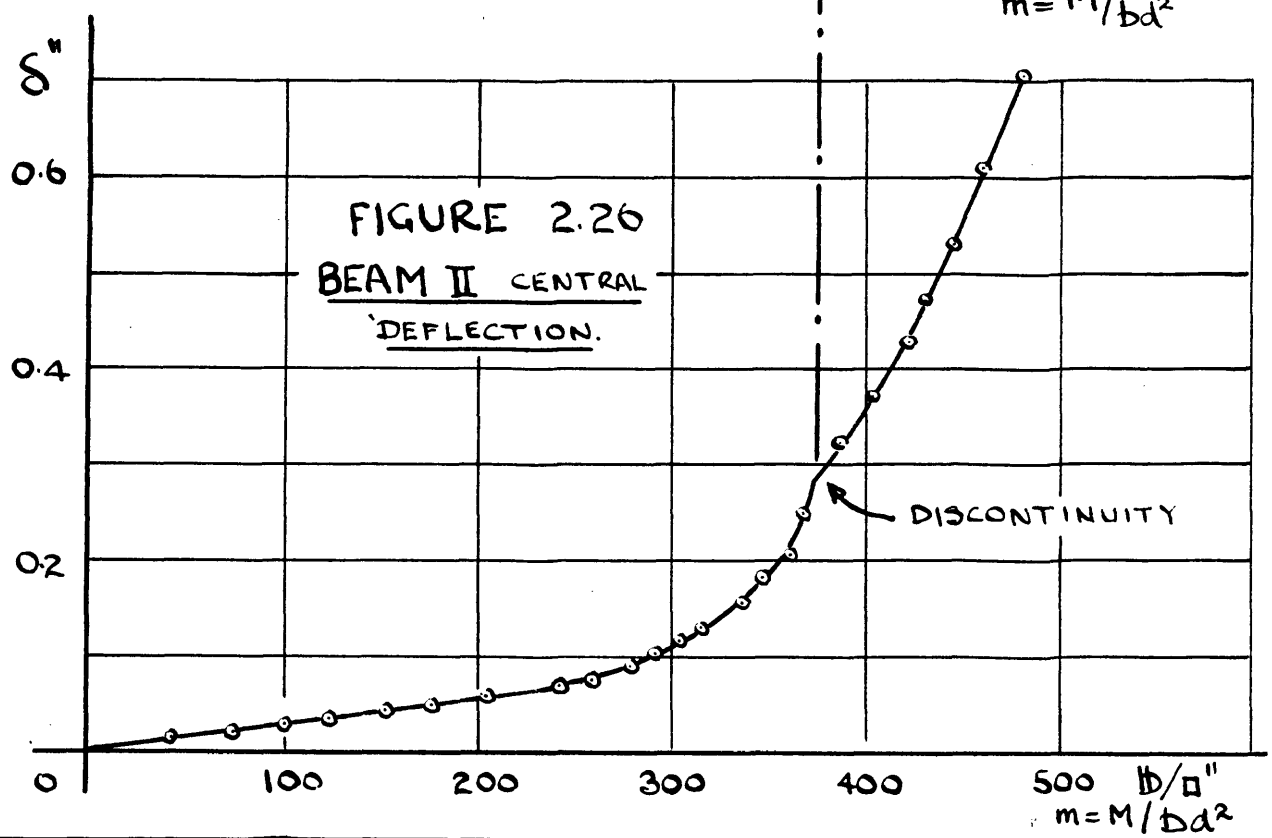

FIGURE 2.26
BEAM II CENTRAL DEFLECTION.

This explains why the corrected steel force (calculated on assumption that the concrete carries no tensile stress) is greater than that calculated on the basis of the strains over the whole gauge length. As the load is increased point B moves towards C and the next crack and eventually slip occurs right through from crack to crack. If the beam were subjected to a uniform bending moment throughout the whole of its length the corrected and uncorrected steel force curves would coincide for all further increases of bending moment. In the case of the beams analysed here the bending moment tapers off outside points L, as in figure 2.28, and slips into the centre section from the ends of the beam and the actual steel force falls below that calculated on the no slip assumption. Under these conditions there can be but very little difference in steel force from point to point over the length of beam subjected to the uniform bending moment. This is verified by the data given in figure 2.25 which shows that although the steel force in two gauge lengths differs somewhat in the transition stage from initial cracking to full slip, there is little difference once full slip is established.

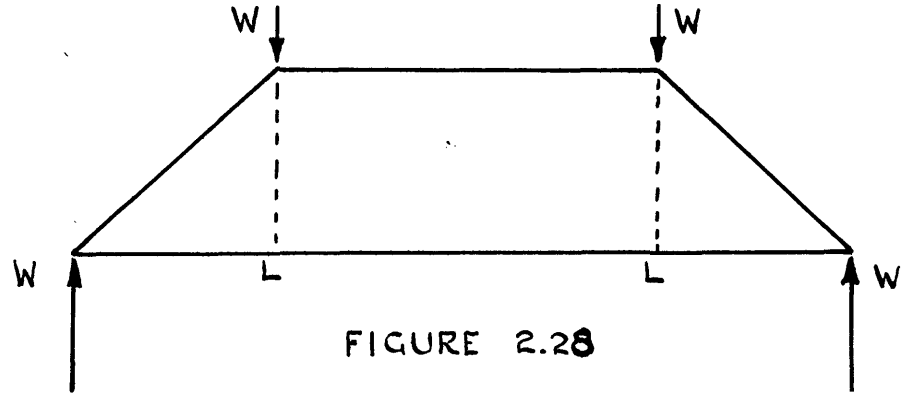

FIGURE 2.28

It is interesting to compare the steel force curves of figure 2.25 with the deflection curve in figure 2.26. There is a definite discontinuity in the latter curve where m equals 375. This value compares well with the discontinuities in corrected steel force curves at 340 and 360. There is an apparent anomaly in the deflection curve as the beam appears to be stiffer after the steel has slipped! The reason is not difficult to find. Comparison of the steel force and deflection curves indicates that the discontinuity in the latter marks the end of the serious slip. This means that just before the discontinuity the steel was slipping through the concrete as the load increased. At an m of 375 the steel had slipped as far as was possible and this relative movement between the steel and the concrete stopped. The effect would have been just the same if the stiffness of the steel and hence of the whole beam had been suddenly increased as suggested by the deflection curve.

BEAM No. III

This beam was of the same cross-section as beam I insofar as the concrete is concerned. The area of steel was greater than that in beam I each cable consisting of 12 high tensile steel wires 2 mm. diameter.

The steel was not bonded to the concrete. Average cube strength 7,500 lb/sq.in.

It was considered inadvisable to pre-stress this beam fully without any load on it because of the danger of cracking the concrete in the top of the beam. The procedure was to put half the desired pre-stress in the steel and to load the beam until it cracked. The load was then maintained whilst the steel force was increased to its full value. Loading was then continued. This results in a discontinuous curve for the steel force, figure 2.29, and the strains. This discontinuity does not cause any difficulty in the determination of the stress strain curve provided that no attempt is made to differentiate across the discontinuity. Although this beam was non-bonded and the steel force was measured by means of dynamometers throughout the test the f_t values for the cracked beam were found to be unsatisfactory. The steel force was corrected as in beam II and the corrected curves are plotted in figure 2.29. There is a substantial difference between these curves and the original one. There appears to be no simple explanation for this. Possibly the steel force measurements were correct and it is the strains or beam dimensions which are in error. There is no way of checking on this.

Fortunately the correction to the steel force make little difference to the corrected stress-strain curve in this case. Figure 2.30 shows the stress-strain curve obtained at the three gauge positions using the 'corrected' steel force. For comparison the curve resulting from use of the uncorrected steel force is superimposed. It can be seen that the difference between the two curves is negligible.

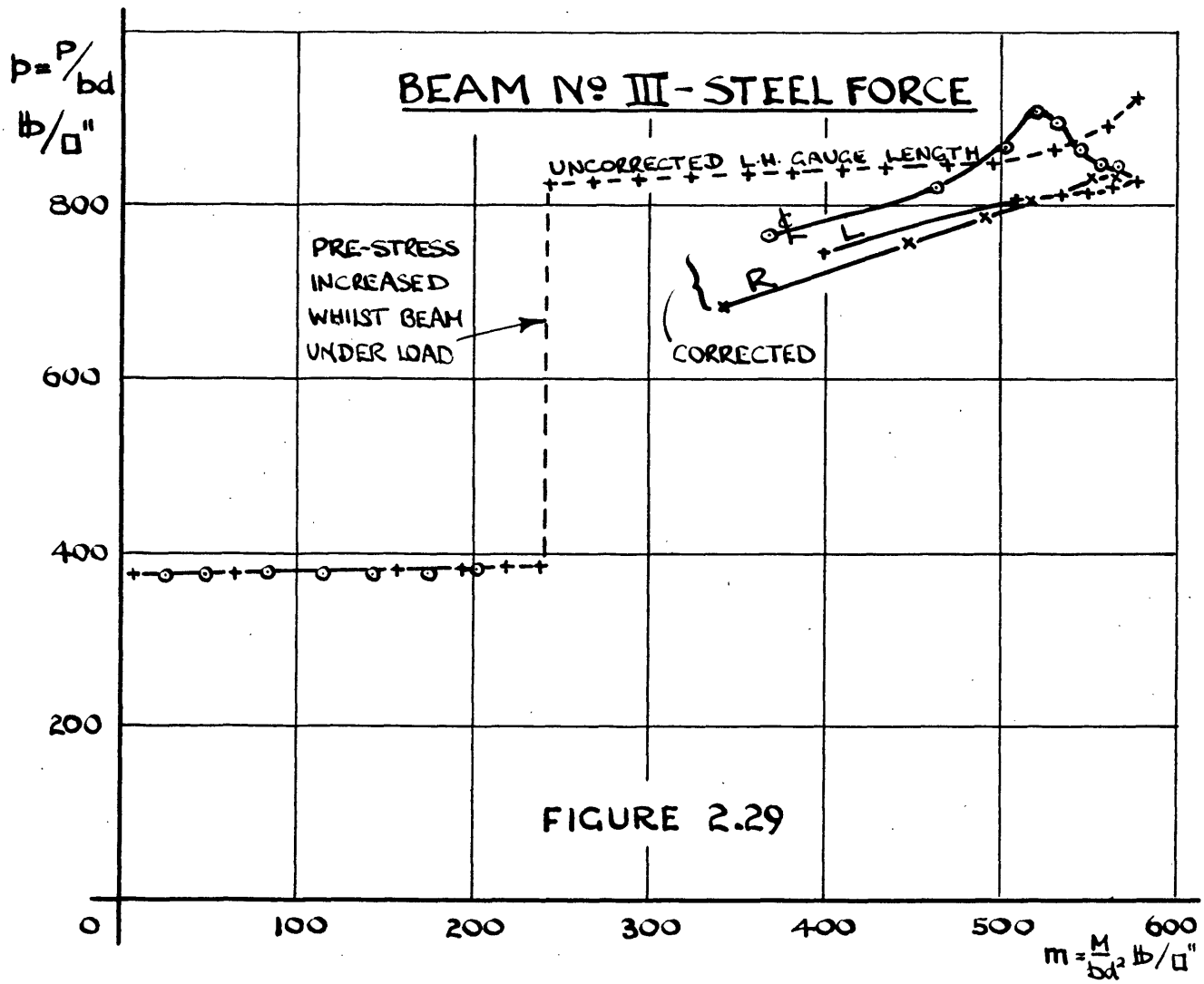

FIGURE 2.29

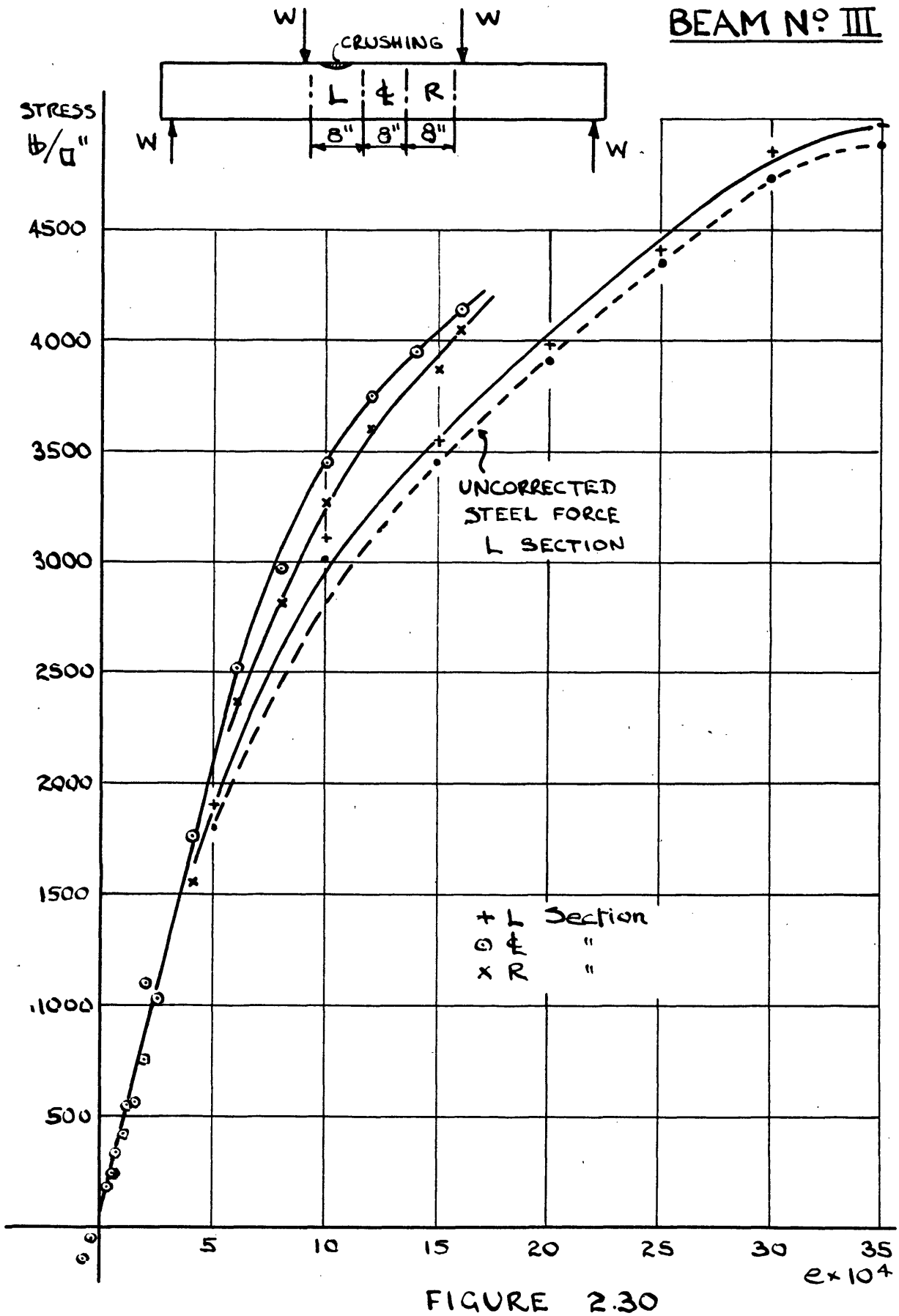
BEAM Nº III
W
W
CRUSHING
L
℄
R
8"
8"
8"
W
W
STRESS
#/□"
4500
4000
3500
3000
2500
2000
1500
1000
500
UNCORRECTED
STEEL FORCE
L SECTION
+ L Section
⊙ ℄ "
× R "
5
10
15
20
25
30
35
ε×10⁴

FIGURE 2.30

BEAM No. IV

This beam was the same as beam III except that the prestressing cables were grouted after pre-stressing. Average cube strength 7,500 lb/sq.in.

The results of the test on this beam call for little comment. The stress-strain curves for the concrete are given in figure 2.31. The steel force was corrected in deducing these curves although the corrections applied were very small as the following figures show.

m		600	650	700	750	780
p	(R section uncorrected)	920	970	1030	1120	1190
p	(R section corrected)	960	1020	1090	1150	1200
p	(℄ " ")	970	1010	1070	1140	1190
p	(L " ")	950	1100	1060	1130	1200

It can be seen that in all cases the corrected values are higher than the uncorrected. This may be ascribed to the phenomenon described on p.75. It appears that complete slip did not take place in the beam until the failing moment was reached (m = 788). It is to be expected that slip should be or less account in the highly pre-stressed beam for in this type of member the low neutral axis results in comparatively small tensile strains (compare the e_c value of the various beams in Appendix 2.2).

BEAM No. IV

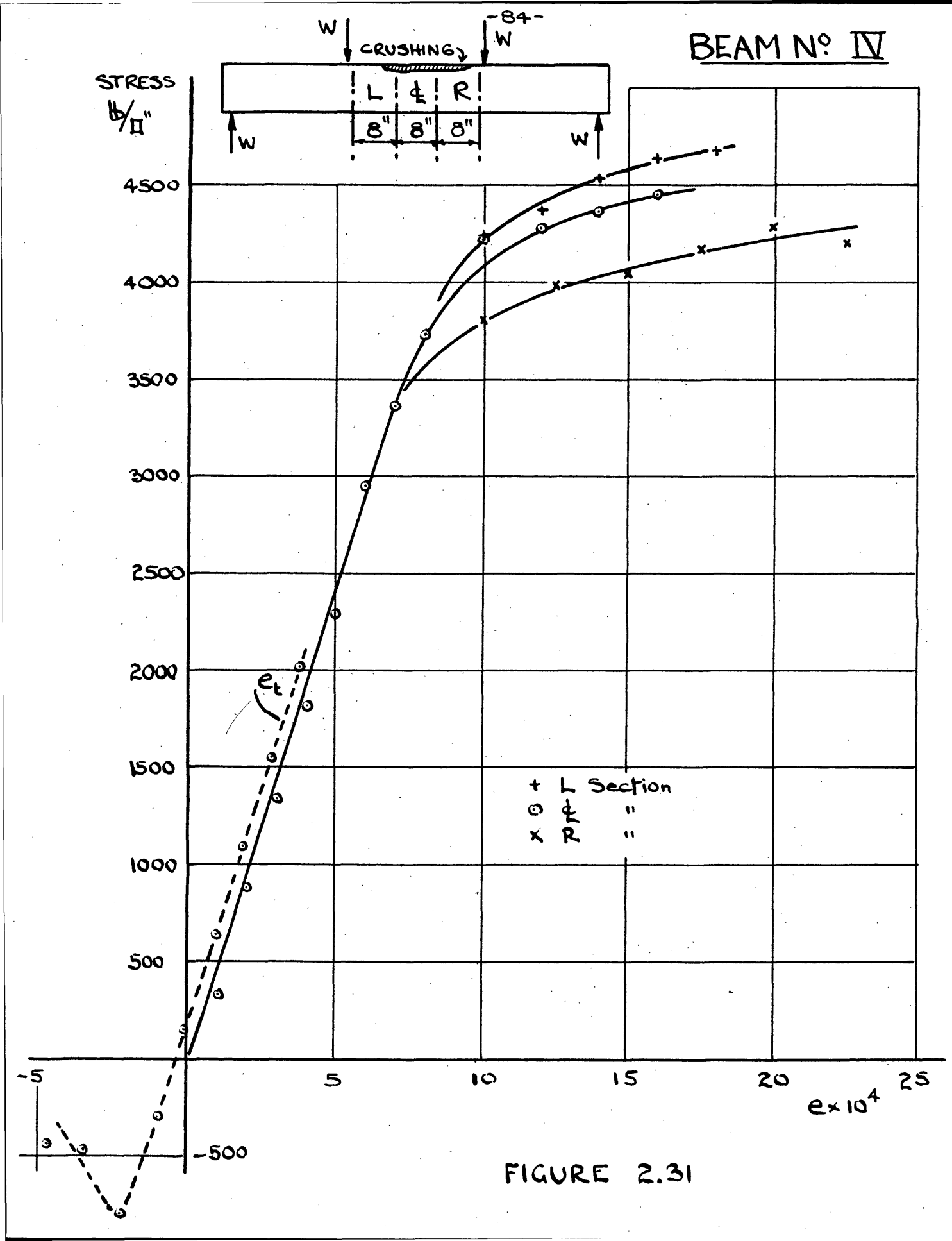

FIGURE 2.31

BEAM No. V

This beam was of the same span as the preceeding beams discussed but of reduced depth. The section is sketched in figure 2.32. The average cube strength was 8,100 lb/sq.in. The reinforcement consisted of four cables each containing twelve tensile steel wires 2 mm. in diameter. The steel was not bonded to the concrete.

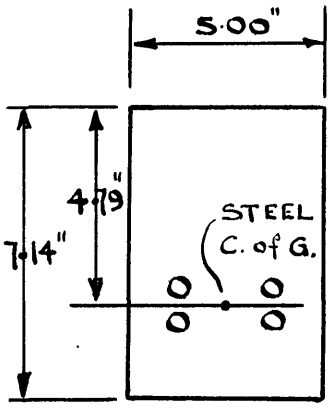

Figure 2.32

A slight difficulty was experienced in analysing the results of this beam. As usual the steel force was at the root of the trouble. During the test the 'measured' p value increased from 1138 at zero moment to 1208 at failure whereas the corrected p was found to be 1388 at failure. The corrected p can be computed only for the cracked beam and if the steel force is in error prior to cracking it is difficult to effect a correction. In this case it was noted that the corrected p was approximately proportional to the measured value and it was assumed that this proportionality was maintained throughout the whole range.

This correction, despite its magnitude made virtually no difference to the positive branch of the stress-strain curve. The f_t values are radically altered in that they

are/

are reduced to zero for the cracked beam and provide for the uncracked beam compressive stress-strain values coindident with the curve obtained from the f_c values. It is this latter fact which justifies correction.

The corrected steel force which was obtained from consideration of the central gauge length, was used to calculate f_c and f_t for the L and R gauge lengths. In both cases the f_t values provided a satisfactory check. The resultant curves are plotted in figure 2.34.

The reader may wonder why the checks described in the last chapter did not reveal such a gross error in the steel force. In fact these checks do reveal the error but they can do no more i.e. they cannot suggest the correct value for the steel force except at the particular load stages at which they are applied.

The steel force may have been wrong due to faulty dynanometers or due to friction between the curved cables and the concrete. Assume that the cable was stretched at end A and that the dynanometer was at B. The steel force at B will be less than that at A due to friction as the cable passes each bend P, Q, R and S.

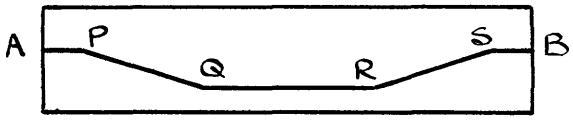

FIGURE 2.33

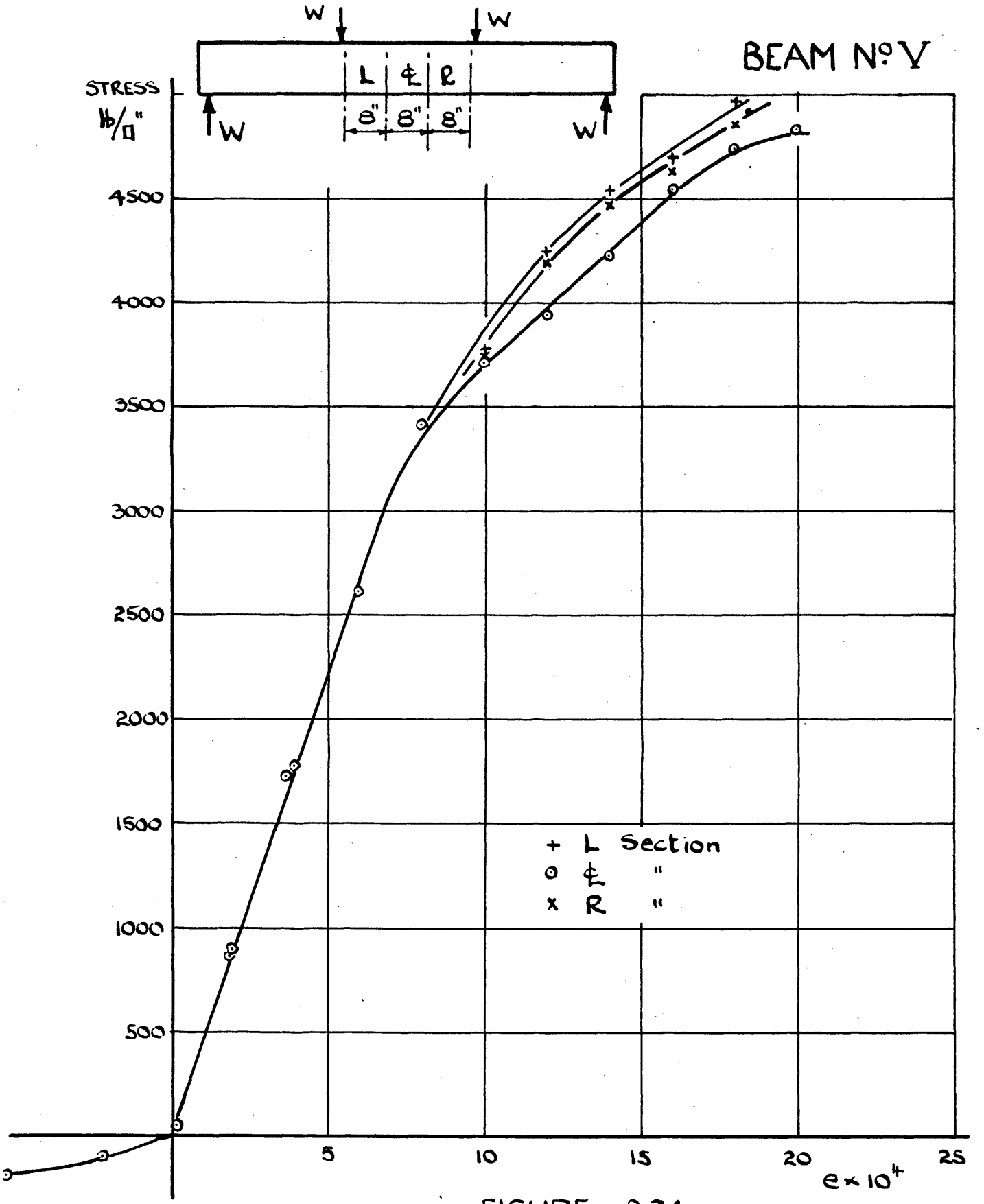
BEAM No V
W
W
L
℄
R
8"
8"
8"
W
W
STRESS
lb/□"
4500
4000
3500
3000
2500
2000
1500
1000
500
5
10
15
20
25
ε × 10⁴
+ L Section
o ℄ "
x R "

FIGURE 2.34

The force in QR will be higher than that recorded at B. For the same reason any increase in the steel force in PQ will be greater than the increase recorded at B.

BEAM No. VI

This beam is very similar in section to the preceding one but in this case the prestressing cables were grouted. The average cube strength was 7,200 lb/sq.in.

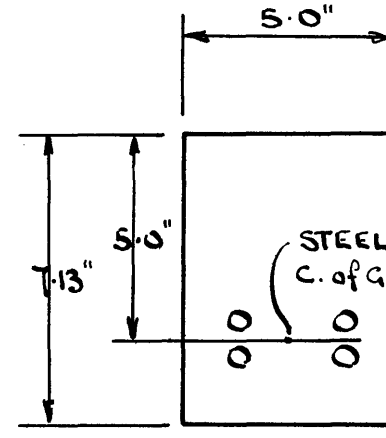

Figure 2.35

The results obtained from this test were of interest as the strains recorded were substantially different in all three gauge lengths. This has not been the case hitherto where, as a general rule, there has been close agreement between two of the three gauge lengths. Even so there is very close agreement between the stress-strain curves obtained for the various gauge positions, see figure 2.36.

As in the case of the other grouted beams it was necessary to correct the steel force. Typical figures showing the amount of correction involved are given below.

m	650	700	750	796
p(L section, uncorrected)	1190	1260	1360	1660
p(L " , corrected)	1190	1250	1350	1490
p(℄ " , ")	1230	1300	1380	1470
p(R " , ")	1190	1240	1350	1450

GENERAL CONCLUSIONS TO II CHAPTERS 3 AND 4

In chapter 3 various ways of reducing the errors involved in the testing of concrete beams were enumerated. This study leads to the conclusion that of all the fundamental quantities involved viz., bending moment, concrete strains, and steel force, it is the latter quantity which is most likely to be in error. Two methods of checking this quantity were given. These are of restricted value because they are applicable only at certain load stages which approximate to the working load, and because they can suggest no remedy if an error is found.

Chapter 3 ends by showing how the author's method of analysing the stress distribution in a beam can be adopted to correct the steel force if it is found to be in error. This method rests on the assumption that the bending moment and concrete strains are correctly measured.

Chapter 4 is devoted to analysing the results of tests on six pre-stressed beams.

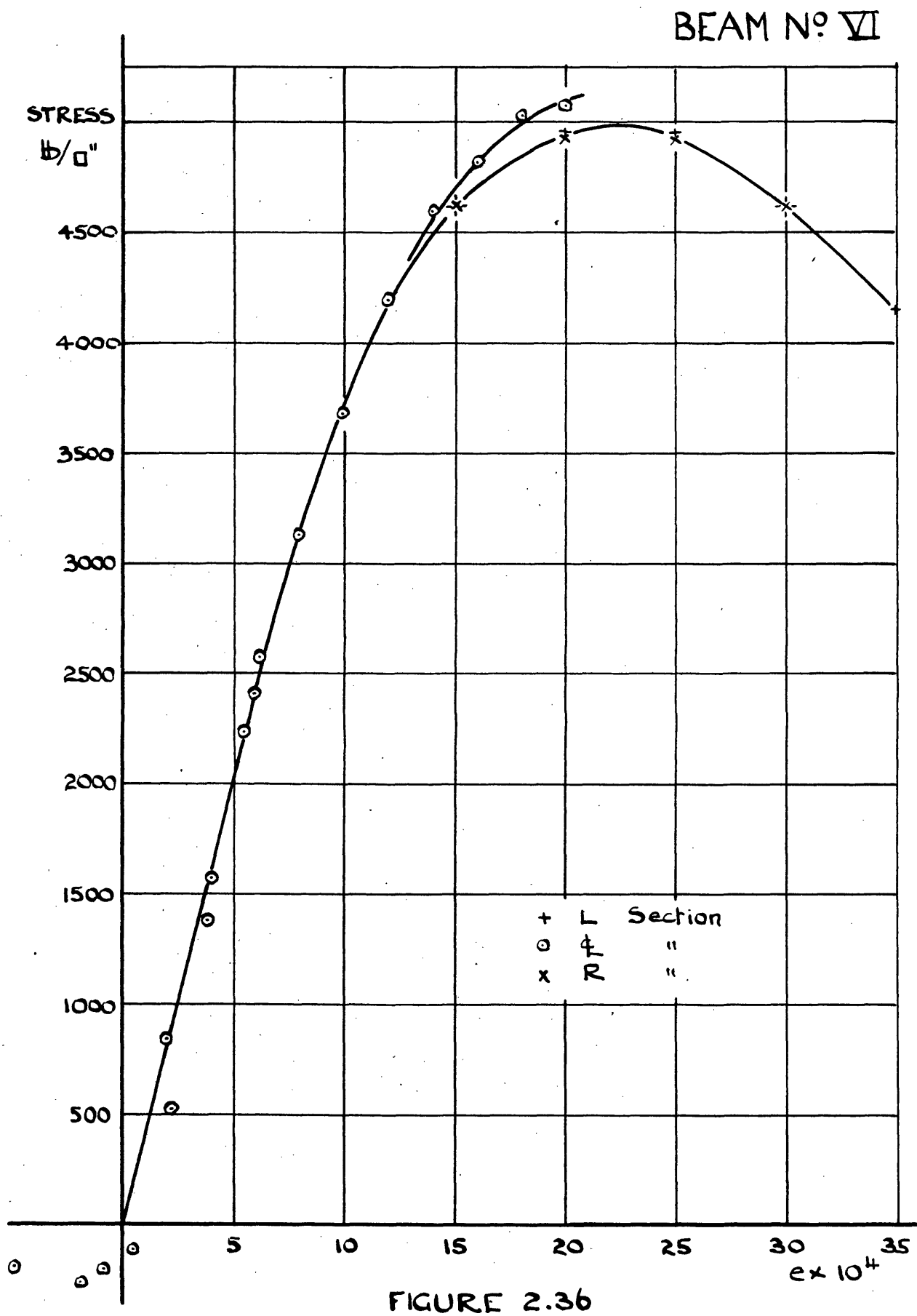
BEAM Nº VI
STRESS
lb/□"
4500
4000
3500
3000
2500
2000
1500
1000
500
0
5
10
15
20
25
30
35
ε x 10⁴
+ L Section
⊙ ℄ "
x R "

FIGURE 2.36

In three of these beams the steel was bonded to the concrete and in three it was 'end-anchored' only. It is a strange feature of the results that the steel force required most drastic correction in the case of the end anchored beams, No's I, III and V. With these beams the steel force was recorded at each load stage by means of dynamometers of the type described on page 42. The results were satisfactory only in the case of beam I. With beams III and V it was necessary to apply corrections of 10% or 12%. In both these cases the effect of the correction on the shape of the concrete stress-strain curve was negligible.

With the bonded beams, No's II, IV and VI the steel force was always estimated in the first instance from the concrete strains assuming no slip to have taken place. In the case of beam IV this assumption appears to have been justified. Beam II is interesting because it shows that the steel force can be higher than that predicted from measurement of average strains as a result of higher steel strains in the immediate vicinity of a crack. This phenomenon is also exhibited to a certain extent in beam VI. The effect does not appear to obtain at failure where slip causes the steel force to be lower than that predicted from the average strains. This is not surprising in the case of the beams described above for bond between the concrete and steel was obtained by injecting grout after pre-stressing.

In such circumstances it is more or less impossible to bond every wire effectively unless spaces are used to separate the wires. Although this is a general practice the small size of the beams rendered the use of spacers impractical in these tests. If steps are taken to ensure good bond either by the use of spacers or by the use of pre-tensioned beams it is possible that even at failure the steel stress will be higher than that predicted from measurement of the average strains (using Baker's terminology $F > 1$). Dr. K. Hajnal-Konyi has recently published a paper in which he suggests that this effect can be considerable (17). Slip is more severe in the beam with a comparatively low pre-stress; this is explained on page 83. This suggests that possibly a lower F factor should be adopted with beams of low pre-stress.

The six beams tested are too few in number to permit general conclusions to be drawn as to shape of the stress distribution in concrete beams. They do provide sufficient evidence to justify the author's method of deriving this distribution. The main support for this contention is given by the agreement obtained between the curves deduced from different sections of the beam. Consider for example figure 2.36 giving the results obtained from beam VI. In this case the compressive strains recorded during the last set of

readings/

readings just prior to failure were .00370 in the left-hand gauge length, .00225 in the central one, and .00326 in the right-hand gauge length. Despite these differences the stress-strain curves obtained from these three gauge lengths are for practical purposes indistinguishable. This is the best example but in all cases the differences are slight.

With the exception of beam II failure occurred in the gauge length giving the lowest peak value for stress. Since these differences between the curves are small it appears that local cracking and slip are as powerful in determining the actual point at which crushing occurs as the local properties of the concrete. Indeed in the case of beam II they are more powerful.

The stress-strain curve obtained for the concrete in tension is sometimes of dubious value for although errors in the steel force have little effect on the f_c values they can introduce errors in f_t of the same order as the tensile strength of the concrete. This portion of the stress-strain curve is of little significance for practical purposes so that one may be permitted to overlook this defect in the analysis.

One would expect creep of the concrete to occur to a greater extent in the gauge length which exhibits the greatest strain and if creep were of significance this would result

in/

in different stress-strain curves being deduced for the gauge lengths in which the measured strains differ. It has been pointed out above that there is generally good agreement between the curves obtained for the different gauge lengths. This indicates that the effect of creep on the distribution of stress is not of great account in short-term tests to destruction. In the tests described the time taken from the start of loading to failure of the beam was about four or five hours.

APPENDIX 2.1

In the following it is proved that if the creep equation can be written in the form

$$c = k.e.\Theta(t)$$

and if the principle of superposition may be applied in respect of strains then; in a homogeneous beam subjected to varying bending moment and end-load the distribution of stress (be it elastic or plastic) is independent of the creep effects.

If superposition may be applied

$$c_T = k\int_{t=0}^{t=T} \Theta(T - t)\,\frac{de}{dt}\,dt. \qquad \text{(i)}$$

but for plane sections to remain plate

$$e_T + c_T = g(T).x \qquad \text{(ii)}$$

where $g(T)$ is some unspecified function of time dependant upon the rate of application of end-load and bending moment.

From (i) and (ii)

$$e_T + k\int_{t=0}^{t=T} \Theta(T - t)\,\frac{de}{dt}\,dt = x.g(T)$$

Integrating

$$e_T + ke_0\Theta(T) + k\int_{t=0}^{t=T} \dot{\Theta}(T - t).e\,dt = x.g(T)$$

Differentiating with respect to e_T

$$1 + 0 + k\frac{\partial}{\partial e_T}\int_{t=0}^{t=T} \dot{\theta}(T-t)\,e\,dt = g(T) \times \frac{dx}{de_T}$$

$$1 + k\dot{\theta}(0) = g(T) \times \frac{dx}{de_T}$$

$$\therefore \quad \frac{de_T}{dx} = g(T)\{1 + k\dot{\theta}(0)\}^{-1}$$

On integrating this we obtain $e_T \propto x$. i.e. the distribution of 'elastic' strain is always linear across the section so that the stress distribution is not affected by creep.

APPENDIX 2.2

The experimental results used in II chapter 4 are given below. The figures have been reduced to a form in which they are most convenient for application of the author's analysis i.e. the bending moment is expressed as m = (Actual moment) $\div bd^2$ and the steel force = = (Total force) $\div bd$. For convenience all strains have been multiplied by 10^4.

The data is given in tabular rather than graphical form in order to save space. This is justified as the results in themselves are not of immediate interest as far as this work is concerned. Typical experimental curves are given see for example figures 2.12, 2.13 and 2.25, in the text. These may be taken as fair examples both as regards accuracy and general shape.

BEAM No. I. Low pre-stress. Non-bonded

m lb/□"	p lb/□"	Strains 'L' e_c	Strains 'L' e_t	Strains '℄' e_c	Strains '℄' e_t	Strains 'R' e_c	Strains 'R' e_t
8	350			-0.5	2.4		
69	350			-0.5	1.5		
132	352			1.3	0.4		
175	354			2.0	-0.2		
201	355			2.4	-0.6		
237	360	2.8	-2.0	3.5	-2.5	2.7	-1.1
263	370	4.9	-7.9	5.9	-8.5	4.0	-3.2
276	386	7.4	-25.1	9.4	-27.6	4.9	-5.8
288	404	10.3	-38.7	11.9	-40.4	6.5	-13.4
302	416	12.5	-47.0	14.0	-55.7	7.1	-16.4
314	437	15.4	-65.7	17.2	-74.0	8.4	-23.4
326	451	16.7	-74.7	19.1	-86.2	9.6	-26.6
338	466	18.7	-85.2	22.7	-109.8	11.8	-40.5
351	482	20.7	-97.8	24.4	-118.5	13.1	-45.1
364	499	24.2	-114.1	29.3	-143.5	14.7	-50.8
377	511	26.1	-123.0	32.0	-161.0	15.5	-58.3
390	532	30.1	-142.0	28.3	-194.0	16.5	-56.8

BEAM No. II. Grouted.

m	p	e_c	e_t	e_c	e_t	e_c	e_t
11				-0.5	2.2		
72				+0.6	1.1		
100				1.0	0.7		
151				1.6	0.1		
204				2.6	-1.0		
255				3.4	-2.4		
279				4.1	-3.7		
291	Not measured. Pre-stressed p = 342	4.8	-5.8	4.7	-4.4	4.5	-3.9
316		6.0	-9.5	5.7	-7.1	6.1	-8.1
339		7.2	-13.3	7.0	-10.6	6.9	-10.1
347		8.2	-17.2	8.1	-14.2	8.0	-13.9
367		10.3	-25.7	9.9	-20.9	9.8	-19.7
387		12.8	-36.1	11.1	-24.0	11.8	-26.4
404		14.3	-43.5	12.7	-31.3	13.2	-31.8
421		16.4	-52.5	14.7	-39.0	14.5	-37.6
444		20.8	-70.8	17.1	-46.1	17.7	-48.3
460		24.0	-83.4	19.3	-54.1	19.7	-55.0
480		29.7	-104	21.0	-59.6	22.3	-63.3
490		42.7	-154	22.8	-60.6	24.5	-70.1

BEAM No. III. High pre-stress. Non-bonded.

m lb/□"	p lb/□"	Strains 'L' e_c	Strains 'L' e_t	Strains '℄' e_c	Strains '℄' e_t	Strains 'R' e_c	Strains 'R' e_t
8	374			-0.8	2.1		
63	376			+0.1	1.3		
108	377			0.9	1.0		
157	378			1.8	0.3		
194	380			2.3	-0.7		
220	382			2.8	-1.3		
239	383			3.6	-2.9		
210	825	2.0	+1.9	1.6	+1.5	1.8	+1.7
269	828			2.4	0.8		
323	832			3.3	0.1		
381	839			4.2	-0.7		
434	842	5.7	-2.4	5.3	-2.3	5.6	-2.5
470	846			6.2	-3.8		
496	852	8.9	-9.4	7.5	-6.7	8.4	-8.5
530	865	13.6	-23.6	11.5	-16.0	11.4	-17.6
560	894	23.6	-59.0	16.5	-37.4	15.9	-32.9
578	924			18.2	-41.9	17.0	-36.0

BEAM No. IV. Grouted.

m	p	e_c	e_t	e_c	e_t	e_c	e_t
26	Not measured. Pre-stressed p = 853			0.1	3.7		
82				0.6	3.2		
127				1.3	2.4		
194				2.0	1.8		
249				2.7	1.2		
314				3.4	0.6		
365				4.2	-0.2		
424				5.1	-1.4		
477		5.5	-1.7	5.6	-1.7	5.8	-1.9
536		6.6	-2.8	6.7	-3.1	7.0	-3.4
590		7.9	-4.9	8.0	-5.1	8.4	-5.7
*629		8.4	-7.4	8.7	-7.5	9.3	-8.4
675		10.2	-11.0	10.5	-11.8	11.2	-13.2
720		13.3	-19.1	13.8	-20.2	15.3	-22.4
749		16.2	-27.2	15.8	-25.0	18.2	-27.9
775		20.2	-37.6	18.8	-31.8	24.4	-46.2
786			No readings taken.				

* Top cable released

BEAM No. V. Very high pre-stress. Non-bonded.

m lb/□"	p lb/□"	Strains 'L' e_c	Strains 'L' e_t	Strains '£' e_c	Strains '£' e_t	Strains 'R' e_c	Strains 'R' e_t
37	1140			0.4	5.1		
89	1142			1.2	4.5		
171	1147			2.3	3.6		
252	1152			3.3	2.5		
334	1153			4.3	1.6		
425	1157			5.6	0.5		
466	1158			6.3	0		
520	1163			7.2	-1.1		
549	1160			7.8	-1.9		
590	1167			8.9	-3.5		
630	1175	10.6	-6.3	11.9	-8.5	10.6	-6.3
664	1184	13.5	-12.7	14.4	-13.3	13.8	-12.7
715	1207	18.3	-22.8	20.6	-27.2	19.6	-26.0

BEAM No. VI. Grouted

m	p	e_c	e_t	e_c	e_t	e_c	e_t
18	Not measured. Pre-stressed p = 1078			-0.3	5.9		
85				+0.6	5.0		
162				1.7	4.3		
235				2.8	3.4		
302				3.8	2.7		
372				4.8	1.6		
442				5.7	0.6		
516				7.0	-0.7		
592		9.0	-3.8	8.8	-3.2	8.5	-4.1
626				10.0	-6.1		
653		12.2	-9.4	11.6	-8.1	12.0	-10.0
696		14.9	-13.4	13.9	-11.6	14.5	-14.7
728		18.0	-19.0	15.9	-16.4	17.7	-22.0
760		21.4	-30.8	18.0	-21.0	20.9	-30.6
783		26.2	-40.4	20.3	-26.0	24.5	-36.8
795		37.0	-59.0	22.5	-29.4	32.6	-53.7

PART III THE EFFECT OF FINITE SPACING OF TENSILE CRACKS ON THE DISTRIBUTION OF STRESS IN CONCRETE BEAMS SUBJECTED TO A PURE BENDING MOMENT

Chapter I. INTRODUCTION

When considering the distribution of stress in concrete beams it is usual to assume that the concrete is incapable of sustaining any tensile stress and to consider the concrete below the neutral axis to be of no account. This leads to the assumption that the distribution of stress in an ordinary reinforced concrete beam, under elastic conditions is as indicated in figure 3.1.

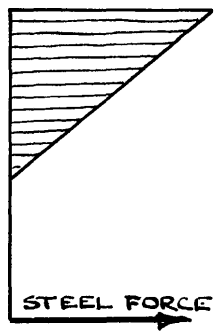

Figure 3.1.

With bonded pre-stressed beams and ordinary reinforced beams these assumptions are justified because the tensile cracks do occur quite close together. With non-bonded beams there is a definite difference the cracks being quite widely spaced. With beam No. I (described in part II) only one major tensile crack appeared whereas beam No. II, which differed only by being grouted, many tensile cracks appeared spaced 4" to 6" apart. It appears unlikely that the stress distribution of figure 3.1 will be realised in the case of beam No. I.

It is the object of this chapter to determine the effect of crack spacing upon stress distribution.

III Chapter II GENERAL REVIEW OF THE PROBLEM

The complexity of this problem, from the analytical standpoint, is such that some severe restrictions must be placed on the work .

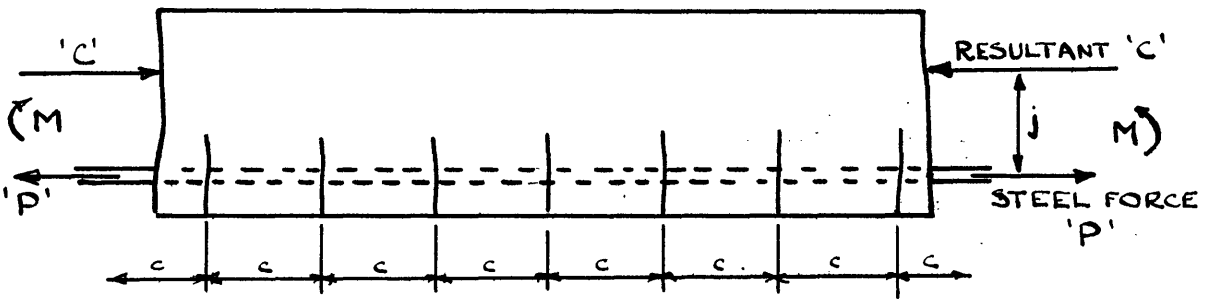

Figure 3.2

It will be assumed that the cracks in the beam are evenly spaced and that the cleavage is in each case in a plane perpendicular to the axis of the beam. The first of these assumptions is realised approximately in practice. The second is sometimes, but frequently the cracks fork. Although the analysis to follow will indicate why this happens quantitative analysis of the phenomenon is hardly possible.

The problem will be restricted to elastic deformations.

An idealised cracked beam is indicated in figure 3.2 Consider the broad statics of the problem. The steel force P = resultant concrete compressive force C and the external moment $M = j.P = j.C$.

Since the steel and concrete are not bonded the concrete stress distribution will be completely unaffected if both P and M are removed to leave only the eccentric compressive force C. That is to say, the concrete beam has become an eccentrically loaded column.

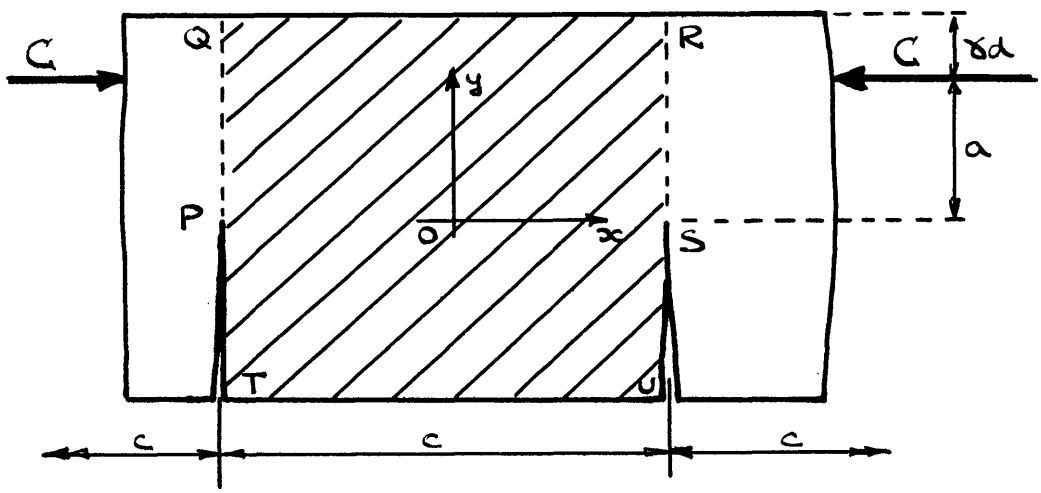

Figure 3.3

The beam can now be regarded as a number of identical blocks, each of length c, placed end to end and subjected to an eccentric end load C. The interface between two blocks c is considered to be incapable of sustaining a tensile stress so that if the compressive force is outside the middle third the cracks will open until the direct stress on the interface is entirely compressive. There may be tensile stresses present <u>within</u> the blocks but no <u>new</u> cracks will be initiated until these stresses exceed the ultimate tensile strength of the material.

We will consider that the beam is fairly thin i.e. in the language of the theory of elasticity the problem is one of plane stress. The presence of the holes through which the reinforcement is passed will be ignored.

MATHEMATICAL STATEMENT OF PROBLEM

Consider the block TQRU in figure 3.3. The equation to be satisfied within these boundaries is the biharmonic equation (18).

$$\nabla^4 \phi = 0$$

where (3.1)

$$\nabla^4 \equiv \frac{\partial^4}{\partial x^4} + 2\frac{\partial^4}{\partial x^2 \partial y^2} + \frac{\partial^4}{\partial y^4}$$

and ϕ is the Airy Stress function. The stresses are obtained from this function as follows:-

$$\frac{\partial^2 \phi}{\partial x^2} = p_{yy} \quad ; \quad \frac{\partial^2 \phi}{\partial y^2} = p_{xx} \quad ; \quad \frac{\partial^2 \phi}{\partial x \partial y} = -p_{xy}$$

The choice of the co-ordinate axes is arbitrary but that given in figure 3.3. is a convenient one.

On boundary TU we have two known stress conditions namely $p_{yy} = p_{xy} = 0$

Hence $$\frac{\partial^2 \phi}{\partial x^2} = 0 \qquad \text{and} \qquad \frac{\partial^2 \phi}{\partial x \partial y} = 0$$

Integrate with respect to x

$$\frac{\partial \phi}{\partial x} = f_1' n(x) \qquad \text{and} \qquad \frac{\partial \phi}{\partial y} = f_2' n(x)$$

Since x is constant along TU both f_1 and f_2 are constants so that

$$\frac{\partial \phi}{\partial x} = k_1 \qquad \text{and} \qquad \frac{\partial \phi}{\partial y} = k_2$$

Integrating the first of these with respect to x

$$\phi = k_1 x + f_3(y)$$

or $\phi = k_1 x + K_1$ where K_1 is a constant.

Since the stresses are obtained by differentiating ϕ twice the values of these stresses will be independent of k_1, k_2 and we can assign arbitrary values to these quantities. For convenience we will set them all to be zero.

The above process will now be repeated for the other boundaries but the constants of integration which appear will no longer be arbitrary. Such constants will be dependent on the values which have been assigned to k_1, k_2 and K_1.

Consider boundaries PT and SU. Here p_{xx} and p_{xy} are zero so that $\frac{\partial^2 \phi}{\partial y^2} = 0$ and $\frac{\partial^2 \phi}{\partial x \partial y} = 0$

Integrate with respect to y

$$\frac{\partial \phi}{\partial y} = f'_3(x) = \text{constant and } \frac{\partial \phi}{\partial x} = \text{constant.}$$

The points T and U lie on TU where $\frac{\partial \phi}{\partial y}$ and $\frac{\partial \phi}{\partial x}$ are both zero hence on PT and SU

$$\frac{\partial \phi}{\partial y} = \frac{\partial \phi}{\partial x} = 0$$

Integrating the first of these it is found that $\phi = 0$.

On boundaries RS and PQ $\frac{\partial^2 \phi}{\partial x \partial y} = 0$ and since $\frac{\partial \phi}{\partial x} = 0$ at P and S it is zero all along both RS and PQ.

A second boundary condition is required and it is given by observing that the stresses must be symmetrical about each of RS and PQ. This is so because all the blocks in the beam are subjected to the same conditions and hence the stresses in them are the same. This only implies that the second derivatures of ϕ must be symmetrical about the interfaces between the blocks. However we have so selected the arbitrary constants on boundary TU that ϕ is symmetrical about the interfaces.

Analysis of the conditions on QR is precisely the same as that for TU and it is found that

$$\phi = k_1' x + K_1 \quad \text{and} \quad \frac{\partial \phi}{\partial y} = k_2'$$

The values of these constants is found by further consideration of boundary RS, on which $p_{xx} = \frac{\partial^2 \phi}{\partial y^2}$

By restricting attention to this line this can be rewritten

$$\frac{d^2\phi}{dy^2} = p_{xx}$$

Integrating

$$\left[\frac{d\phi}{dy} \right]_{y=S}^{y=R} = \int_S^R p_{xx}\, dy$$

$$= C, \text{ the total compression.}$$

$\frac{\partial \phi}{\partial y}$ is zero at S $\therefore \left[\frac{\partial \phi}{\partial y} \right]_{y=R} = C$

i.e. $k_2' = C$

Consider now

$$y \frac{d^2\phi}{dy^2} = y \cdot p_{xx}$$

Integrate

$$\left[y \frac{d\phi}{dy} \right]_{y=S}^{y=R} - \int_S^R \frac{d\phi}{dy}\, dy = \int_S^R y \cdot p_{xx}\, dy.$$

$$C(a + \gamma d) - [\phi]_S^R = C.a$$

$$(\phi)_S = 0 \qquad \therefore \quad (\phi)_R = C.\gamma d$$

(γd is used to preserve uniformity with the preceeding sections of this thesis)

This analysis applies equally to boundary PQ and

$$(\phi)_Q = C\gamma d$$

Hence $k_1' = 0$ and $K_1' = C\gamma d$.

The above statement of the problem is summarised in figure 3.4 below.

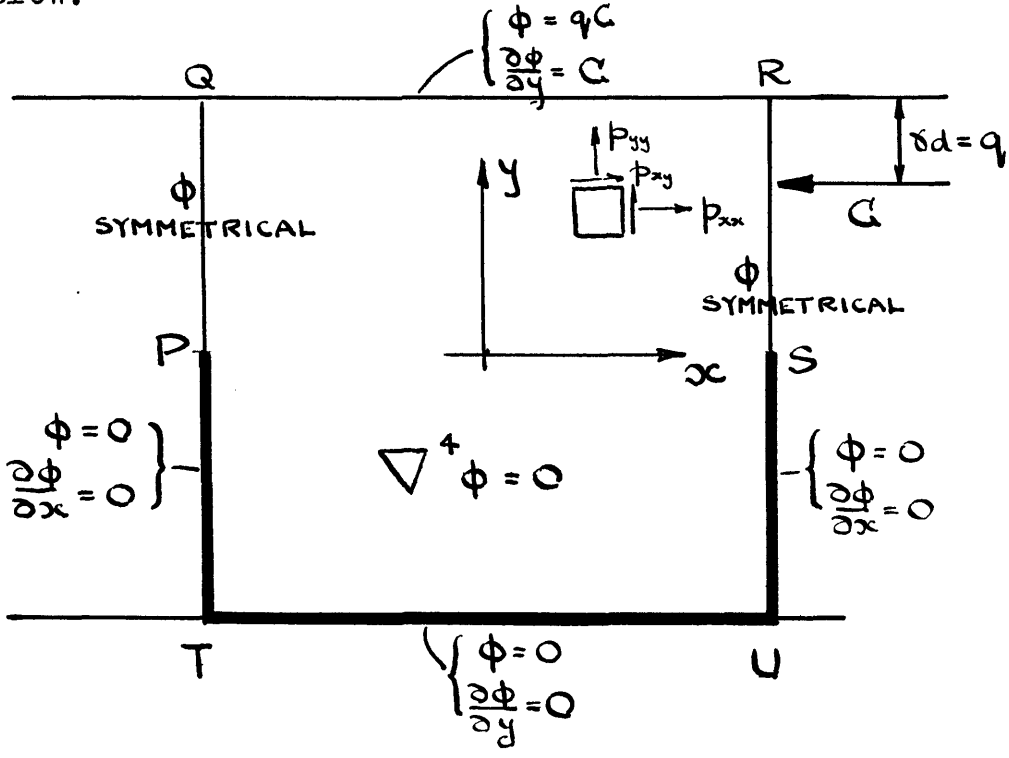

Figure 3.4

Unfortunately figure 3.4 does not give a complete statement of the problem for the positions of S and P depend upon the position of the resultant C. An arbitrary selection of point S when q is specified will result in p_{xx} having some value other than zero at S. It cannot be tensile becuase the S would shift up and the crack would open more. On the other hand a positive value would close the crack. The required solution is given when p_{xx} at S is just zero.

ANALYTICAL SOLUTION OF THE PROBLEM.

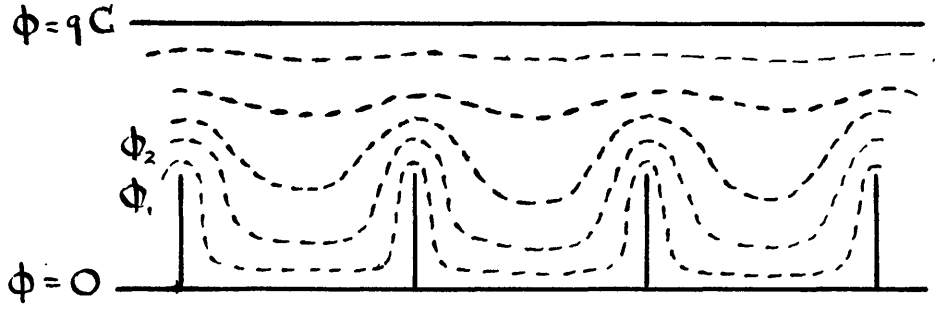

Figure 3.5

An explicit solution of the problem requires the determination of the function

$$\phi = g(x, y)$$

where ϕ satisfies the biharmonic equation and all the boundary conditions. Having obtained such a solution it would be possible to plot equi-ϕ lines which might appear as in figure 3.5.

The function $\phi = 0$ would give the bottom boundary including cracks and as ϕ is increased to γC the curves would degenerate into a straight line. It appears that a solution in the form of a harmonic series could be found but the author has been unable to discover one.

The above paragraphs were written before the author obtained the relaxation solutions given below. As will be seen in figure 3.9 the equi-ϕ lines do not altogether follow the pattern suggested in figure 3.5. The proper solution is modified by the appearance of negative ϕ contours. Figure 3.5 is, however, left in its original form as it is a part of the sequence of reasoning which led to the final solution of the problem and as there is nothing to indicate that one should assume a-priori the existence of the negative ϕ values.

RELAXATION SOLUTION

As it appeared unlikely that an explicit solution to the problem could be found readily the author decided to use relaxation methods. As relaxation is now a standard method of solving field problems details of technique need not be considered here. The general method of dealing with the biharmonic equation has been given in a paper by Fox and Southwell (19).

In solving the problem above difficulty arises as a result of the undefined dependence of the crack depth on the position of the resultant force C.

This difficulty is solved by splitting the solution into two parts. The author is indebted to Mr. D.N. de G. Allen for suggesting that the problem might be tackled in this way. Instead of solving the complete problem as stated in figure 3.4 the two independent components given in figure 3.6 are each solved separately.

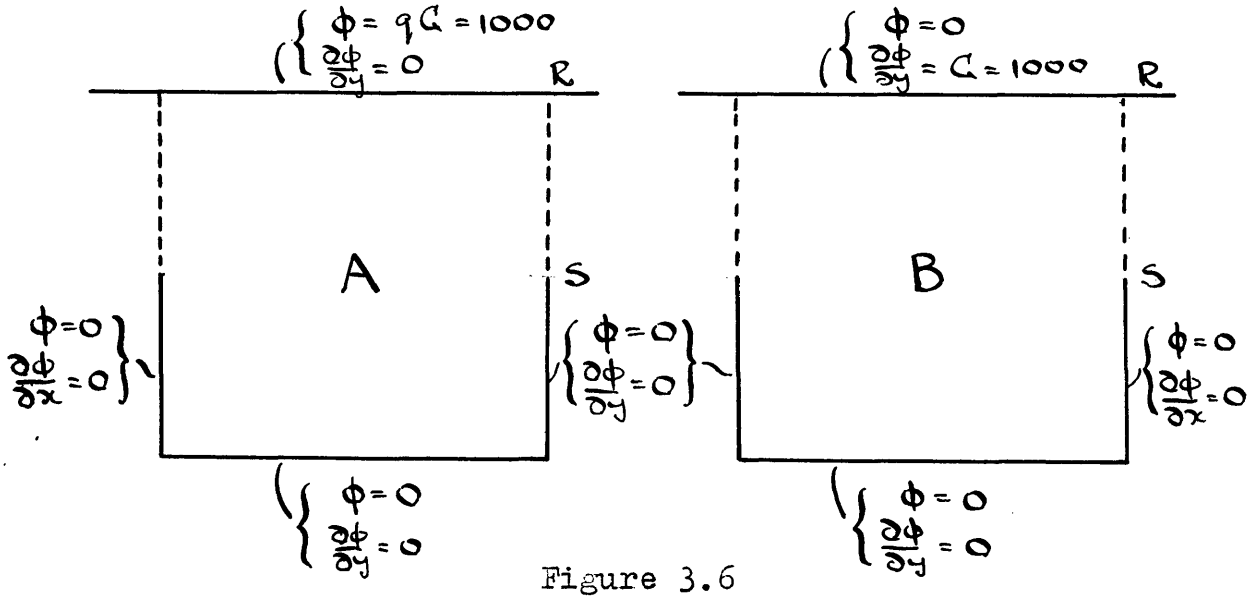

Figure 3.6

The final solution is then of the form A + λ B λ so chosen that the resultant p_{xx} is zero at point S.

In the case of a square block with the crack extending to half the depth of the beam the distribution of p_{xx} along SR is as given in figure 3.7. It will be seen that in this case $\lambda = -\frac{486}{648} = -0.75$.

It is not necessary to evaluate the stresses in this way as the value of λ can be obtained directly by consideration of the ϕ's . It is stated above that $\phi_{xx} = \frac{\partial^2 \phi}{\partial y^2}$. At some point such as M in figure 3.8 this equation, when written in finite difference form, becomes $(\phi_{xx})_m = (\phi_L - 2\phi_M + \phi_N) \div h^2$ For simplicity the mesh length h can be made unity (this is done without loss of generality) so that we can write

$$(\phi_{xx})_M = \phi_L - 2\phi_M + \phi_N .$$

At S, $\frac{\partial \phi}{\partial y} = 0$ because ϕ is constant along SU. At the imaginary mesh point 2 we have ϕ_2 which must $= \phi_1$ Thus at S where $\phi = 0$, $\phi_{xx} = \phi_1 + \phi_2 = 2\phi_1$. So that λ is found simply by dividing $(\phi_1)_B$ into $(\phi_1)_A$.

In figure 3.9 the two components A and B are plotted alongside the resultant A + λ B for the case of a square block with a crack extending half-way up the section. The solution is of little value in this form so that only this one example will be given. It is, however, quite typical.

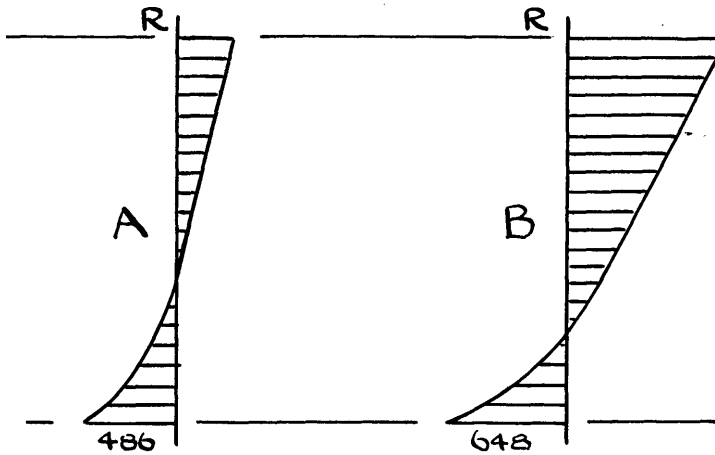

FIGURE 3.7

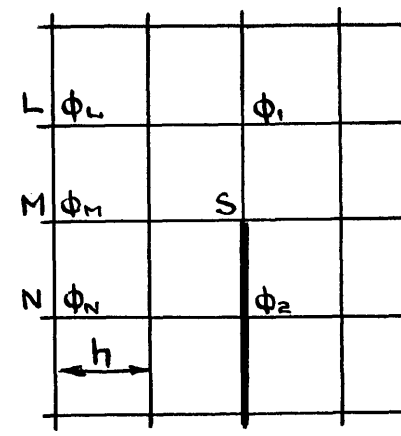

FIGURE 3.8

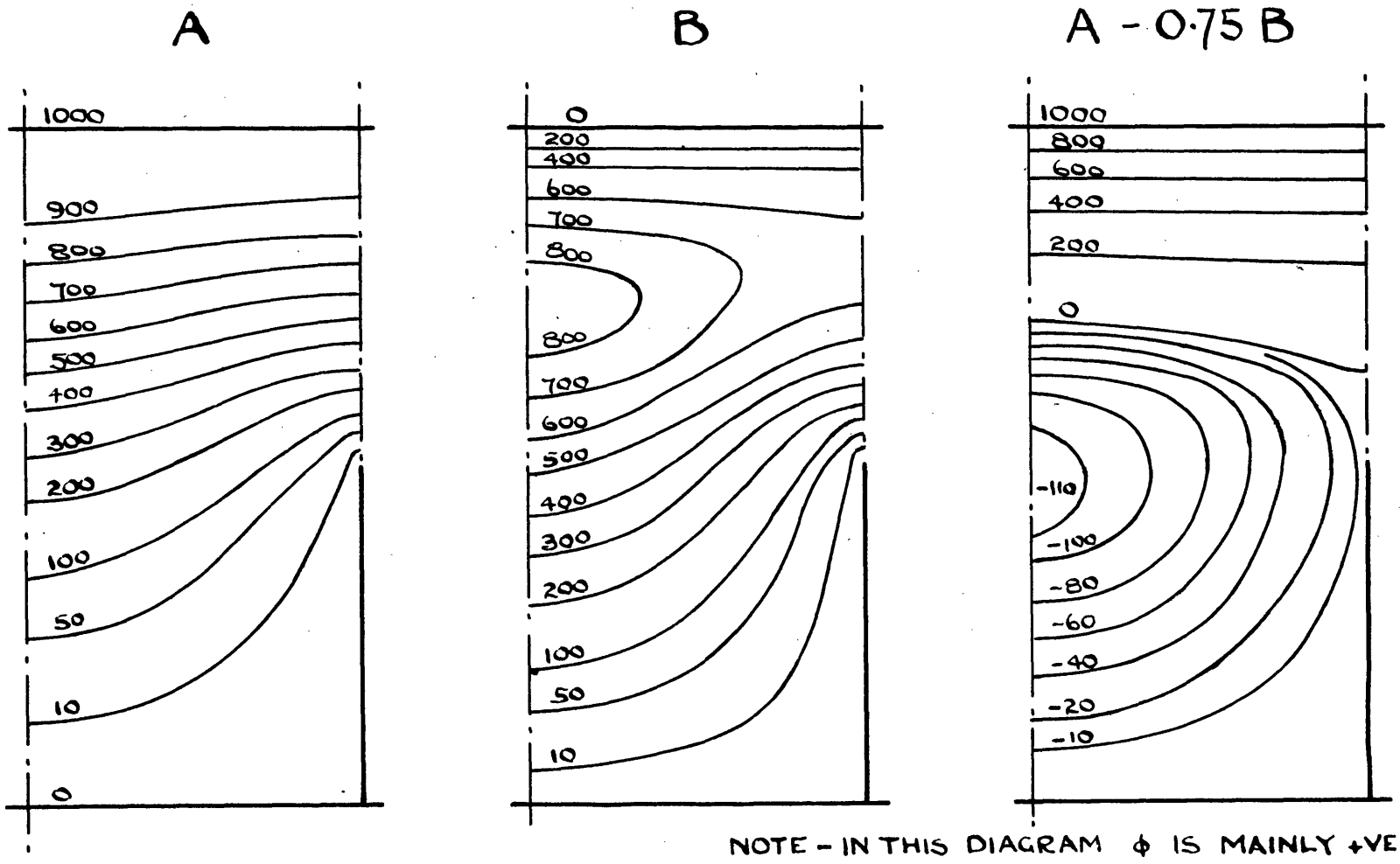

FIGURE 3-9

NOTE - IN THIS DIAGRAM ϕ IS MAINLY +VE. WITH THE STRESS DEFINITION GIVEN ON PAGE 104 THIS MAKES C TENSILE. FOR SUBSEQUENT DIAGRAMS C IS COMPRESSIVE.

RANGE OF SOLUTIONS

The general purpose of this section of the work is to investigate the effect of crack spacing and crack depth on the stress distribution in a beam. It was necessary, therefore, to solve a whole series of problems. In all cases the side of the mesh length of the relaxation pattern was unity with a beam depth of 8 units. The total of cases considered are given in the table below.

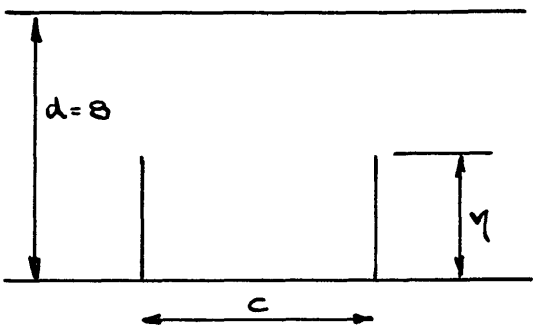

Figure 3.10

TABLE 3.1

c	η = 0	1	2	3	4	5	6	7	8
2			X		X		X		X
4			X		X		X		X
8	X	X	X	X	X	X	X	X	X
16			X		X		X		X

The square block was considered in much detail because the author has observed the crack spacing in non-bonded beams to be very approximately equal to the beam depth. The other values of c were chosen to give a fairly wide range.

III Chapter III DISCUSSION OF RESULTS OBTAINED FOR A PARTICULAR CASE

In giving the solution of a problem in stress analysis it is not easy to decide how to make the most comprehensible and useful presentation. One way is to plot an orthogonal set of trajectories directed in the directions of principal stress together with contours giving the local intensity of the two principal stresses. The advantage of this method in so far as concrete is concerned is that it indicates immediately the value and direction of the tensile stresses which tend to cause cracking. Alternatively contours giving the intensity of the component stresses p_{xx}, p_{xy}, p_{yy} can be plotted. This latter method is much the simpler as the stresses are calculable directly from the ϕ's whilst the principal stresses can only be determined by further calculation. As interest is centred on p_{xx}, the p_{xy} and p_{xy} contours can be omitted. Local values can be given at the nodes of the relaxation network.

Both methods of presentation are given in figures 3.11 and 3.12. The example chosen is that of the square block with a crack running to one half beam depth.

Consider first figure 3.11 which gives the principal stresses. There are three main areas of interest:-

(a) The general area above the cracked zone.

In this region the numerically largest principal stress is compressive in a direction which is, for all practical purposes, parallel to the axis of the beam (b) The area of tensile stress at the bottom of the centre line midway between two cracks. This stress acts parallel to the axis of the beam. (c) The large tensile stress at the top of the crack acting parallel to the crack. All stresses not mentioned in these three categories are small and of little consequence.

It can now be seen that figure 3.12 shows all the important information enumerated above. The stress contours in the compression zone of the beam are almost identical to the principal stress contours of figure 3.11 whilst the latter shows the directions of the principal stress deviates but slightly from the xx direction. The tensile stress in region (b) is p_{xx} for as this stress is on a boundary it must be a principal stress. The tensile stress at the top of the crack is not indicated by any contours in figure 3.12. The value is given by the figures printed at the nodal points and since the stress is on a boundary and a line of symmetry it must be a principal stress.

This particular case has been discussed in order to demonstrate that, as far as the object of this section is concerned,/

C=1000

FIGURE 3.11

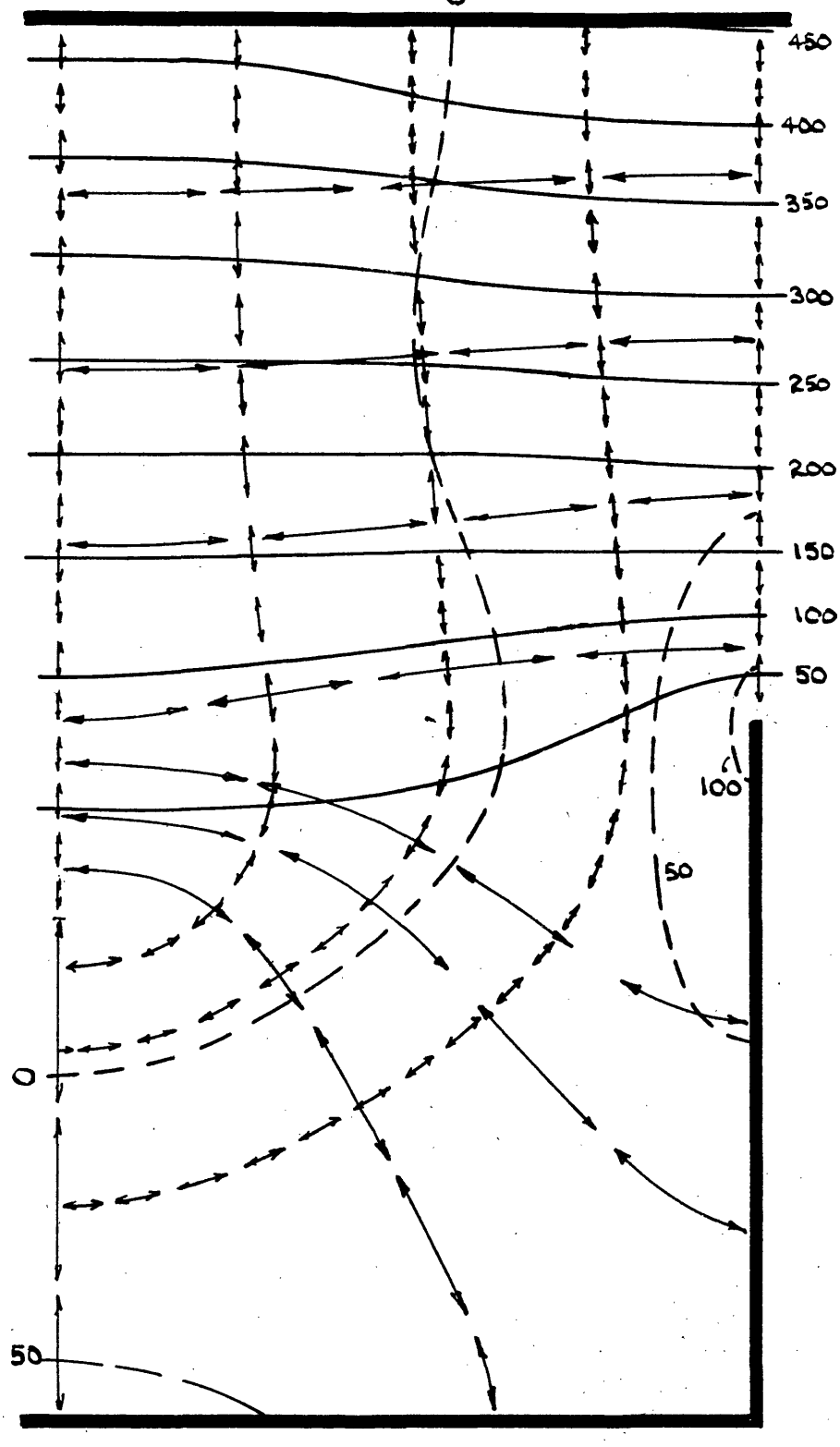

LONG ARROWS GIVE DIRECTION OF MAJOR PRINCIPAL STRESS
SHORT " " " " " MINOR " "
FULL LINES ARE CONTOURS OF MAJOR " "
BROKEN " " " " MINOR " "
COMPRESSIVE STRESSES ARE POSITIVE
LAYER TINTS SHOW TENSILE STRESSES

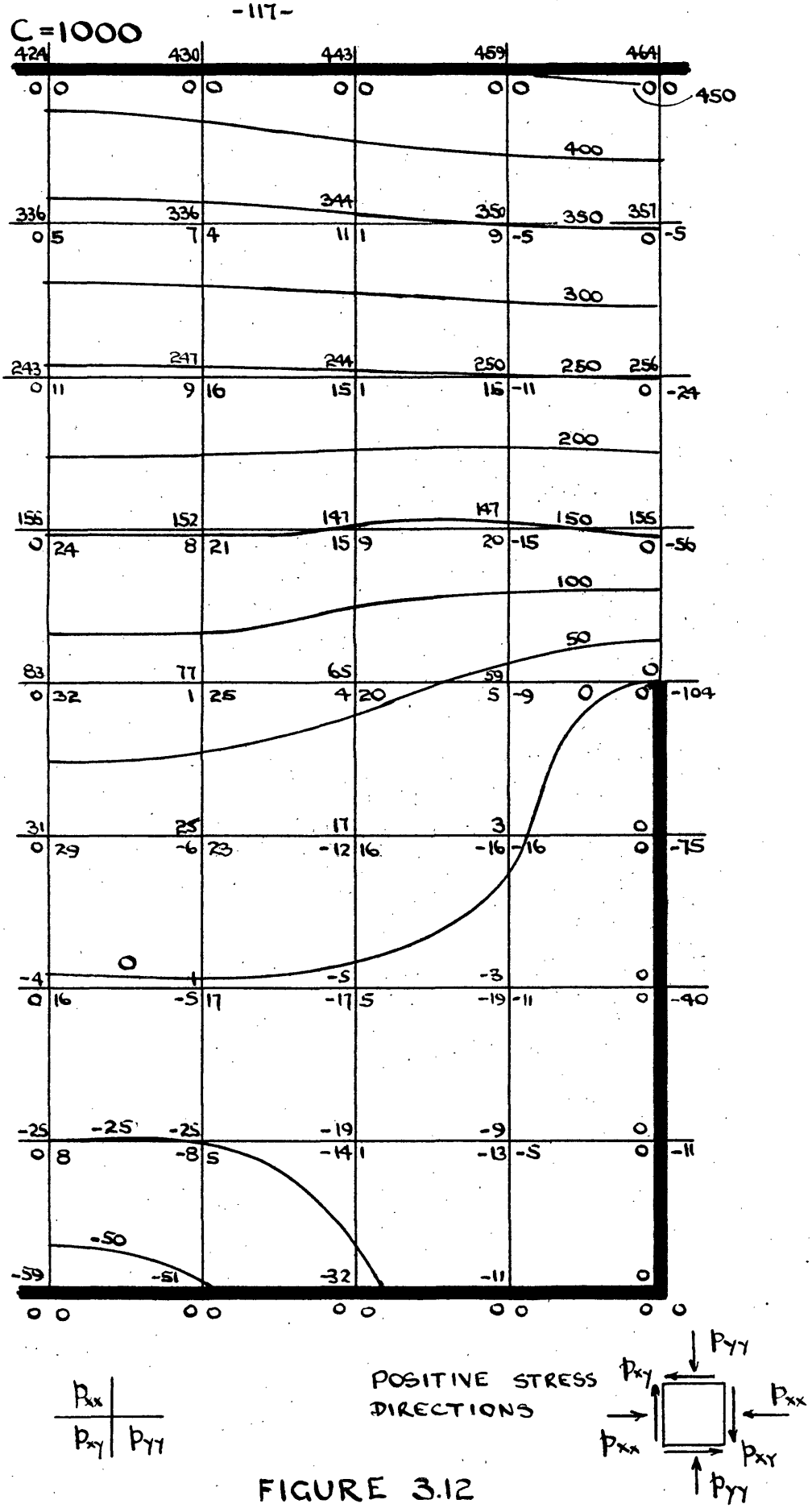
C=1000
424
430
443
459
464
450
400
336
344
350
350
357
300
247
244
250
250
256
200
152
147
150
155
100
50
77
65
59
0
25
17
3
0
-6
-12
-16
-16
-75
-5
-17
-19
-11
-90
-25
-19
-9
-8
-14
-13
-5
-11
-50
-51
-32
-11
P_{xx}
P_{xy}
P_{yy}
POSITIVE STRESS DIRECTIONS

FIGURE 3.12

concerned, it is not necessary to consider the distribution of the principal stresses in detail but that all relevant information can be put on diagrams of the type 3.12.

III Chapter IV DISCUSSION OF SOME OF THE GENERAL RESULTS

It will now be more convenient to consider specific points which emerge from all the cases considered rather than to deal with each complete case by itself.

DISTRIBUTION OF p_{xx} ABOVE A CRACK

Figure 3.13 illustrates the effect of crack spacing on the distribution of stress on the plane containing the crack. This figure gives the results for the crack extending to one half beam depth whilst the remaining results are given in table 3.2.

It can be seen that as the crack spacing is increased the stress distribution ceases to follow the triangular distribution normally assumed and which can be realised only when the distance between cracks becomes zero. The deviations are small and are practically negligible. The maximum difference recorded amounting to only 7% of its corresponding top fibre stress. The general effect of the wide crack spacing is a slight decrease in the top fibre stress and an increase in stress nearer the neutral axis. This means a slight lowering of the centre of compression.

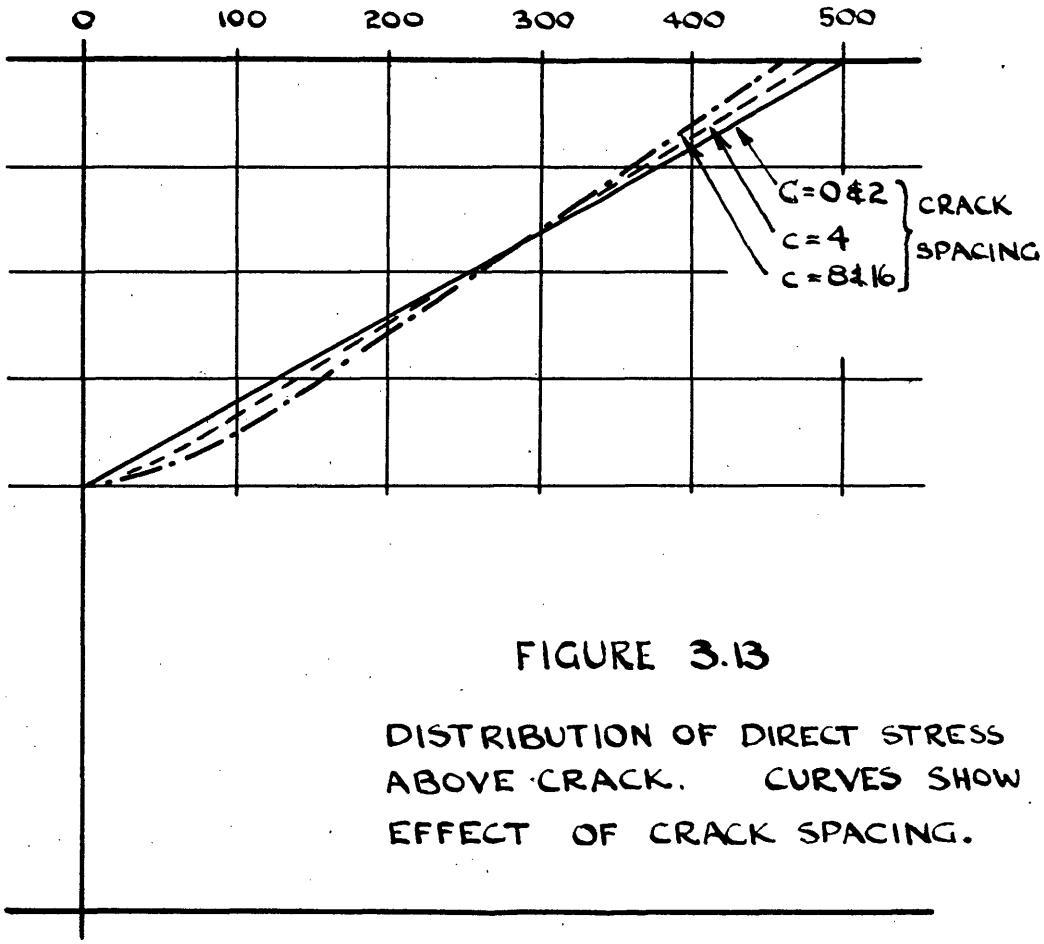

FIGURE 3.13

DISTRIBUTION OF DIRECT STRESS ABOVE CRACK. CURVES SHOW EFFECT OF CRACK SPACING.

TABLE 3.2 p_{xx} at cracked section for G = 1000

	y =	0	1	2	3	4	5	6	7	8
η = 0	c=0→∞	0	31	63	94	125	156	187	219	250
η = 2	c=0	0	0	0	56	111	167	222	278	333
	2	0	0	0	61	110	169	220	274	331
	4	0	0	0	67	116	166	219	274	318
	8	0	0	0	71	120	167	218	264	315
	16	0	0	0	67	124	167	218	267	314
η = 4	c=0	0	0	0	0	0	125	250	375	500
	2	0	0	0	0	0	128	251	373	496
	4	0	0	0	0	0	141	252	366	481
	8	0	0	0	0	0	155	256	357	464
	16	0	0	0	0	0	156	256	354	466
η = 6	c=0	0	0	0	0	0	0	0	500	1000
	2	0	0	0	0	0	0	0	505	990
	4	0	0	0	0	0	0	0	514	971
	8	0	0	0	0	0	0	0	511	968
	16	0	0	0	0	0	0	0	510	980

In table 3.2 the stress values for finite crack spacing are all obtained by relaxation. The stresses for zero distance between cracks have been obtained by calculation from the known triangular distribution. In making the comparison between the 'completely' cracked case and the cases where the crack spacing is finite the errors inherent in the relaxation process must be borne in mind. These errors are small if the mesh dimensions are small compared with the main dimensions of the body i.e. where the cracks are spaced 8 and 16 mesh lengths part. They become more significant where $c = 4$ whilst $c = 2$ can only be regarded as a rather crude approximation. A better solution would be obtained by taking a smaller mesh size but in view of these practical limitations on the value of this analysis the author feels that the extra labour involved in doing this would be unjustified. The purpose of this analysis is to determine general effects rather than mathematically precise quantities which are obviously of dubious practical value. These remarks apply also as the crack depth becomes very deep e.g. $\gamma = 6$. Then the depth of the compression zone is comparable with the mesh size. In this case the effect of replacing the differential equation by a finite difference equation can be investigated quite easily. Table 3.3 compares the exact stress values with those obtained by relaxation for $c = 0$.

TABLE 3.3

'Exact' p_{xx}	0	31.25	62.5	93.75	125	156.25	187.5	218.75	250
Relaxation Values (8 meshes)	0	32	63	95	124	153	185	217	251
Relaxation Values (4 ")	0		62		123		188		250
Relaxation Values (2 ")	0				125				250

Table 3.3. shows that in this particular example the errors introduced by relaxating on a coarse mesh are negligible Such close agreement between the 'precise' and relaxation values could hardly be expected for cases where $c \neq 0$ but there is indication that a reasonable picture is obtained even with a coarse network.

DISTRIBUTION OF p_{xx} ON SECTION MIDWAY BETWEEN TWO CRACKS

One of the questions that the author hoped to decide by this analysis was - What are the main factors influencing crack spacing in a non-bonded beam?

Close to a crack the stress in the bottom fibres of a beam is zero. As the point considered is moved away from the crack a tensile stress builds up. This stress is a maximum midway between two adjacent cracks. All other things being equal, the greater the distance between these cracks the greater will be the tensile stress and the more likely it becomes that a new crack will be initiated there.

Figure 3.14 shows the distribution of p_{xx} on the plane midway between two cracks for a variety of crack spacings and crack depths. It shows that there is practically no build-up of tensile stress in the bottom fibres for crack spacings of $\frac{1}{4}$ and $\frac{1}{2}$ beam depth (c = 2 and 4). At the other extreme where the crack spacing is twice the beam depth (c = 16) the tensile stress builds up practically to the maximum possible. This is shown by comparing these curves with those for infinite crack spacing. The top diagram in figure 3.14 shows the effect of the crack extending to full depth. This is included because it shows the maximum possible effect of increasing crack depth. It is of little practical interest because it implies infinite stresses in the infinitely small compression zone above the crack.

In figure 3.15 the bottom fibre tensile stress is plotted to show the effect of crack depth and crack spacing.

Figure 3.15 shows that the bottom fibre tensile stress only increases with crack depth for the wider crack spacings. For example when c = 4 the tensile stress increases with for η less than 2 and that it decreases as the crack gets deeper. This is assuming that the steel force remains constant. Thus provided that the increase in steel force is not too great and the crack spacing is small the tendency to form more cracks between those already established decreases as the original cracks become deeper.

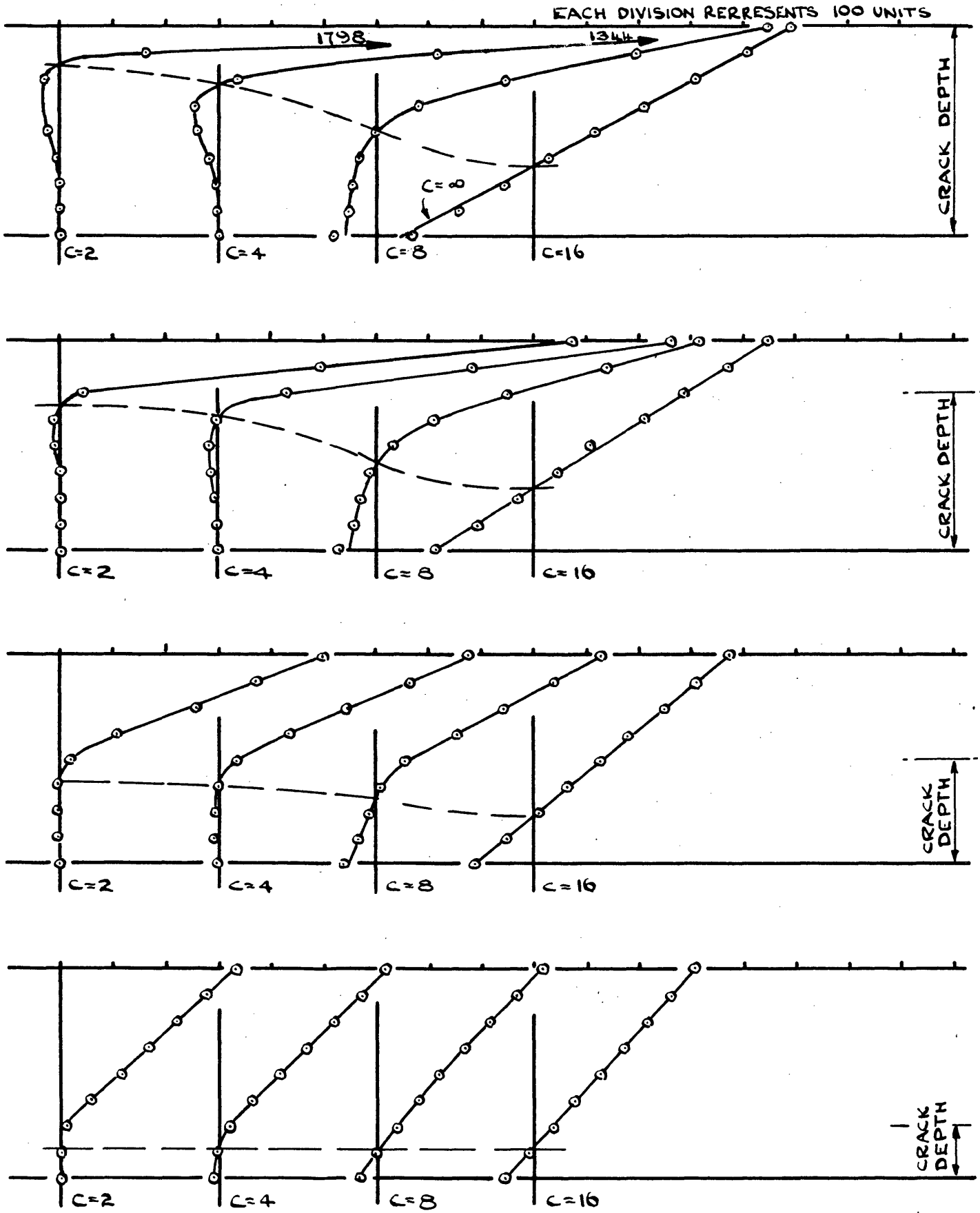

FIGURE 3.14

C=1000

STRESS DISTRIBUTION ON PLANE MIDWAY BETWEEN TWO CRACKS

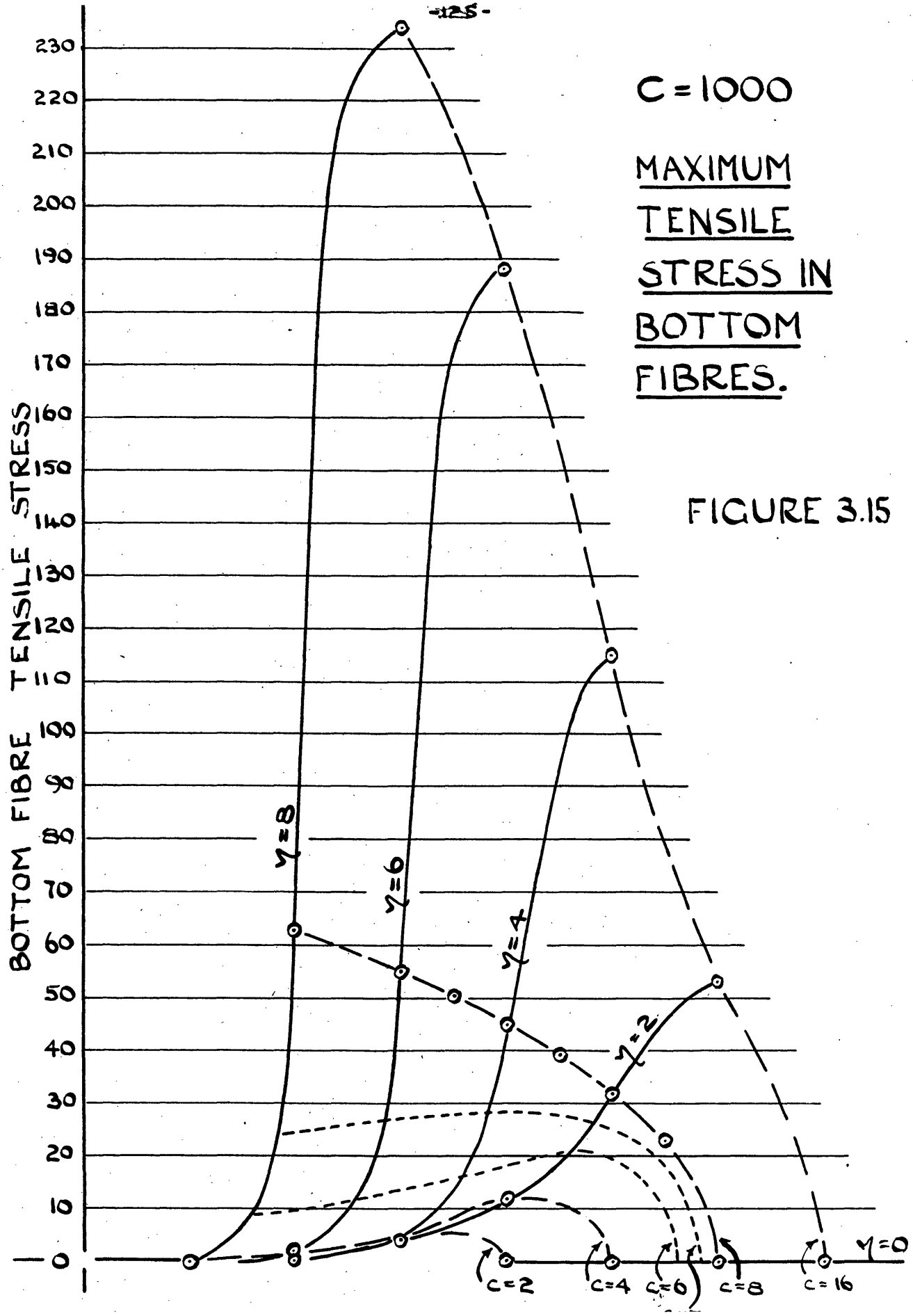
C = 1000
MAXIMUM TENSILE STRESS IN BOTTOM FIBRES.
BOTTOM FIBRE TENSILE STRESS
230
220
210
200
190
180
170
160
150
140
130
120
110
100
90
80
70
60
50
40
30
20
10
0
γ=8
γ=6
γ=4
γ=2
γ=0
C=2
C=4
C=6
C=8
C=16

FIGURE 3.15

The upper limit to the crack spacing is obtained by sketching in the curves for c = 6, and 7 in figure 3.15. The method of plotting used enables this to be done with fair accuracy (ref. 20). The result gives c = 7 (i.e. as d = 8 this means a crack spacing of $\frac{7}{8}$ beam depth) as the limiting value. For $c > 7$ the bottom fibre tensile stress increases with η, and for $c < 7$ the stress decreases once η is greater than $\frac{1}{4}$ beam depth.

This can be summed up by saying that if the cracks are spaced closer than $\frac{1}{8}d$ then further cracking will not take place unless (a) the steel force increases substantially or (b) the crack depth is less than $\frac{1}{4}d$. It can be seen that neither of these exceptions is likely. In non-bonded beams the steel force does not increase very much. This is verified by reference to the experimental results given on pages 89-91. In beam No.1 p.89 increases from 360 at cracking to 532 at failure, in beam No. 111 the increase is from 825 to 924 and in beam No.V from 1167 to 1207. At first glance the increase in beam I appears to be substantial, 48%. There is a corresponding increase in the tensile stress, but as we shall see below the increase is not sufficient to increase the tensile stress to the value which originally caused cracking.

It is suggested in the preceeding paragraph that crack depth/

depth is not likely to be less than one quarter of the beam depth. This is demonstrated by considering the stress distribution immediately before and after cracking. The two conditions are indicated in figure 3.16.

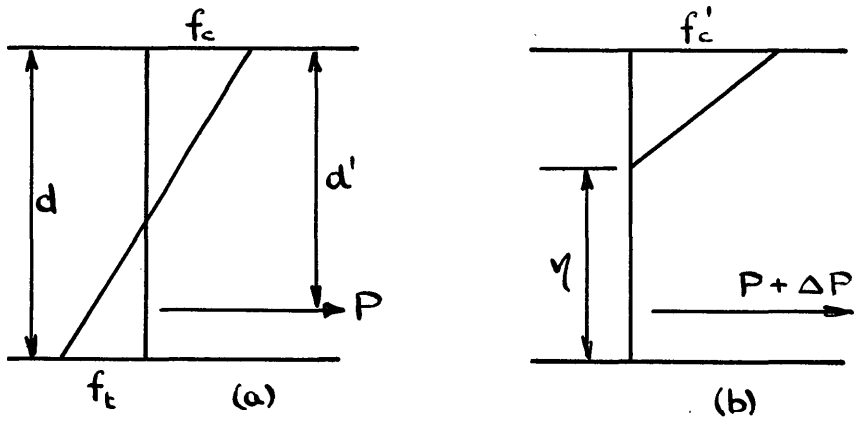

Figure 3.16

Just before cracking we have compressive and tensile stresses f_c and f_t. On cracking f_c increases to f_c' and the steel force increases from P to P + Δ P. Let this take place at moment M.

Take moments about the bottom fibre for the uncracked case

$$M = \frac{1}{3} f_c b D^2 - \frac{1}{6} f_t b D^2 - P(D-d)$$

equating forces

$$P = \tfrac{1}{2}(f_c - f_t)\, bD$$

After cracking

$$M = (P + \Delta P)\left(d - \frac{1}{3}\overline{D-\gamma}\right)$$

Eliminate M and f_c from these equations and we get

$$2\eta P + 6\,\Delta P\left(d - \frac{1}{3}(D - \eta)\right) = f_t b D^2.$$

Experience shows that ΔP is only about 1% P and so may be neglected in the above equation. This gives

$$\frac{\eta}{D} = \frac{f_t b D}{2P}$$

The results of II chapter 4 give f_t = 1/20 to 1/10 the cube strength (C_u).

In practice the top fibre stress for zero bottom stress will be 1/6 to 1/3 of the C_u so that $2P/bd$ = (1/6 to 1/3)C_u. Substituting for f_t and P we find $\frac{\eta}{D}$ = 3/20 to 3/5. The higher value occurs with the lower pre-stress. The initial crack depth is seen to vary over a fairly wide range but will be at least 0.15 D and that it will only be so small for concrete with rather low tensile strength. Experiments show that the crack deepens very rapidly at first so that the critical value of $\frac{1}{4}$D will soon be passed even if the crack is not initially so deep.

In the table below f_t is calculated for P(=C) of 1000 with b = 1 and D = 8 whilst η is varied.

η =	1	2	3	4	5	6	7	8
f_t =	16	31	47	63	78	94	110	125

This table together with figure 3.15 makes it possible to say whether or not there is a possibility of the creation of new cracks between those already developed. Two examples will illustrate this:-

(i) Suppose that two cracks appear 7 units apart and that the depth of the cracks, η , is 4 units. The above table shows that for c = 1000, f_t (that is the tensile stress just before cracking) = 63 units. Referring now to figure 3.15 we see that no matter how deep the cracks become the bottom fibre stress cannot reach the original cracking value unless the steel force increases. In fact the tensile stress will have its maximum at the instant of cracking for as the crack depth increases the tensile stress decreases slightly. The maximum value of the stress is 28 units so that the steel force must more than double itself before the original cracking stress is exceeded.

(ii) Suppose that the critical crack depth is 3 units whilst the spacing is 8 units. The table gives the cracking value of $f_t = 47$. Referring to figure 3.15 we see that this stress will be reached when $\eta \approx 4\frac{1}{2}$.

Before concluding the observations on the likelihood of new cracks being formed between those already established it/

it is necessary to define the limits of the arguments used above. The calculated values of the bottom fibre stresses apply only as long as the basic assumptions are true. The most important of these is the assumption that the cracks rise vertically. This is approximately true until the cracks become deep when there is a tendency to bifurcate. Sometimes the two branches continue to rise as the bending moment is increased and sometimes they run practically parallel with the axis of the beam and new vertical cracks rise from the main branch.

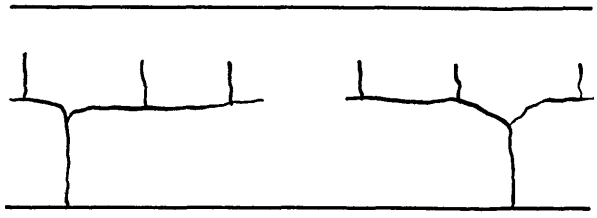

The shape of the cracks is indicated in figure 3.17.

Figure 3.17

The reason why the cracks split into two branches is indicated in figure 3.11. At the top of the crack there is a large tensile stress parallel to the crack. When this stress exceeds the tensile strength of the concrete the material urptures at right angles to the original crack.

The author has stated already that he considers any attempt to trace the subsequent course of the cracking to be beset by great computational difficulties. It is also his opinion that the expenditure of effort would not be justified.

However, having demonstrated the existence of the stress which causes the cracks to fork it is possible to explain the subsequent behaviour in general terms.

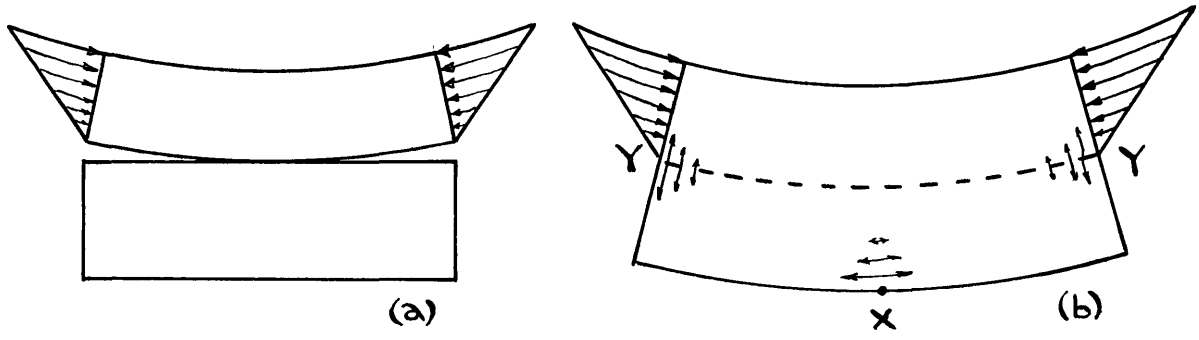

Figure 3.18

Imagine the block contained between two vertical cracks to be sliced away from the upper section of the beam. The latter will bend as indicated in figure 3.18(a) whilst the lower section will be stress-free and underformed. In order to rejoin the two peices the lower section must be bent round the upper section and the joint must be capable of sustaining the tensile stress indicated in 3.18(b). At the same time tensile bending stresses are introduced into the lower fibres of the completed beam. The bottom fibre stress has been examined in detail. If it exceeds the tensile strength a crack forms at X, we shall see that this has the effect of lowering the tensile stress at Y and thus reducing the tendency for the cracks to fork. If, on the other hand, the stress at Y exceeds that at X

then/

then it is more likely that the existing cracks will fork rather than that a new crack will be formed at X. Once the existing cracks do fork the effect is to lower the stress at X for the material between two cracks tends to straighten out as indicated in figure 3.18(a). When this happens the material below the cracks is effectively no longer part of the beam and the author has seen cases where two horizontal cracks have joined, and but for the fact that the reinforcement passed through the isolated block the latter would have fallen out. The 'new' beam is much shallower than the original one so that the new vertical cracks which are formed are much closer together than the original ones. This is indicated in figure 3.17 and is borne out by experience.

Values for the tensile stress at Y for C=1000 are tabulated below.

TENSILE STRESS AT THE TOP OF A CRACK

η =		0	1	2	3	4	5	6	7	8
c =	2	0	-	8	-	18	-	62	-	-
	4	0	-	24	-	52	-	115	-	-
	8	0	9	41	58	104	169	288	-	-
	16	0	-	33	-	112	-	302	-	-

These values can be compared with the stresses at X given in figure 3.15. It is found that the stress at Y exceeds that at X in all cases to the right and above the heavy zig-zag line. It is evident that when the crack spacing is less than the beam depth the existing cracks will fork rather than permit the formation of intermediate cracks. The reverse is the case for wider crack spacing except when the existing cracks become deep and extend more than half-way up the side of the beam.

The general conclusion to be drawn is that the average crack spacing in non-bonded beams will be approximately equal to the beam depth. Experience shows this to be so.

III Chapter V THE BEARING OF THE ABOVE ANALYSIS ON THE INTERPRETATION OF STRAIN GAUGE READINGS

The distribution of strain in concrete beams is generally determined as described in Part II Chapter III, that is by attaching a series of strain gauges down the depth of the beam. Reference has already been made to the work of Mygind and Binns (16) who showed that short gauge lengths are undesirable because of the tendency to record abberations caused by local lack of homogeneity. Below we shall study the effect of varying the gauge length upon the strain recorded when the material is 'perfect' but in which the stress distribution is not the ideal triangular one usually assumed.

DERIVATION OF STRAIN FROM RELAXATION SOLUTIONS

A strain gauge records the average strain over the gauge length. Thus if we wish to calculate the reading which would be obtained from a strain gauge we must integrate the total movement over the gauge length to obtain the average value. This is done quite simply from the relaxation solutions already obtained.

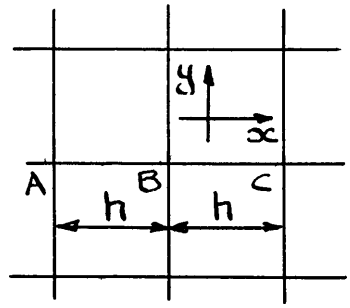

Figure 3.19

The strain in the x direction at point A (figure 3.19) is

$$e_{xx} = \left\{ p_{xx} - \sigma p_{yy} \right\} / E$$

σ being Poisson's ratio and E Young's modulus. The change in the length AC is

$$\frac{h}{2} e_{xx}(A) + h e_{xx}(B) + \frac{h}{2} e_{xx}(C)$$

The average strain over length AC is this latter quantity divided by AC so that

$$e_{xx}(AC) = \tfrac{1}{2}\left\{ \tfrac{1}{2} e_{xx}(A) + e_{xx}(B) + \tfrac{1}{2} e_{xx}(C) \right\}$$

If the gauge length extends over n mesh lengths then

$$e_{xx}(AN) = \frac{1}{n}\left\{ \tfrac{1}{2} e_{xx}(A) + e_{xx}(B) + \cdots + e_{xx}(M) + \tfrac{1}{2} e_{xx}(N) \right\}$$

The stress which will be interpreted from such a gauge reading is $e_{xx}(AN) \times E = \bar{p}_{xx}(AN)$. and

$$\bar{p}_{xx}(AN) = \frac{1}{n}\left\{ \tfrac{1}{2} p'_{xx}(A) + p'_{xx}(B) + \cdots \cdots \tfrac{1}{2} p'_{xx}(N) \right\}$$

where

$$p'_{xx} = p_{xx} - \sigma p_{yy}$$

Figure 3.12 shows that the most severely stressed transverse section of a beam is that containing a crack whilst the least severe section is that midway between two cracks. It is the maximum stresses which are of greatest significance and correspondence between these and the measured strains will be poorest when the latter are taken symmetrically about a line midway between two cracks.

It is this worst case which will be considered in the following work. The effect of varying the gauge length on the correspondence between p_{xx} and p_{xx} (at crack) will be demonstrated.

It has been shown by Jones (21) that Poisson's ratio for concrete varies between 0.2 and 0.3. An average value of 0.25 will be used here.

The work of the last chapter has shown that the cracks are unlikely to rise vertically if the crack spacing is greater than the beam depth so that in the following work there is little point in considering the case where $c < d$. We will study two crack spacings, one with $c = d$ and the other $c = \frac{1}{2}d$.

Figure 3.20 gives the stress distribution deduced from strain gauge readings when the crack depth is three-quarters of the beam depth. When the crack spacing is equal to the beam depth the discrepancy between the measured and 'actual' stresses is considerable even when the gauge length equals the crack spacing. When the crack spacing is halved the discrepancy becomes quite small. When the cracks are widely spaced the gauge length has a large effect upon the value of the measured stress whilst with the smaller spacing the effect is small.

The best basis for comparison is to express the difference between the measured and 'actual' stress at any level as a percentage of the maximum (i.e. top fibre) stress. This has been done in figure 3.21.

The following can be inferred from this diagram:-

(a) The errors in stresses deduced from strain gauge readings can be very much in error if the crack spacing is wide and the cracks are deep. With a crack depth of $\frac{3}{4}$d a gauge length equal to the crack spacing the error is less but still considerable at 22%.

(b) With a crack depth not greater than one half the beam depth the error in the top fibre stress is less than 10% whatever the gauge length.

(c) There is always a fair error at the neutral axis. This is because the measured neutral axis is always lower than the top of the crack.

This latter point deserves of a little elaboration. When the strains are plotted for a gauge length equal to the crack spacing it is found the distribution is linear above the top of the crack. This can be seen in figure 3.20 where the stresses deduced from readings on the long dashes above the top of the crack.

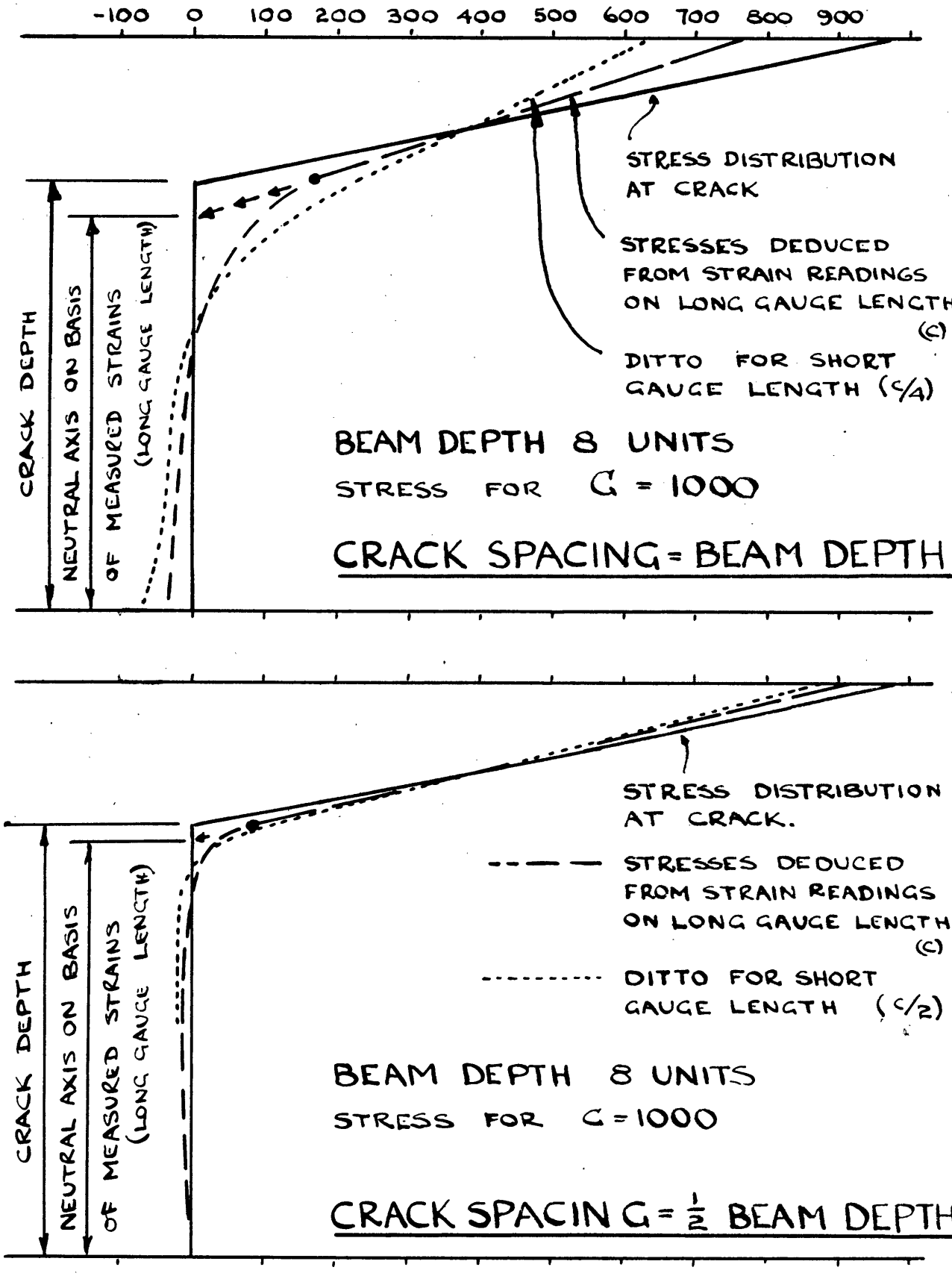
-100 0 100 200 300 400 500 600 700 800 900
CRACK DEPTH
NEUTRAL AXIS ON BASIS OF MEASURED STRAINS (LONG GAUGE LENGTH)
STRESS DISTRIBUTION AT CRACK
STRESSES DEDUCED FROM STRAIN READINGS ON LONG GAUGE LENGTH (c)
DITTO FOR SHORT GAUGE LENGTH (c/4)
BEAM DEPTH 8 UNITS
STRESS FOR G = 1000
CRACK SPACING = BEAM DEPTH
CRACK DEPTH
NEUTRAL AXIS ON BASIS OF MEASURED STRAINS (LONG GAUGE LENGTH)
STRESS DISTRIBUTION AT CRACK.
STRESSES DEDUCED FROM STRAIN READINGS ON LONG GAUGE LENGTH (c)
DITTO FOR SHORT GAUGE LENGTH (c/2)
BEAM DEPTH 8 UNITS
STRESS FOR G = 1000
CRACK SPACIN G = ½ BEAM DEPTH

FIGURE 3.20

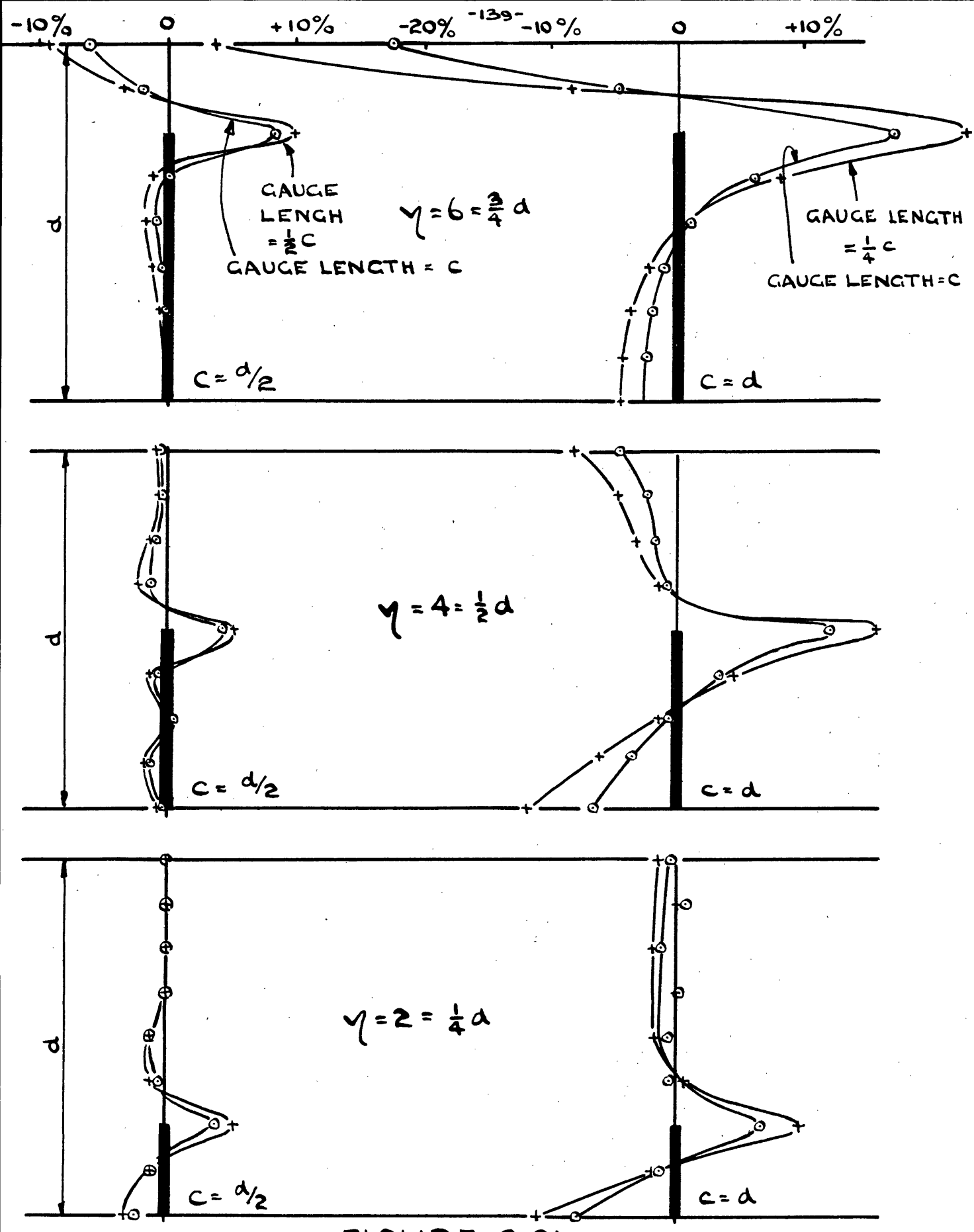
-10%
0
+10%
-20%
-10%
0
+10%
d
GAUGE LENGH = ½C
GAUGE LENGTH = C
η = 6 = ¾ d
C = d/2
GAUGE LENGTH = ¼ C
GAUGE LENGTH = C
C = d
d
η = 4 = ½ d
C = d/2
C = d
d
η = 2 = ¼ d
C = d/2
C = d

FIGURE 3.21

Over the length between the two heavy dots the distribution is quite linear. This result is implicit in the basic assumptions and so provides a check on the work. It is assumed that an infinity of blocks are loaded by an eccentric compressive force. On this basis the interface between two blocks must remain plane. This is accounted for in the boundary conditions by making the shear stress at the interface zero. The neutral axis fails to coincide with the top of the crack because in translating strains into stresses we have assumed that $p_{xx} = E\, e_{xx}$. This has been done tacitly as it usually is when analysing the results of tests. p_{xx} is zero at the top of a crack but $e_{xx} \neq 0$ because of the stresses parallel to the crack. When the position of the neutral axis is determined by plotting the horizontal strains the depth of the compression zone will always appear greater than the actual depth. This is illustrated in figure 3.22.

It can be seen that with the wider crack spacing the depth of the neutral axis as given by strain readings over a long gauge length may be appreciably in error. With the closer spacing the error is not great. If a smaller gauge length is used on the line midway between two cracks the errors will be worse.

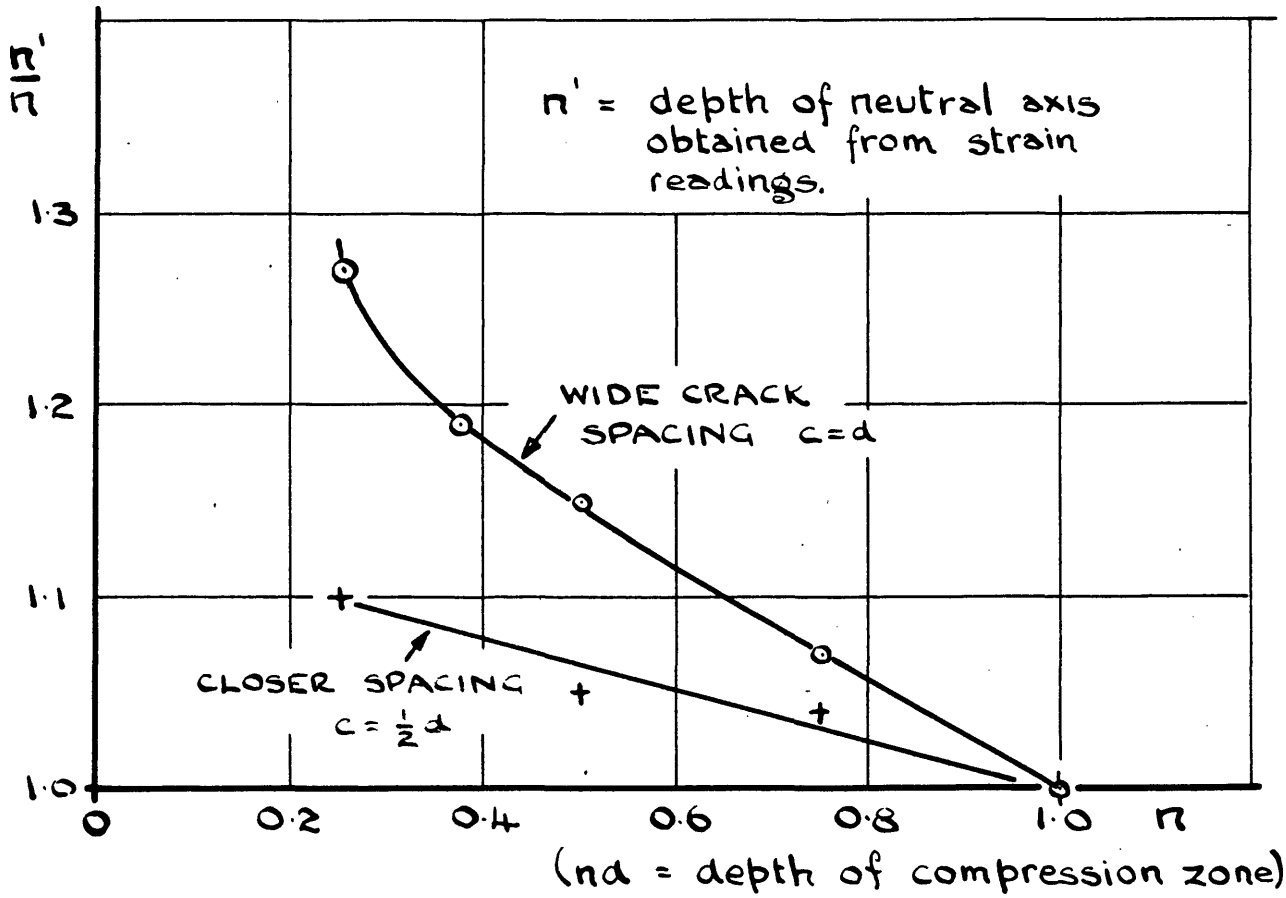
n'/n
n' = depth of neutral axis obtained from strain readings.
1·3
1·2
1·1
1·0
WIDE CRACK SPACING c=d
CLOSER SPACING c = ½d
0
0·2
0·4
0·6
0·8
1·0
n
(nd = depth of compression zone)

FIGURE 3.22

III Chapter VI THE EFFECT OF THE PHENOMENA DESCRIBED ABOVE ON THE STRESS STRAIN CURVE DEDUCED FROM READINGS ON A BEAM.

It was stated on p.18 that the author's method of determining the stress strain curve from measurements on a test beam depends solely upon the validity of the assumptions on which it is based. These assumptions are given on p.21 A further assumption is also generally made in practice. It is that the strains can be measured directly by a strain gauge. We have seen that the strains so measured contain a component due to the stresses induced at right angles to the axis of the beam. Strictly speaking this component should be deducted from the measured strains before applying the analysis to determine the stress-strain curve. It would be very difficult to do this and in practice the analysis must be applied to the uncorrected readings. This means that the neutral axis will appear to be rather low giving a deeper compression zone which in turn will tend to cause the analysis to give a low value for the top fibre stress. This is counteracted by the shorter lever arm tending to increase the stress. If a long gauge length is used this stress will be related to a strain which will also be lower than the peak value above the crack. It is found in practice that measurement of the strains below the neutral axis does not give results of any value and the bottom

fibre/

fibre strain has to be determined by extrapolation from the strains above the neutral axis. This procedure will be followed using the strains calculated in the last chapter. Figure 3.23 shows the depth of the neutral axis plotted against measured top fibre stress for C = 1000.

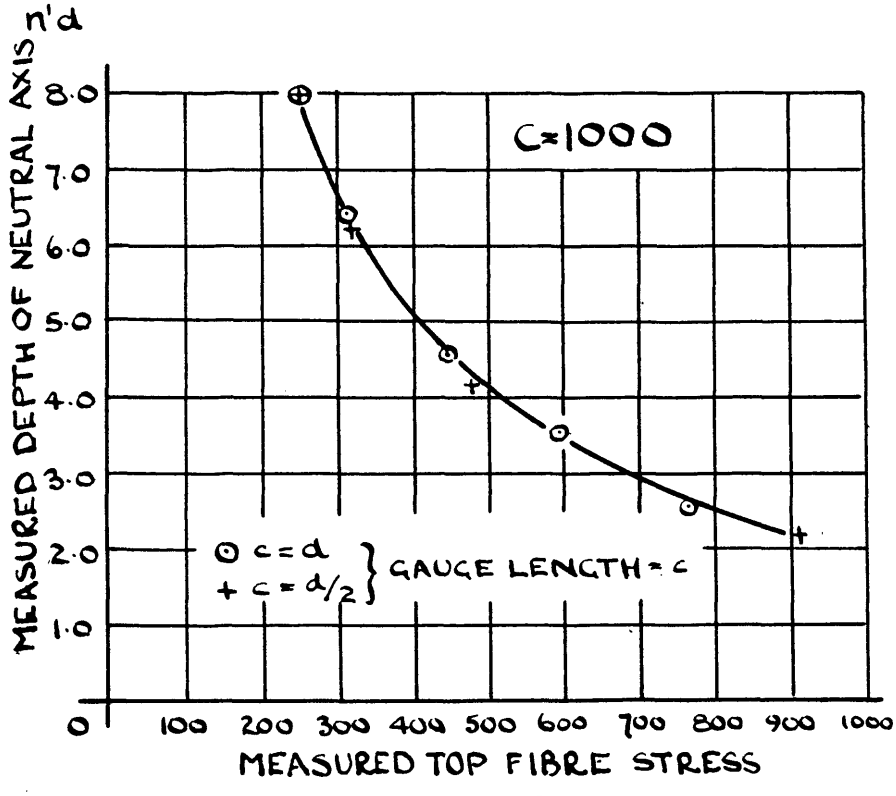

FIGURE 3.23

This data has been plotted for two crack spacings one equal to beam depth and one equal to one half beam depth. In each case the gauge length equals the crack spacing. It will be noticed that the two curves are indistinguishable and so will lead to the same stress strain curve.

On page 21 the following relationship is given for a cracked beam

$$\int_c b\,d = \frac{d}{de_c}\{P(e_c - e_t)\}$$

In a non-bonded beam P does not increase very much as the results on pages 98-100 show and if it is taken to be a constant the conditions will approximate to these in a non-bonded beam. The above equation then becomes

$$\int_c b\,d = P\left(1 - \frac{de_t}{de_c}\right)$$

Using this equation and the data given in figure 3.23 we can compute the stress strain curve which would be deduced from the strain readings and compare it with the actual stress strain curve. e_t is obtained by using the equation

$$e_t = \frac{nd-d}{nd} \times e_c$$

Since de_t/de_c is dimensionless it is not necessary to convert the measured top fibre stress to strain in this expression. The calculation is conveniently tabulated as below.

$e_c.E$	250	300	350	400	450	500	550	600	650	700	750
nd	8.0	6.68	5.78	5.10	4.57	4.15	3.80	3.45	3.16	2.90	2.69
$e_t.E$	0	-59	-135	-228	-337	-464	-607	-791	-994	-1230	-1480
$-de_t/de_c$		1.35	1.69	2.02	2.36	2.70	3.27	3.87	4.39	4.86	5.30
$1-de_t/de_c$		2.35	2.69	3.02	3.36	3.70	4.27	4.87	5.39	5.86	6.30
f_c	250	294	337	378	420	463	535	610	674	732	788

The figures in the bottom line have to be compared with those in the top line. The latter is labelled e_c but it is actually the stress corresponding to e_c, e_c being the measured strain in the top fibre. If the figures in this line were divided by E and then used as a base for the bottom line of figures we should get the stress strain curve for the material as obtained by the author's method of analysis. The curve has been plotted in figure 3.24 without the introduction of E.

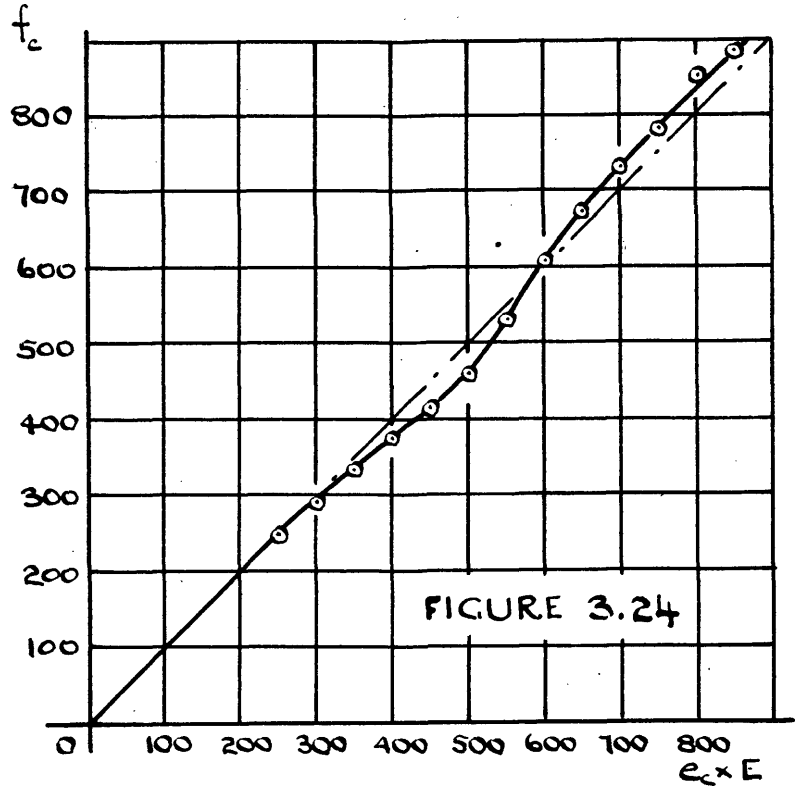

FIGURE 3.24

It seems that the agreement is very good and that the method of analysis will give a fair interpretation of stress-strain curve despite the inaccuracies in measuring the top fibre strain and the position of the neutral axis. It appears that these two discrepancies just counteract each other. The low neutral axis results in a low stress being computed but as this is compared with the low strain resulting from the measurement of the mean rather than the peak value the resultant point lies very close to the proper stress-strain curve.

It seems likely that if the analysis were extended into the plastic range the discrepancy would worsen.

It is interesting to compare the computed top fibre stress in figure 3.24 with the actual peak stress above a crack. This is done in figure 3.25. All quantities are plotted to the base $e_c xE$ i.e. the measured strain xE.

For the smaller crack spacing (one half beam depth) the discrepancies are very small, and it is fair to say that the measured top fibre strain is a fair measure of the peak top fibre strain.

Furthermore the author's analysis also gives reasonable agreement with the actual stress.

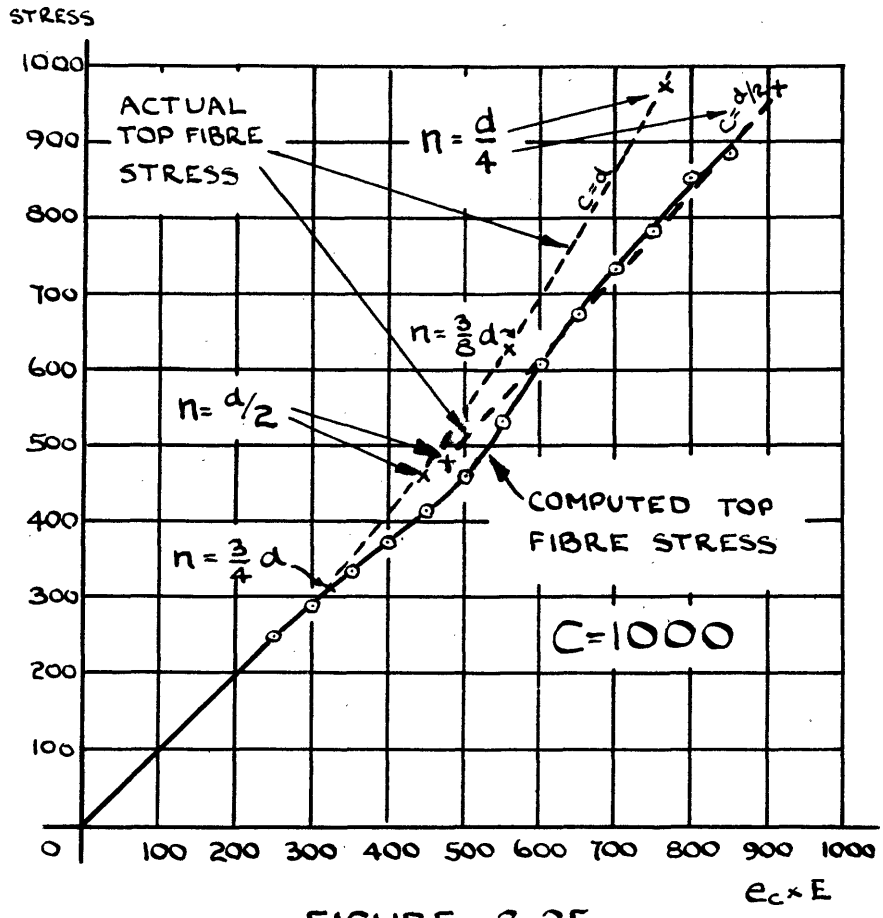

FIGURE 3.25

With the wider crack spacing (c = d) agreement is not so good especially where the cracks become deep. Provided that the cracks do not extend beyond one half beam depth there is little variation between the measured, computed and actual stresses agreement is still reasonable when the cracks extend to $\frac{5}{8}$ beam depth but beyond that accuracy will be poor.

We have already seen that in non-bonded beams the crack spacing is likely to be approximately equal to the beam depth and the general conclusion to be drawn from the above is that the author's analysis cannot be expected to give a very precise stress strain curve once the cracks extend more than half-way up the beam. Matters are complicated because of the tendency for the cracks to fork. If this happens it is very difficult to assess the accuracy of the deduced stress-strain curve and it cannot be assumed that the result is more than a rough approximation.

With bonded beams the cracks are much more closely spaced and it seems that the author's analysis will give fair results however deep the cracks become.

PART IV THE DISTRIBUTION OF STRESS IN A CUBE WHEN COMPRESSED BETWEEN RIGID ROUGH PLATES.

Chapter I INTRODUCTION.

It is well known that the strength of concrete depends very much on the shape of the specimen tested. The Handbook on the B.S. Code of Practice for Reinforced Concrete (CP 114) for instance points out that the concrete strength realised in columns is about two-thirds of that obtained by crushing a 6" cube of the same type of concrete. Mr. C.S. Whitney gives the ratio of column to cylinder (i.e. 12" x 6" dia.) strength as 0.85 (6). This variation in strength is due to varied degrees of end restraint. In a column with no binding reinforcement the lateral expansion of the concrete is unrestrained whilst in cube and cylinder tests lateral restraint is effected by friction between the specimen and the plates between which it is compressed. This lateral support enables the concrete to sustain a greater stress than is possible in the unsupported case. The restraining effect is greater with the cube than with the cylinder because of the decreased height to breadth ratio.

The aim of the work in the following pages is to determine the nature of the stresses set up by this frictional restraint/

restraint and to attempt to assess the value of the stress strain curves obtained in 'simple' compression tests.

The analysis is confined to consideration of the elastic behaviour of the material. Any conclusions drawn from this work as to the plastic behaviour of test specimens will therefore be somewhat tentative. This restriction is irksome but as yet unavoidable as present-day methods of analysis are inadequate for extending the investigation into the plastic range. It will be seen that even with elastic behaviour the analysis is very complex.

HISTORICAL REFERENCES.

The problem of determining the distribution of the stress in a circular cylinder compressed between rigid rough plates was attacked by Filon in 1902 (22). The general solution is given for the stress distribution in a circular cylinder subject to the following boundary conditions:-

(i) The total force over the plane ends is $\pi a^2 Q$, the actual distribution of normal pressure being unknown.

(ii) The ends are constrained to remain plane.

(iii) The ends do not expand along the perimeter. This condition is satisfied by allowing a shear stress of unknown distribution over the plane ends.

Of these conditions only (iii) calls for comment. This assumption implies that although no overall expansion is permitted at the ends slip is permitted provided that it does not occur at the perimeter. The ideal solution would be obtained if no slip at all were permitted. Filon regards the possibility of attaining this end in the following words:- "The analytical complexity of such a complete solution would be very great and would render it quite beyond the reach of arithmetical expression, and consequently valueless for the purposes of the engineer and physicist". This was written before the advent of electronic computers and Filon's pessimism may no longer be justified. However, as we shall see modern methods of attack which concentrate on obtaining a numerical solution to a particular problem enable Filon's difficulty to be avoided. Filon evaluates his general solution for the case where the ratio of the height to diameter is $\pi/3$ and Poisson's ratio is $\frac{1}{4}$.

The same problem has been investigated by Edelman (23) using an approximate method developed by Prager and Synge (24). This method enables Edelman to assume complete fixity at the ends but as the solution is an approximate one it is not possible to say without supplementary evidence whether or not it gives a better picture than Filon's solution.

Edelman's analysis is for a cylinder of height equal to its diameter and of a material having a Poisson's ratio of 1/3. The stress distribution which he obtains is not published.

Recently a solution has been found for a cylinder of height to diameter ratio of unity and Poisson's ratio of $\frac{1}{4}$ by use of relaxation methods (25). The author (Markland) refers to two other papers by Pickett (26) and d'Appolonia and Newmark (27). Markland adequately sums up these two papers as follows:-

"Pickett adopts Fourier-Bessel series expansions for u and w and uses the boundary conditions to obtain the coefficients in the series. Two sets of coefficients are involved, and the expression for a single coefficient of one series involves all the coefficients of the other, so that the series are terminated at the fourth terms in order to calculate numerical results. At the plane ends the expressions for stresses are found to converge very slowly, and although methods appropriate to slowly converging oscillating series were used, there is some doubt as to the distribution of stress over the ends.

D'Appolonia and Newmark have used a lattice analogy, in which the cylinder is replaced by a lattice of elastic bars/

bars of certain properties. Consideration of the equilibrium of every node of the lattice under the action of bar forces and of extremely applied loads load to a sufficient number of simultaneous linear equations for the components of displacement at each node to be calculated".

The author has used the Prager-Synge technique to attack the problem of determining the stress distribution in a cube (28). In the published paper the author gives Poisson's ratio the value 1/3. This value was chosen in order that the solution might be compared with Edelman's (the author was not then aware of Pickett's paper and Markland's paper had still to be written). 1/3 is, however, too high for concrete and the analysis has been repeated for Poisson's ratio of $\frac{1}{4}$ and 1/6. In the work to follow a detailed compression is made between Filon's solution, Markland's and the author's due attention being given to the fact that the latter is for a cube whilst the other two are for a cylinder.

As far as he is aware the author alone has published a solution for the cube problem although there are solutions to two allied problems. A. and L. Foppl (29) have considered the case of a square-prism compressed at the ends which are taken to be sufficiently far apart to enable them/

them to be considered separately i.e. friction at one end is considered to have no effect at the other end. One would clearly be unjustified in using this method for a cubic specimen in which the height equals the breadth.

The allied problem of an infinite bar of square cross section compressed through a pair of lateral faces between rigid rough plates has been solved by Greenberg and Truell (29). Here the Prager-Synge method was used with Poisson's ratio equal to 1/3.

IV Chapter 2. THE DISTRIBUTION OF STRESS IN AN ELASTIC CUBE COMPRESSED BETWEEN RIGID ROUGH PLATES.

The author has already published a solution of this problem and a copy of this paper is given below. The method is one of successive approximation employing two basic theorems, one the theorem of minimum strain energy and the other a complementary theorem of maximum strain energy.

The fundamental quantity calculated is the strain energy of the body. If a stress system can be found which satisfies all the following

(1) the equilibrium equations

(2) the compatability equations

(3) the boundary conditions on stress

(4) the boundary conditions on displacement

then the solution will be exact and the true value of the strain energy is found. If, because of the complexity of the problem such a solution cannot be found then we have to be content with one which satisfies only some of these conditions. For example in the cube problem we can ignore (1) and (3) above and select a stress strain system which satisfies (2) and (4). The theorem of minimum strain energy tells us that the strain energy of this stress system will be in excess of the true value.

It is a fairly simple matter to select a number of stress systems which will satisfy the simplified problem. The Prager-Synge method combines any number of these simple systems so that they are used to the greatest advantage, that is so that the strain energy of the combined system has its lowest possible value. By adding further systems the strain energy is reduced so that approaches the true strain energy.

The maximum strain energy theorem is applied similarly except that with successive approximation the strain energy approaches the true strain energy from below.

In this way it is possible to bracket the true strain energy between upper and lower limits. The closer that these are, the more exact is the solution. Ultimately the strain energy of the body can be stated as the mean of the two limits plus or minus one half the difference expressed as a percentage. Unfortunately this does not mean that the stresses or the displacements are calculated to the same accuracy.

The method of solution is given in the printed paper for a proof of which the reader is referred to the original papers by Prager and Synge. A brief resume of the calculations is given in the Appendix.

NUMERICAL RESULTS

The printed solution is not correct. An arithmetical error was made in calculating the upper limit. The appropriate figures have been altered in the original paper and corrected ones are given below.

The error was an unfortunate one in that it suggested the solution to be very much better than it is. One of the drawbacks of the Prager-Synge method lies in the fact that there is great difficulty in checking the results when an isolated example is considered. As Hartree has pointed out recently: "One kind of 'check' is so inadequate as to be almost worthless, namely, repetition of a calculation by the same individual that did it originally. It is much too easy to make the same mistake twice ...". (31) Unfortunately this seems to be the only possible check on the evaluation of the scalar products $S_i.S_j$. The original error was discovered only when new calculations were made for a different value of Poisson's ratio, it was then possible to effect a moderately independent cross-check.

THE APPARENT YOUNG'S MODULUS

One effect of the frictional restraint of the loading plates is to increase the value of Young's modulus computed by dividing the average compressive stress by the overall longitudinal strain.

The ratio of the apparent to the true Young's modulus is given for varying Poisson's ratio in the table below.

Poisson's Ratio	True Young's Modulus / Apparent Modulus
1/3	92.9% ± 1.5%
1/4	96.1% ± 0.7%
1/6	98.3% ± 0.3%
	100%.

The above figures show that frictional restraint has little effect upon the overall strain of a cube. This does not mean that the stress distribution is modified only to a small degree as the work to follow shows. One conclusion of moderate importance can however be deduced from the above figures. It is that for most practical purposes the stress strain curve can be derived by simple overall movement of the plates of the testing machine and that there is little point in attaching strain gauge to the surface of a cube.

FRICTION STRESSES AT ENDS

The set of stresses which first claim the interest are those at the ends. Here the local shear (friction) stress must be less than the local compressive (p_{zz}) stress multiplied by the coefficient of friction or there will be slip.

ON THE COMPRESSION OF A CUBE BETWEEN RIGID ROUGH PLATES

By J. M. PRENTIS (*Imperial College, London*)

[Received 13 March 1951]

SUMMARY

The problem is to determine approximately the mode of deformation of a cube of elastic material compressed between rigid plates sufficiently rough to prevent any relative movement between the plates and the ends of the specimen. A method of solving this type of problem has been given by Prager and Synge (**1**) and is applied here to determine the relationship between the true Young's modulus and the apparent modulus obtained by a test of the type described above. As two other papers have recently been published (**2, 3**) applying the same method to similar problems, the work is given in outline only.

1. Introduction

THE method of analysis evolved by Prager and Synge for the approximate solution of elastic boundary solution problems requires the selection of a number of comparatively simple stress states which, in the aggregate, approximate to the natural stress conditions. The method of selecting the artificial states separates them into two classes, called the associated and the complementary. In one class the restrictions imposed by the equilibrium equations and the boundary conditions on stress are relaxed, whilst in the other class the compatibility equations and the imposed boundary conditions on displacements are ignored. Consideration of these two classes enables upper and lower bounds to be placed upon the total strain energy of the body. If a sufficient number of approximate states are taken in each class these bounds can be narrowed, allowing the total strain energy to be calculated to any desired degree of accuracy.

2. Following the method used by Edelman (**3**), the problem P_0 (see Fig. 1 for details) may be resolved into two components. We shall consider P_c in which the cube is subjected to a uni-axial compression, the lateral expansion being unrestricted, and P such that $P+P_c = P_0$.

3. Symmetry allows us to confine our attention to one-eighth of the body, $0 \leqslant x, y \leqslant b$, and $0 \leqslant z \leqslant h$, b and h being the breadth and height of the specimen, respectively.

The boundary conditions of P are:

$$\left.\begin{array}{ll} u_x(0,y,z) = 0 & u_x(x,y,z=h) = -\sigma a x \\ u_y(x,0,z) = 0 & u_y(x,y,z=h) = -\sigma a y \\ u_z(x,y,0) = 0 & u_z(x,y,z=h) = 0 \end{array}\right\} \text{for displacements,} \qquad (1)$$

σ being Poisson's ratio, and

$$\left.\begin{aligned} &p_{xy},\ p_{xz} = 0 \text{ for } x = b \text{ or } 0 \\ &p_{xy},\ p_{yz} = 0 \text{ for } y = b \text{ or } 0 \\ &p_{xx} = 0 \text{ for } x = b \\ &p_{yy} = 0 \text{ for } y = b \end{aligned}\right\} \text{ for stresses.} \tag{2}$$

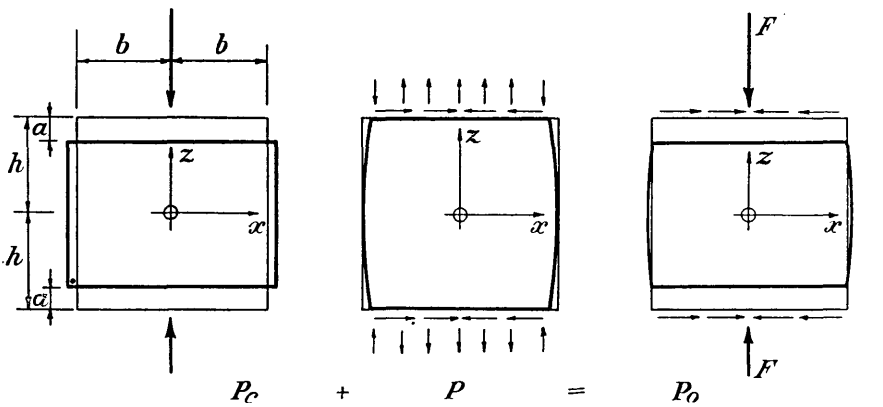

FIG. 1.

4. This is a displacement boundary condition problem and for its solution Prager and Synge require a series of states:

(*a*) The completely associated state **S***, the deformations of which must satisfy equations (1) and the strains must satisfy the compatibility equations,

$$u_{i,j}+u_{j,i} = 2e_{ij}, \tag{3}$$

where $u_{i,j}$ stands for $\partial u_i/\partial u_j$.

(*b*) A sequence of states $\mathbf{S}'_1, \mathbf{S}'_2, \ldots, \mathbf{S}'_m$, called the homogeneous associated states which must also satisfy equations (3) whilst the u' are required to vanish wherever they are prescribed on the boundary by equations (1).

(*c*) A sequence of states $\mathbf{S}''_1, \mathbf{S}''_2, \ldots, \mathbf{S}''_n$, called the complementary states selected to satisfy equations (2) and the equilibrium equations,

$$p_{ij,i} = 0. \tag{4}$$

Except that they must satisfy the required conditions given above, the states are all quite arbitrary.

5. Defining the scalar product of two states as

$$(\mathbf{S}.\mathbf{S}') = \int e_{ij}\, p'_{ij}\, dv,$$

Prager and Synge show that

$$\sum_{q=1}^{n}(\mathbf{S}^*.\mathbf{I}''_q)^2 \leqslant S^2 \leqslant (\mathbf{S}^*.\mathbf{S}^*)-\sum_{p=1}^{m}(\mathbf{S}^*.\mathbf{I}'_p)^2, \tag{5}$$

where $\mathbf{I}'$ (and $\mathbf{I}''$) are orthonormal sequences $= \sum_{r=1}^{p} c_r \mathbf{S}'_r$ and the c_r are chosen to satisfy the conditions,

$$(\mathbf{I}'_p.\mathbf{I}'_r) = \delta_{qr},$$

δ_{qr} being the Kronecker delta, and where $S^2 = (\mathbf{S}.\mathbf{S}) = 2\times$the total strain energy of the state P.

6. Selection of the states

It is necessary to specify Poisson's ratio and the relative dimensions of the specimen. We have taken $\sigma = \frac{1}{3}$ and $b = h = 1$.

The associated states selected are given in Table I, where for convenience in computation E and a are temporarily put equal to unity. The strains

TABLE I

The associated states

	u_x	u_y	u_z
S'_1	0	0	$-z(1-z^4)$
S'_2	$-xz^2(1-z^4)$	$-yz^2(1-z^4)$	0
S'_3	0	0	$-z(1-z^4)(x+y)$
S'_4	$-x^2z^2(1-z^4)$	$-y^2z^2(1-z^4)$	0
S'_5	0	0	$-z(1-z^4)(x^2+y^2)$
S^*	$-xz^4/3$	$-yz^4/3$	0

corresponding to each state are obtained from equations (3) and the stresses from

$$p_{ij} = \tfrac{3}{4}(e_{xx}+e_{yy}+e_{zz})\delta_{ij}+\tfrac{3}{4}e_{ij}.$$

The complementary states are most easily selected by use of Maxwell's stress functions ψ_i $(i = x, y, z)$, the stresses being obtained from these functions as follows:

$$p_{xx} = \frac{\partial^2\psi_y}{\partial z^2}+\frac{\partial^2\psi_z}{\partial y^2}, \quad \text{etc.},$$

and

$$p_{xy} = -\frac{\partial^2\psi_z}{\partial x\partial y}, \quad \text{etc.}$$

Thus defined, the stresses automatically satisfy the equilibrium equations. The only restrictions placed on the choice of the ψ's is that equations (2) must be satisfied. The strains are obtained from the stresses by using

$$e_{ij} = \tfrac{4}{3}e_{ij}-\tfrac{1}{3}(p_{xx}+p_{yy}+p_{zz})\delta_{ij}.$$

In selecting the complementary states, deformations are not considered, so that the compatibility equations are not, in general satisfied, and

no corresponding displacements exist. The functions used are given in Table II.

TABLE II

The complementary states

	ψ_x	ψ_y	ψ_z
S_1''	$\frac{1}{4}z^4(1-y^2)^2$	$\frac{1}{4}z^4(1-x^2)^2$	0
S_2''	$-y^2/4$	$-x^2/4$	0
S_3''	$-y^4/12$	$-x^4/12$	0
S_4''	0	0	$-\frac{1}{4}(1-x^2)^2(1-y^2)^2(1-z^4)$

7. Computation of the apparent E

Using the selected functions it is found that

$$\sum_{q=1}^{4}(\mathbf{S}^*.\mathbf{I}_q'')^2 = 0{\cdot}060697a^2E = L, \text{ say}$$

and

$$(\mathbf{S}^*.\mathbf{S}^*) - \sum_{p=1}^{5}(\mathbf{S}^*.\mathbf{I}_p')^2 = \text{0·063000}\,a^2E = U, \text{ say.}$$

The strain energies of P_c and P may be superimposed by simple addition so that $S_0^2 = S_c^2 + S^2$. It is easily seen that $S_0^2 = \frac{1}{4}Fa$ and that $S_c^2 = a^2E$. Substitution in equation (5) gives

$$L + a^2E \leqslant S_0^2 \leqslant U + a^2E.$$

Putting $\frac{1}{4}F$, the average stress, equal to f and, since $h = 1$, $a\,(= a/h) = \epsilon$, the mean e_{zz}, we obtain

$$0{\cdot}94278f/\epsilon \geqslant E \geqslant \text{0·94079}f/\epsilon,$$

or, averaging, $E = \text{0·94178}f/\epsilon$ with a maximum possible error of $\pm$0·1 per cent.

Thus, in a test of this type the true Young's modulus is 94·2 per cent. of the apparent modulus as given by the overall relative movement of the plates.

REFERENCES

1. W. PRAGER and J. L. SYNGE, 'Approximations in elasticity based on the concept of a function space', *Quart. of Applied Math.* **5** (1947), 241.
2. H. J. GREENBURG and R. TRUELL, 'On a problem in plane strain', ibid. **6** (1948), 53.
3. F. EDELMAN, 'Compression of a short cylinder between rough end blocks', ibid. **7** (1949), 334.
4. M. O. PEACH, 'Simplified technique for constructing orthonormal functions', *Bull. Amer. Math. Soc.* **50** (1944), 556.

The distribution of the resultant shear stress and of the direct stress are shown in figure 4.2 for a Poisson's ratio of 0.25. It can be seen that the tendency to slip is greatest along the diagonal of the quadrant shown. The necessary values for the coefficient of friction are tabulated below.

COEFFICIENT OF FRICTION NEEDED TO PRESENT SLIP ON DIAGONAL.

$$= \sqrt{p_{xz}^2 + p_{yz}^2} \quad / p_{zz}$$

σ	x=y=0	0.2	0.4	0.6	0.8	1.0
1/3	0	0.217	0.343	0.344	0.220	0
1/4	0	0.152	0.251	0.256	0.169	0
1/6	0	0.095	0.159	0.170	0.116	0

As a rough approximation it can be said that the coefficient of friction needed is approximately equal to the value of Poisson's ratio. The author has carried out some simple tests to determine the value of the coefficient of friction for concrete on steel. Weights were piled on to the top of a concrete cube standing on a steel plate and the lateral force necessary to move the cube was determined by means of a spring balance.

The results of these tests are given in figure 4.3. The coefficient of friction for concrete on steel is seen to vary between 0.36 and 0.79.

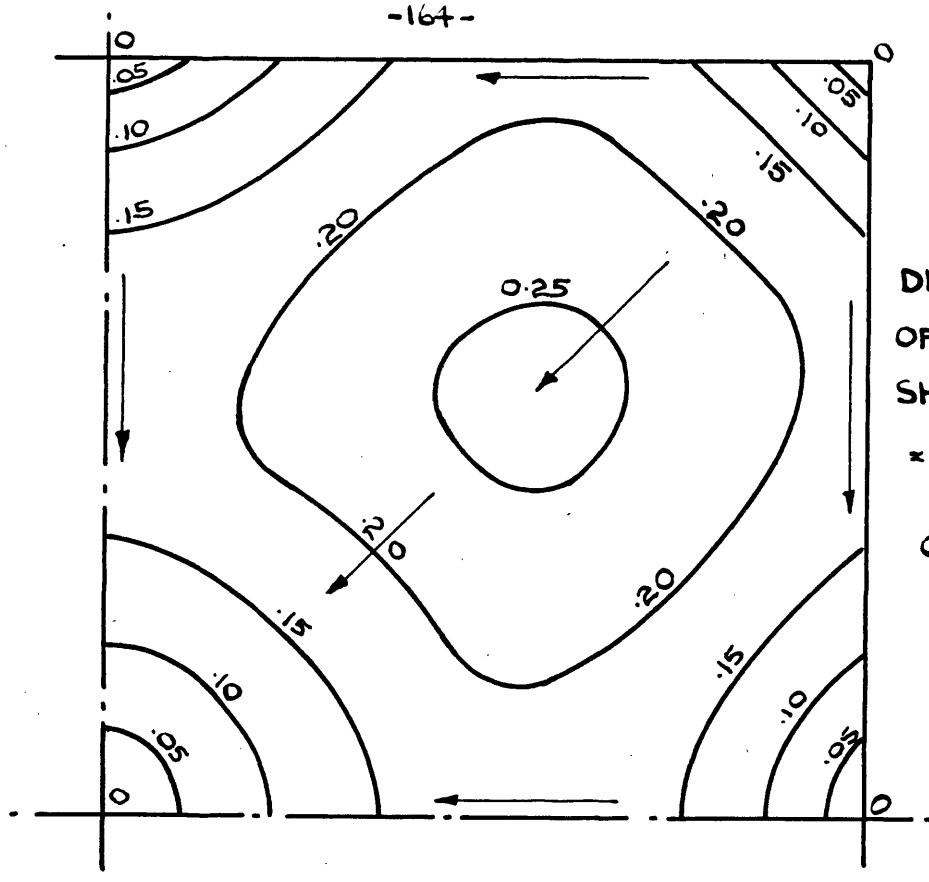
0
.05
.10
.15
.20
0.25
PLANES
$z = \pm 1$
DISTRIBUTION OF RESULTANT SHEAR STRESS
$= \sqrt{p_{xz}^2 + p_{yz}^2}$
$\sigma = 0.25$

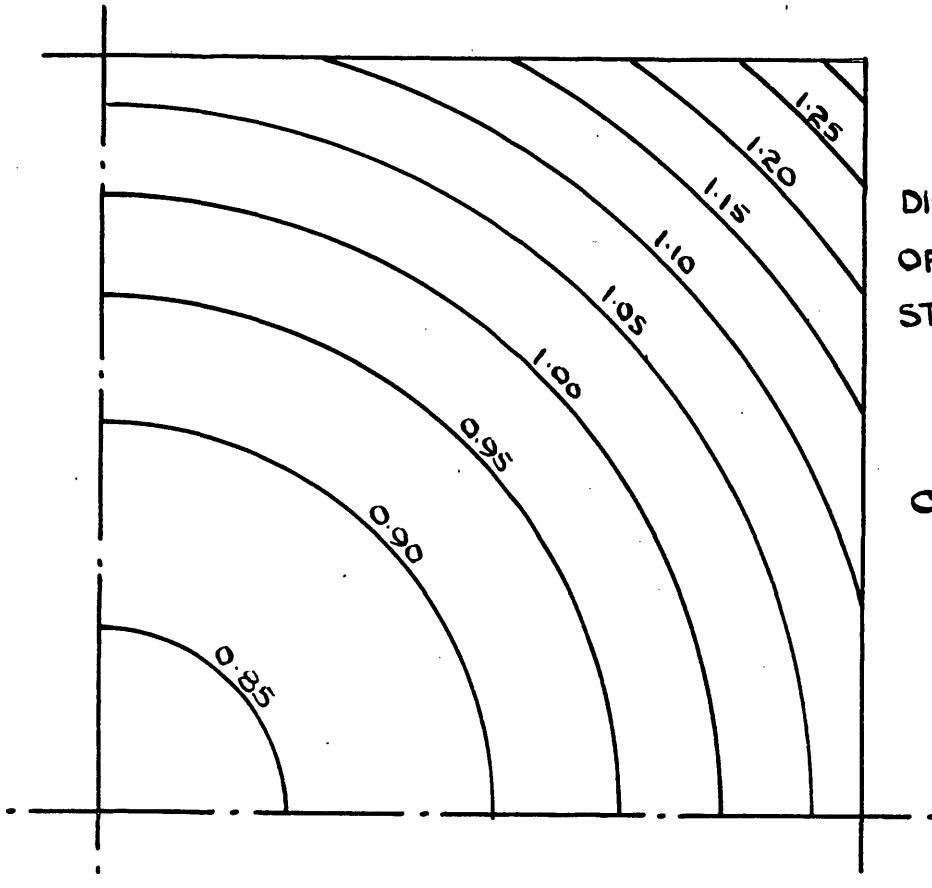
1.25
1.20
1.15
1.10
1.05
1.00
0.95
0.90
0.85
DISTRIBUTION OF DIRECT STRESS p_{zz}
$\sigma = 0.25$

FIGURE 4.2

These results were obtained for a very low contact pressure but there seems to be no reason why the coefficients should not apply to the higher stresses encountered in a practical cube test. It seems likely that the coefficient at higher contact pressures will be increased for it was found that grit particles between the forces in contact lowered the friction force. The cube tended to roll over these particles With greatly increased contact pressure such particles would become embedded in the surface of the cube or plate tending to increase the friction force.

The tests lead to the conclusion that there is little liklihood of slip for even a very high Poisson's ratio.

This observation is true provided that the stress distribution derived by the above analysis is reasonably correct. This point is dealt with in more detail later in the chapter.

Figure 4.2 shows that the stress functions assumed lead to a distribution of p_{zz} such that it is proportional to the radial distance from the axis of the cube. The maximum stress is accordingly at the outer corner. The effect of varying Poisson's ratio is seen from the results plotted in figure 4.4.

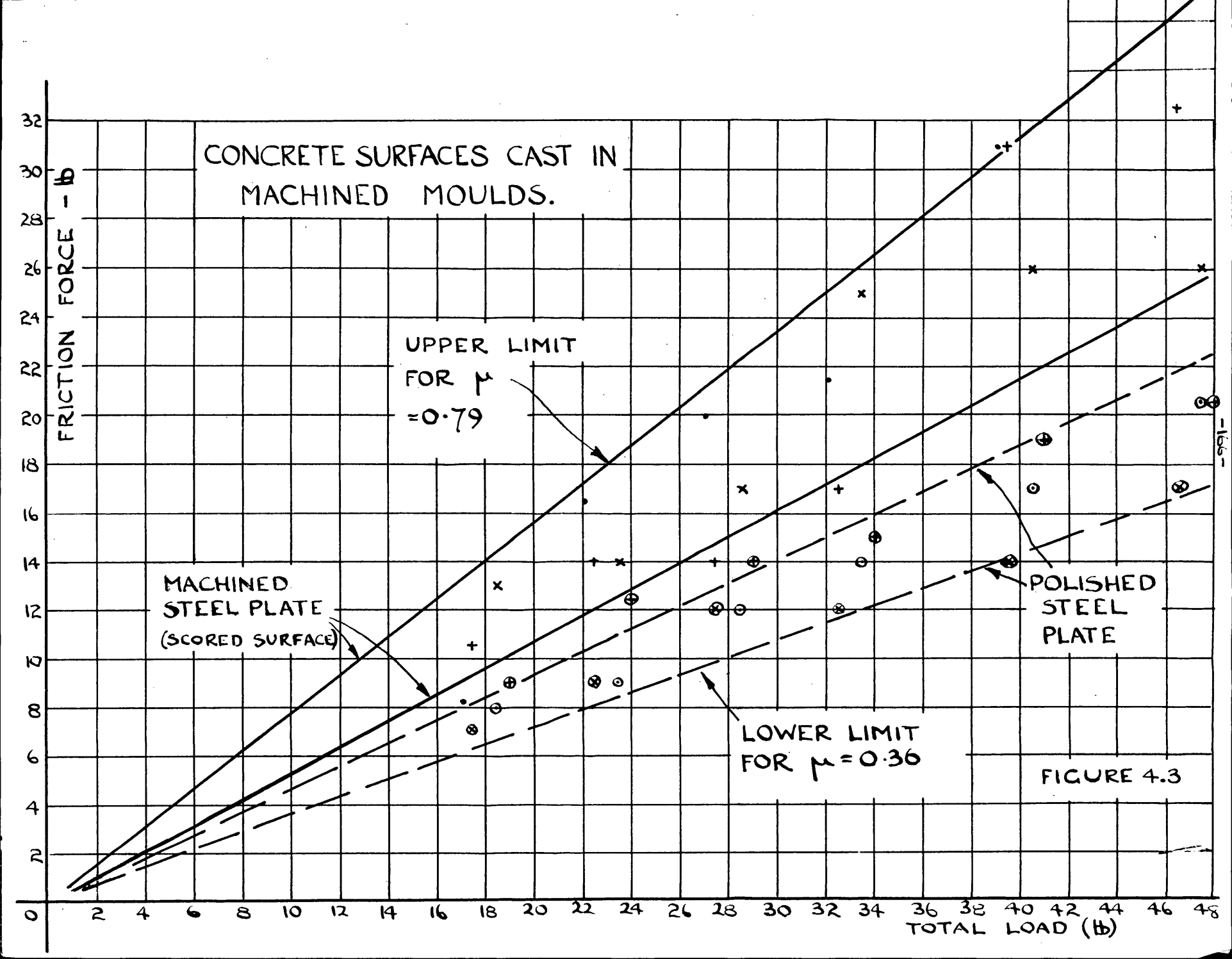
CONCRETE SURFACES CAST IN MACHINED MOULDS.
FRICTION FORCE - lb
TOTAL LOAD (lb)
UPPER LIMIT FOR μ =0·79
LOWER LIMIT FOR μ=0·36
MACHINED STEEL PLATE (SCORED SURFACE)
POLISHED STEEL PLATE
0
2
4
6
8
10
12
14
16
18
20
22
24
26
28
30
32
34
36
38
40
42
44
46
48

FIGURE 4.3

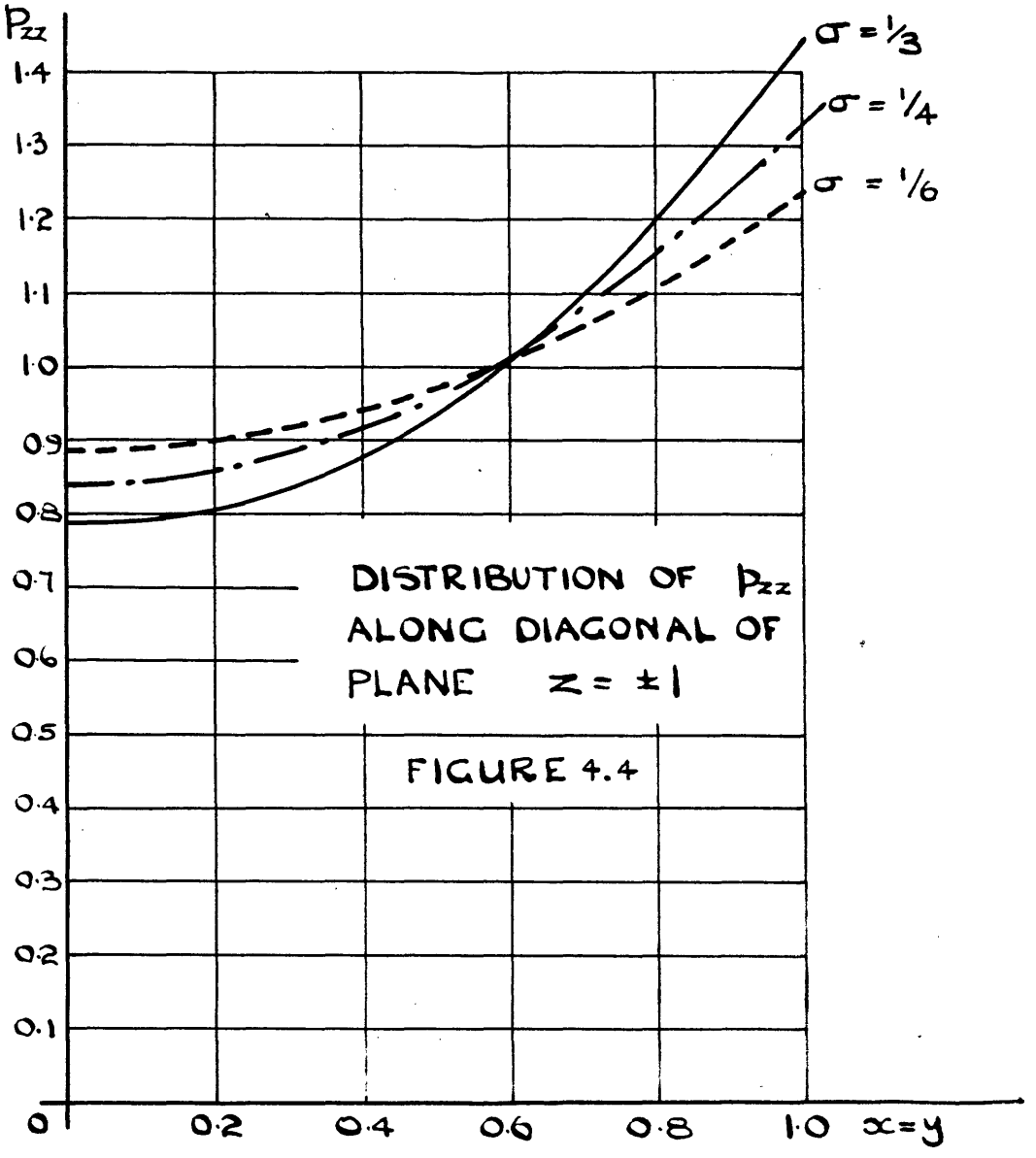
p_{zz}
1·4
1·3
1·2
1·1
1·0
0·9
0·8
0·7
0·6
0·5
0·4
0·3
0·2
0·1
0
0·2
0·4
0·6
0·8
1·0
x=y
σ = 1/3
σ = 1/4
σ = 1/6
DISTRIBUTION OF p_{zz} ALONG DIAGONAL OF PLANE z = ±1

FIGURE 4.4

STRESSES ON PLATE $y = 0$. The Axial Plane.

The stress distribution on the central plane parallel to the load is of interest because it provides a fairly complete picture of the effects of frictional restraint.

Figure 4.5 shows the distribution of the maximum principle stress parallel to the plane, this stress is everywhere compressive as is the minor principal stress. It is interesting to observe that at the ends the largest stress occurs at the outer surfaces of the cube whilst the reverse is true on the central plane, $z = 0$. The variations from the average value of unity are nowhere very large, the greatest increase in stress being a little over 5%. The last value of the stress occurs at the central point of the end plane.

The corresponding distribution published by Filon is reproduced for comparison. A number of points must be borne in mind in comparing the two figures: Firstly, Filon's solution is for a cylinder whilst the author's is for a cube: Secondly, Filon has solved precisely the case for a cylinder which is prevented from lateral movement at the outer surface on the plane ends, whilst the author's solution is an approximate one for a cube which is prevented from moving laterally all over the end planes.

DISTRIBUTION OF MAXIMUM PRINCIPAL STRESS ON AN AXIAL PLANE OF A CYLINDER AND A CUBE.

AVERAGE $p_{zz} = 1$ POISSON'S RATIO 0.25

CYLINDER - FILON'S SOLUTION.

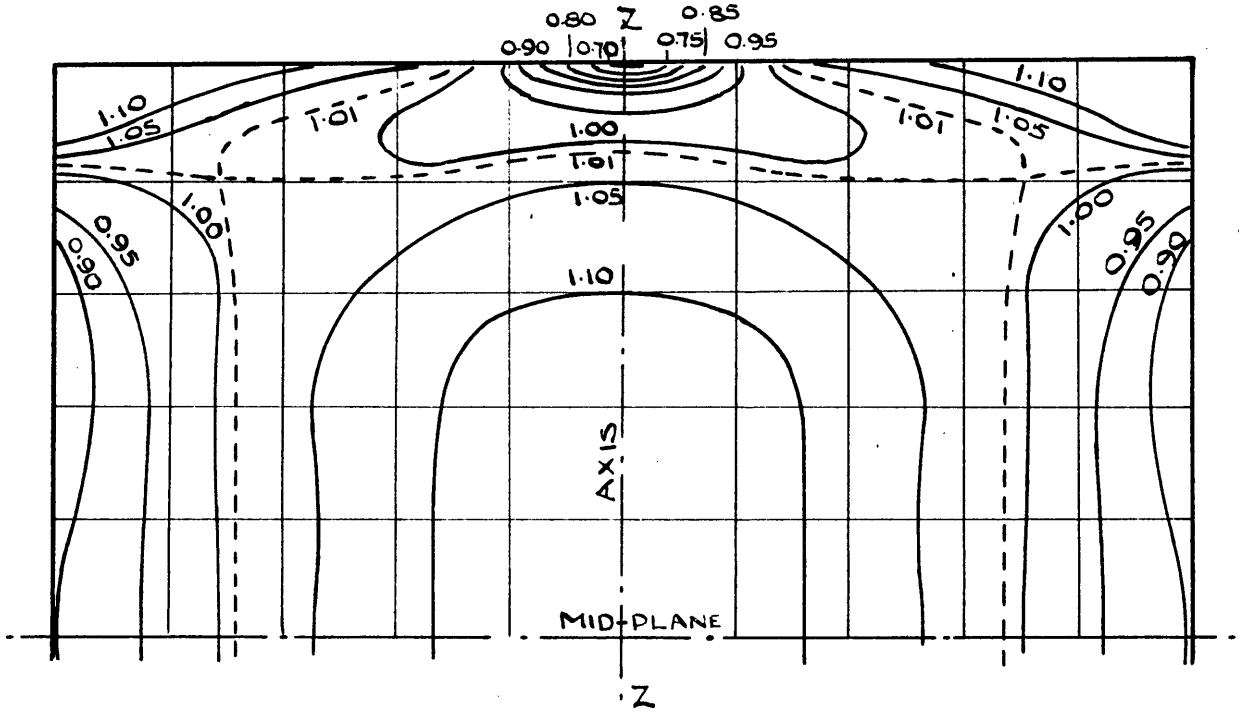

CUBE - AUTHOR'S SOLUTION

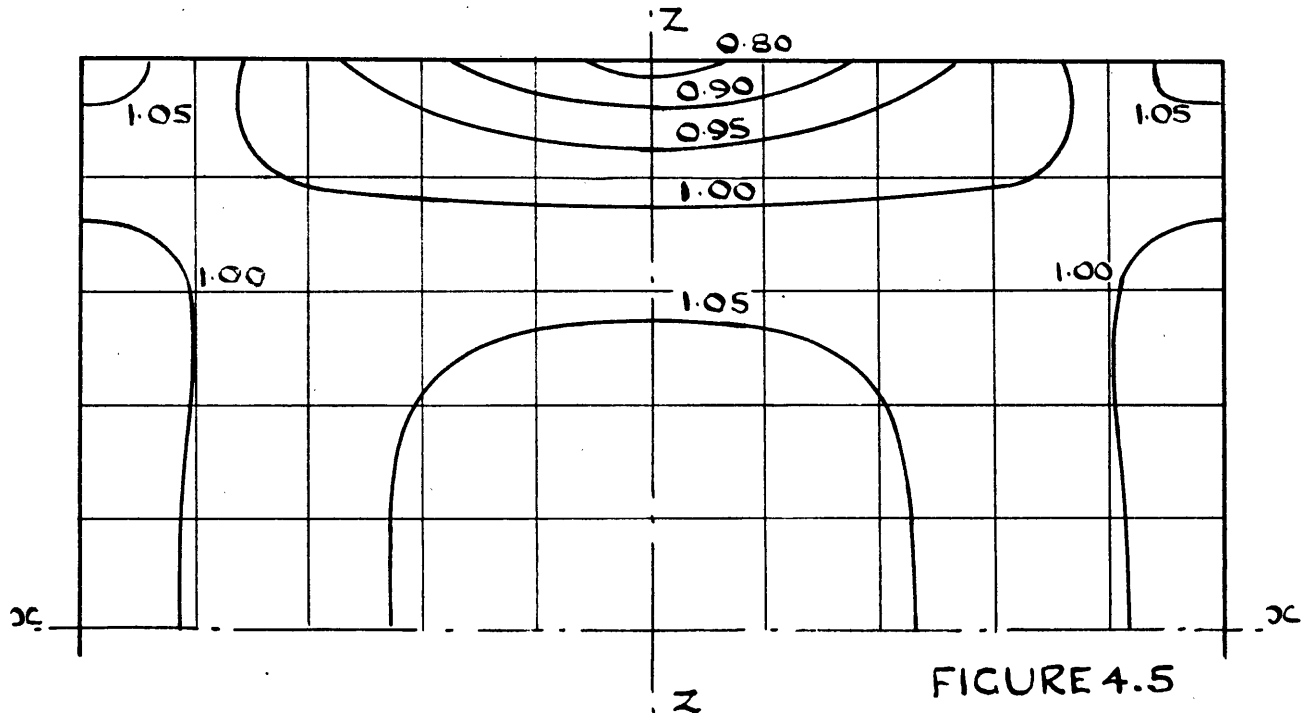

FIGURE 4.5

Despite these reservations the two sets of curves are strikingly similar. The main difference is that in Filon's solution the variations are more pronounced. This is to be expected because the ratio of cross sectional area of cube to its length is greater than it is for a cylinder. As this ratio is increased the stress at the central point on the upper surface will approach unity, the value it will have if the lateral dimensions are made large compared with the length.

In using relaxation methods to solve the problem of the cylinder (25) Markland is able to consider lateral restraint to be effected over the whole of the plane ends. In the tables below all three solutions are compared.

prr (Cylinder) or pxx (Cube).

Z		r=x=0	1/6	1/3	½	2/3	5/6	1.0
1.0	F	0.897		0.659		0.100		0
	M	0.302	0.301	0.300	0.302	0.310	0.341	0.477
	A	0.358	0.338	0.283	0.201	0.111	0.033	0
2/3	F	0.253		0.205		0.092		0
	M	0.134	0.127	0.112	0.094	0.058	0.007	0
	A	0.173	0.163	0.136	0.097	0.053	0.016	0
1/3	F	0.051		0.042		0.176		0
	M	0.034	0.034	0.029	0.018	0.008	0.002	0
	A	0.056	0.053	0.044	0.031	0.017	0.005	0
0	F	0.003		0.002		0.001		0
	M	0.016	0.011	0.007	0.004	0.001	0.002	0
	A	0.016	0.015	0.013	0.009	0.005	0.002	0

$p_{\theta\theta}$ or p_{yy} (Brackets indicate tension).

Z		r x=0	1/6	1/3	½	2/3	5/6	1.0
1.0	F	0.897		0.777		0.482		0.438
	M	0.302	0.301	0.300	0.302	0.310	0.341	0.477
	A	0.358	0.358	0.358	0.358	0.358	0.358	0.358
2/3	F	0.253		0.223		0.152		0.063
	M	0.140	0.132	0.122	0.112	0.095	0.068	0.039
	A	0.172	0.171	0.168	0.162	0.155	0.140	0.133
1/3	F	0.051		0.041		0.015		(0.020)
	M	0.034	0.034	0.031	0.023	0.013	0.002	(0.013)
	A	0.056	0.054	0.050	0.044	0.035	0.016	0.009
0	F	0.003		0.003		(0.017)		(0.033)
	M	0.016	0.013	0.007	0.001	(0.006)	(0.012)	(0.014)
	A	0.016	0.015	0.011	0.004	(0.005)	(0.024)	(0.032)

p_{zz}

1.0	F	0.686		0.750		0.928	1.082	1.686
	M	0.907	0.903	0.900	0.903	0.931	1.022	1.430
	A	0.835	0.842	0.863	0.897	0.945	1.007	1.082
2/3	F	1.080		1.054		1.006	0.985	0.882
	M	1.005	1.004	1.004	1.008	1.010	1.007	0.954
	A	1.027	1.026	1.022	1.017	1.009	0.999	0.987
1/3	F	1.133		1.100		1.013	0.951	0.872
	M	1.054	1.054	1.050	1.040	1.020	0.984	0.924
	A	1.071	1.068	1.059	1.044	1.024	0.970	0.964
0	F	1.134		1.100		1.007	0.948	0.894
	M	1.072	1.064	1.056	1.036	1.001	0.975	0.944
	A	1.074	1.071	1.061	1.046	1.025	0.997	0.963

p_{zx} or p_{rz}

1.0	F	0		0.354		0.442		0
	M	0	0.035	0.072	0.112	0.161	0.228	0.354
	A	0	0.078	0.141	0.179	0.176	0.122	0
2/3	F	0		0.059		0.086		0
	M	0	0.022	0.045	0.062	0.070	0.056	0
	A	0	0.023	0.042	0.053	0.052	0.036	0
1/3	F	0		0.004		0.002		0
	M	0	0.014	0.024	0.030	0.027	0.012	0
	A	0	0.003	0.005	0.007	0.007	0.004	0
0	F	0	0	0	0	0	0	0
	M	0	0	0	0	0	0	0
	A	0	0	0	0	0	0	0

Before considering the details of these tables it is as well to stress the fundamental difference between Markland's and Filon's solution. The latter allows slip at the ends except on the perimeter whereas Markland is able to solve for no slip everywhere. This is the only significant difference between the assumptions upon which the two solutions are based but its effect appears to be appreciable. It comes as a surprise to note that there is generally better agreement between the author's solution (for a cube) and Markland's solution (for a cylinder) than there is between the two solutions for the cylinder. Consider for example the distribution of the stress p_{zz} on the end plane (see figure 4.6). The author's distribution agrees quite well with Markland's except at the outer corner ($r = 1$) whilst Filon's values are very different. The difference between Markland's and the author's value for p_{zz} when $r = 1$ exists for two possible reasons; firstly, it may be due simply to the different shape of the two specimens, it is to be expected that differences should be accentuated at the corners; secondly the assumed functions which are used to determine the stresses are such that it is not possible for the curve to take the sudden bend that Markland's does. If terms including higher power of x were included better agreement would probably result. Furthermore Markland's values may not be very precise as the finite difference approximations made tend to cause errors where the function changes its value rapidly.

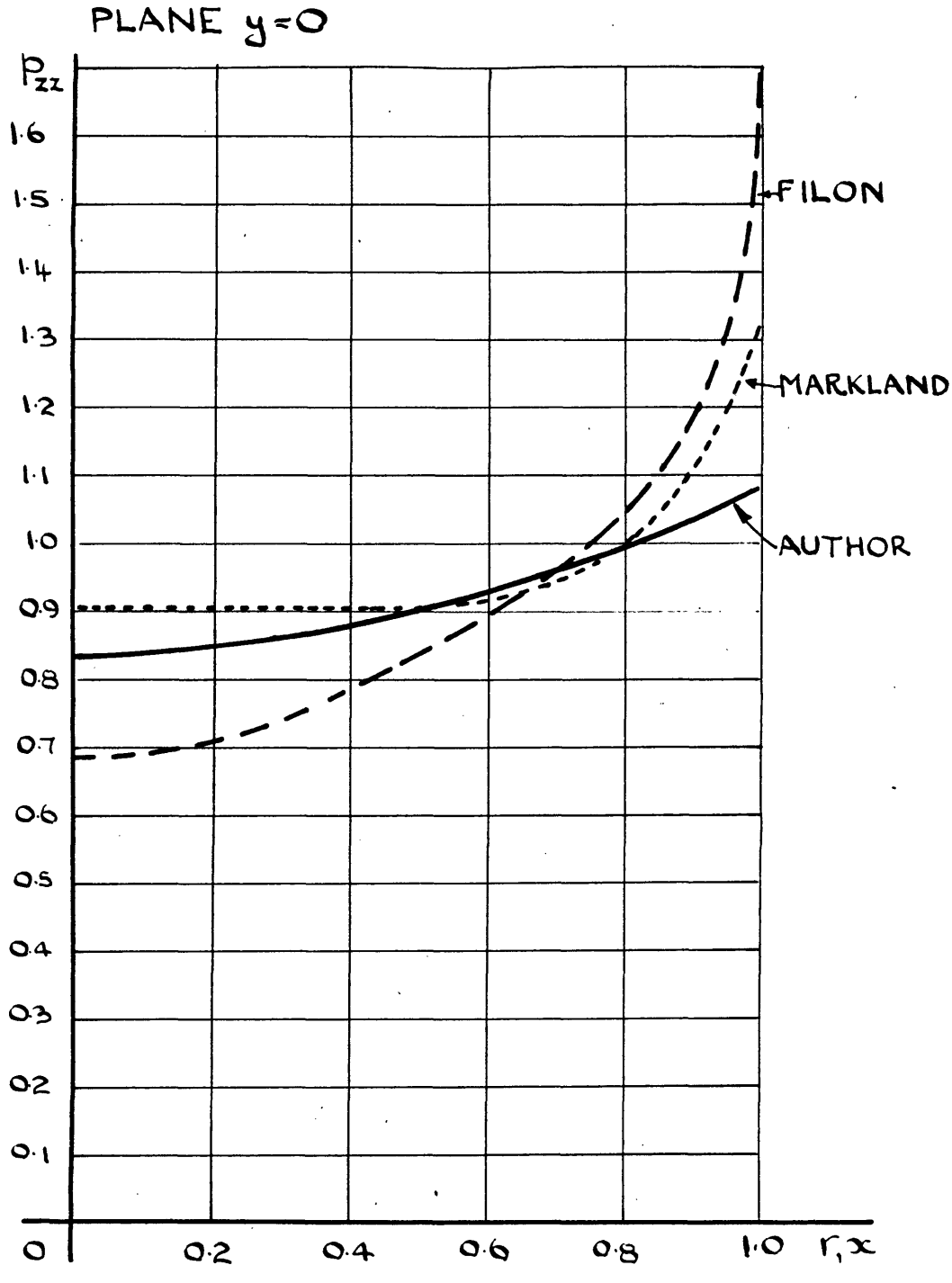
PLANE y=0
p_{zz}
1.6
1.5
1.4
1.3
1.2
1.1
1.0
0.9
0.8
0.7
0.6
0.5
0.4
0.3
0.2
0.1
0
0.2
0.4
0.6
0.8
1.0
r, x
FILON
MARKLAND
AUTHOR

FIGURE 4.6

This difficulty can be overcome by using a finer mesh. For values of z other than 1.0 the agreement between the author's and Markland's values for p_{zz} is remarkably good.

Turning now to the shear stress it can be seen that there is complete disagreement between all three solutions. Matters are complicated because Markland gets p_{rz} double valued for $z = r = 1.0$. This point will be considered in detail below. Much the same can be said for p_{rr} (or p_{xx}) except that here the author and Markland compare quite well for values of z other than 1.0.

On the whole there is quite good agreement between $p_{\theta\theta}$ and p_{yy} in Markland's and the author's solutions respectively. Again Filon's solution does not compare very well.

Why is there such disagreement between Filon's solution and Markland's solution? Superficially it appears that by preventing movement at the perimeter of the plane end Filon has a very good approximation. This point requires further investigation. Let us compute the actual movement of the plane ends for values of r other than 1.0. The radial strain $e_{rr} = \frac{1}{E}\left\{p_{rr} - \sigma (p_{zz} + p_{\theta\theta})\right\}$, and this equation and the tabulated values of the stresses enable $e_{rr} \times E$ to be calculated. The results are plotted in figure 4.7. Since $e_{rr} = \frac{\partial u}{\partial r}$ the integral of this curve gives $u \times E$, also plotted on figure 4.7.

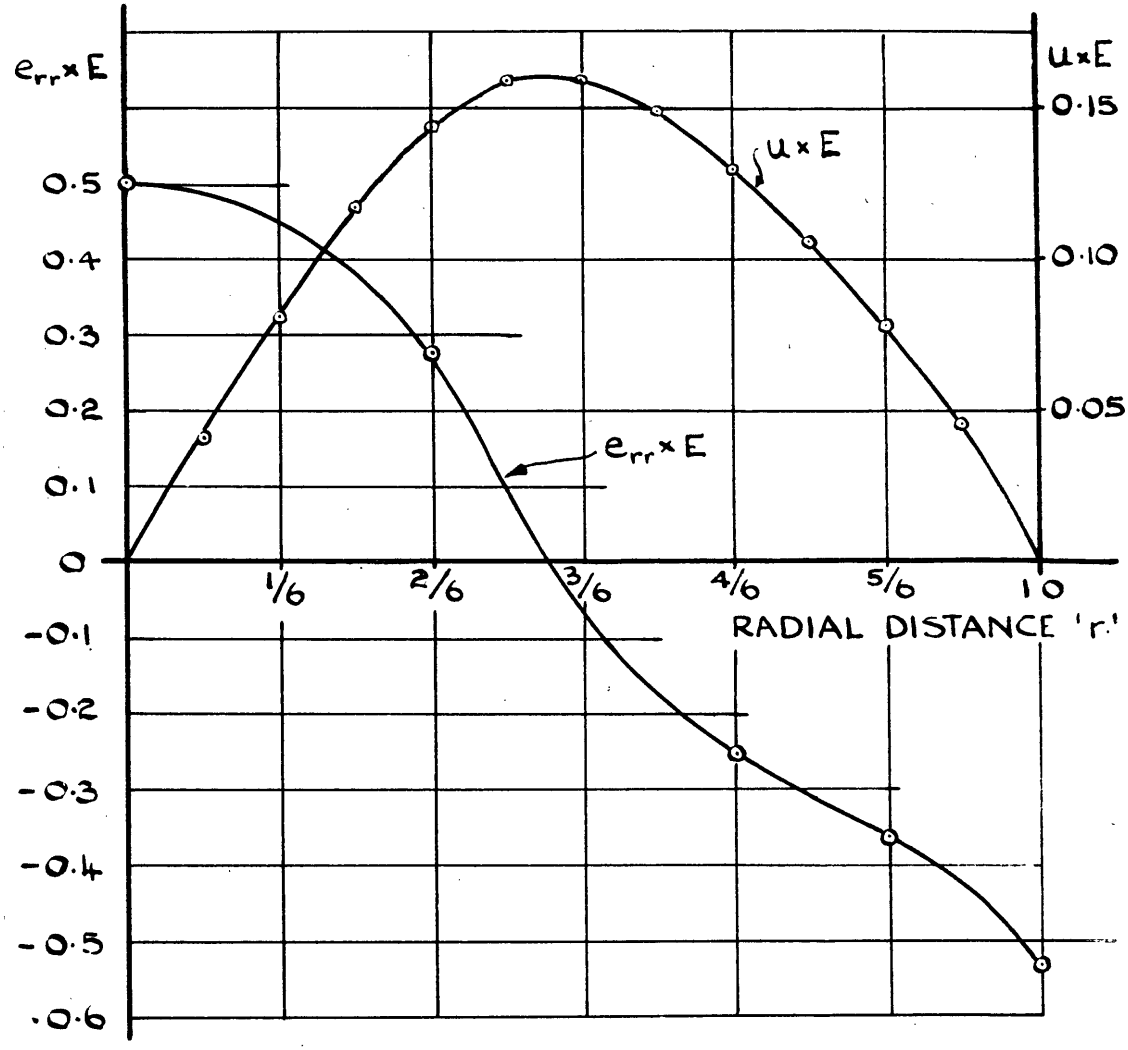

FIGURE 4.7

It will be seen that the maximum slip occurs at half radius to the value 0.163/E. Compare this with the movement in the Z direction. Filon's computation gives the apparent modulus as 1.0498E so that the movement of the loading plate relative to the central plane (z = 0) will be $\frac{1}{1.0498E} \times \frac{\pi}{3}$ (the total height of Filon's prism is $\frac{\pi}{3}$ x diameter), which equals 0.998/E. Thus the maximum slip is over 16% of the compressive movement.

This is far from being negligible and it can readily then be accepted as the difference between Filon's stresses and Markland's stresses.

In determining the approximate stress distribution by the Prager-Synge method the equations of compatability are ignored so that any movements calculated from the author's stresses would be meaningless. Different values would be obtained for different paths of integration! The final solution was selected on the basis of total strain energy and there is no guarantee that the stress distribution presents an accurate picture. The close agreement with Markland's solution is therefore to a certain extent fortuitous. We would expect the actual stress distribution on the central plane of a cube to be practically the same as that on an axial plane of a cylinder of the same dimensions. The fact that Markland's and the author's solution do agree enables it to be said with confidence that the latter's solution provide a tolerable picture of the stresses throughout the cube.

One further point calls for comment: The relaxation solution gives finite values to p_{rr} and p_{rz} at the perimeter of the plane end ($r = z = 1$). This arises because, as Markland points out, the conditions

$$\left.\begin{aligned} u &= 0 \\ w &= \text{constant} \end{aligned}\right\} \text{ on plane } z = 1.0$$

and $p_{rr} = p_{rz} = 0$ on the cylindrical surface are incompatible.

This point can be illustrated quite simply as follows:

All the solutions agree that p_{zz} tends to increase the point $r = z = 1$ so that p_{zz} is not zero there. However on the upper surface there is no radial straining and $e_{rr} = e_{\theta\theta} = 0$. This gives $p_{rr} = p_{\theta\theta} = \left(\frac{1-\sigma}{\sigma}\right) p_{zz}$. As p_{zz} is not zero p_{rr} cannot be. Hence the incompatability. This means that in fact some slip must occur at the perimeter or else plastic yield of the material must take place. The latter invalidates the analysis in the immediate locality of the perimeter.

This difficulty does not arise with either Filon's solution or with the author's solution. Filon's solution, as we have seen, does not permit slip right on the perimeter but does allow it elsewhere. This means that e_{rr} need not be zero so that $p_{rr} \neq \left(\frac{1-\sigma}{\sigma}\right) p_{zz}$. The Prager-Synge method used by the author deliberately ignores the compatability equations in determining the stress system and is able to impose the condition that p_{rr} be zero at any desired point.

STRESSES ON PLANE $y = 1$. The Outer Surface

It is to be expected that failure will be initiated on the outer surface of the cube so that the stress distribution there is very interesting. The stresses referred to Cartesian co-ordinates are given in the table below for Poisson's ratio of 0.25.

p_{xx} (Brackets indicate tension)

z	x=0	0.2	0.4	0.6	0.8	1.0
1.0	0.358	0.330	0.253	0.147	0.046	0
0.8	0.210	0.194	0.148	0.086	0.027	0
0.6	0.101	0.093	0.071	0.041	0.013	0
0.4	0.026	0.024	0.018	0.011	0.003	0
0.2	(0.018)	(0.016)	(0.013)	(0.007)	(0.002)	0
0	(0.032)	(0.030)	(0.023)	(0.013)	(0.004)	0

p_{zz}

z	x=0	0.2	0.4	0.6	0.8	1.0
1.0	1.082	1.092	1.122	1.171	1.240	1.329
0.8	1.012	1.013	1.018	1.025	1.035	1.048
0.6	0.979	0.976	0.968	0.955	0.937	0.914
0.4	0.966	0.962	0.950	0.930	0.901	0.865
0.2	0.963	0.959	0.945	0.924	0.893	0.853
0	0.963	0.959	0.945	0.923	0.892	0.852

p_{zx}

z	x=0	0.2	0.4	0.6	0.8	1.0
1.0	0	0.092	0.160	0.183	0.137	0
0.8	0	0.047	0.082	0.094	0.070	0
0.6	0	0.020	0.034	0.040	0.030	0
0.4	0	0.006	0.010	0.012	0.009	0
0.2	0	0.001	0.001	0.001	0.001	0
0	0	0	0	0	0	0

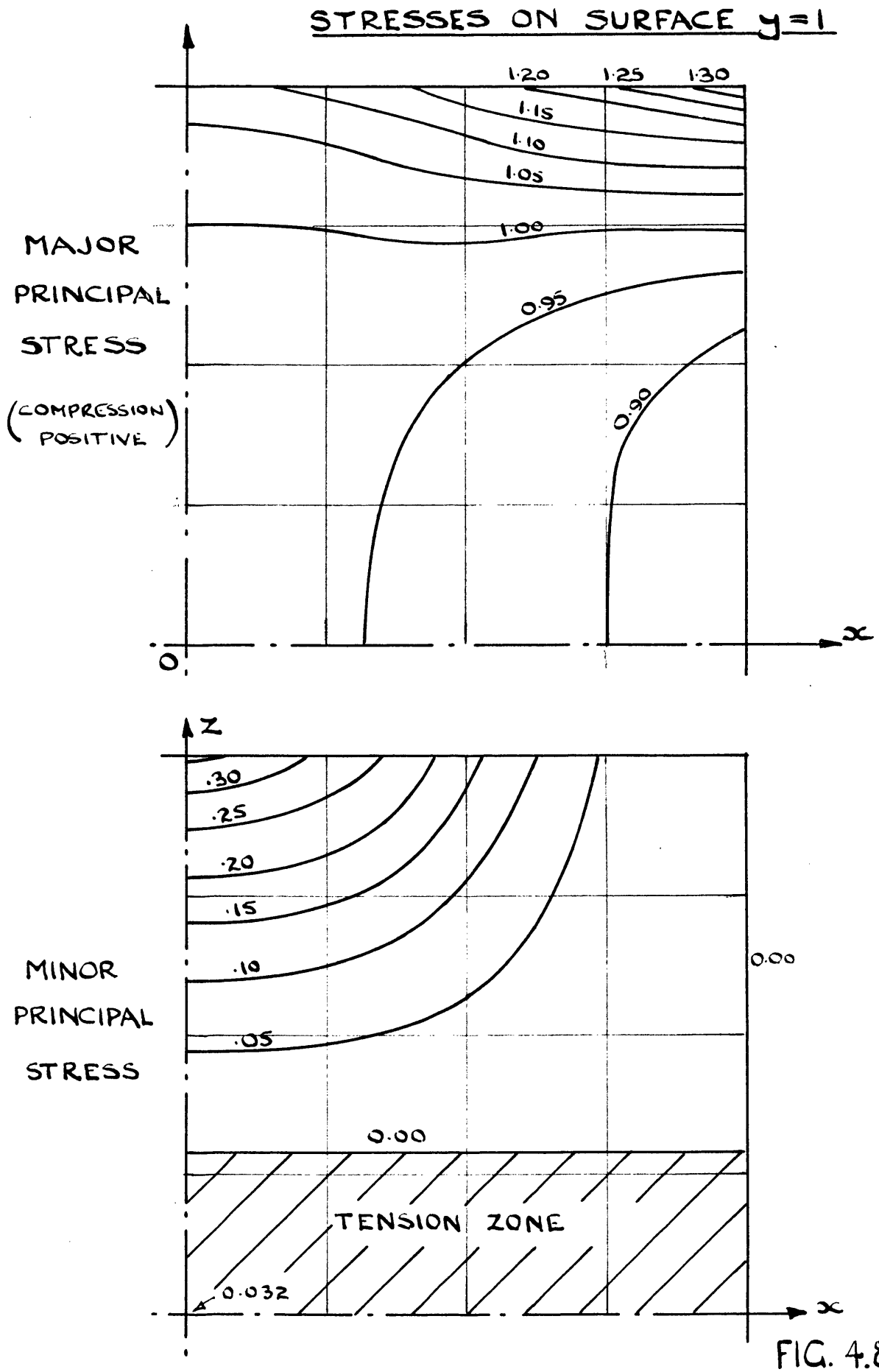
STRESSES ON SURFACE y=1
MAJOR PRINCIPAL STRESS
(COMPRESSION POSITIVE)
1·20
1·25
1·30
1·15
1·10
1·05
1·00
0·95
0·90
O
x
z
MINOR PRINCIPAL STRESS
·30
·25
·20
·15
·10
·05
0·00
0·00
TENSION ZONE
0·032
x

FIG. 4.8

Figure 4.8 shows the principal stresses at the surface. At the corners of the cube the major principal stress reaches a value 33 per cent in excess of the average compressive stress. As the other principal stresses at this point are zero the maximum shear stress is 33 per cent greater in a cube subjected to frictional restraint than in one where friction is absent. Dr. H.J. Cowan suggests the principal shear stress to be the criterion governing a crushing failure (32) which implies that friction should reduce the load bearing capacity of a cube. This is quite contrary to experience. Dr. Cowan's theory is not necessarily invalidated by this argument: Firstly, we cannot be sure that the compressive stress at the corner is anything like as high as the calculations suggest because of the incompatability between the strains and the stresses at this point. Secondly, even if the stresses are high at the corner under elastic conditions it may be that local plasticity is sufficient to redistribute the stresses so that no visible failure occurs until the load on the cube has been increased considerably.

Dr. Cowan quotes Nadai as saying that the maximum strain theory is one which has experimental support when applied to brittle materials such as concrete, but he appears to consider a combination of Rankine's maximum stress/

stress theory and Coulomb's maximum shear theory to be more suitable. Nevertheless the way in which a cube fails suggests that it is possible that the tensile strain is the governing factor. It often happens when a cube is tested to destruction that cracks such as 'A' form perpendicular to the faces of the cube tending to cause the corners to break away whilst in the shaded region the surface of the cube flakes off. The flakes are often quite thin. This may be due to the surface layer of mortar coming away from the aggregate but it may also be explained by saying that cracks are formed in planes parallel to the surface due to the tensile strain perpendicular to it. It is instructive therefore to evaluate the surface strains in the cube and to see if they can account for observed failure of the above type.

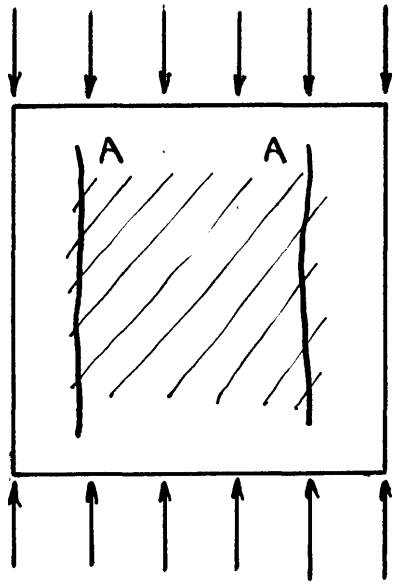

Figure 4.9

STRAINS ON PLANES y=0 and y=1

In evaluating the stresses we have more or less ignored the fact that the Prager-Synge method leads to two stress systems; one due to the associated states, the other/

other due to the complementary states. When stresses are considered it is natural to use the complementary states because these are chosen to satisfy the boundary conditions on stress. Were the displacements required it would be natural to use the associated states. The strains are, as it were, one calculation removed from both the stresses and the displacements and one cannot say categorically that either one of the associated or the complementary states should be used in preference to the other for determining them. Figures 4.10 and 4.11 compare the strains as given by both stress systems.

Figure 4.10 shows the strains on the axial plane $y = 0$. It will be seen that the agreement between the strain values for the two systems is remarkable insofar as the direct strains are concerned except at the intersection of the outer surface and the end plane. The incompatability of stresses and strains at this point naturally leads to difficulties here. Another discrepancy may be noticed in the distribution of the strains is the x direction. On the plane $z=1$ the lateral strains e_{xx} and e_{yy} are zero, as given by the associated states whilst the complementary states, which take no account of the displacements, give them non-zero values. However, the contours of the complementary states which pass through the plane $z = 1$ very quickly align themselves with their fellows of the associated states.

STRAINS ON AXIAL PLANE $y=0$ $\sigma = \frac{1}{4}$

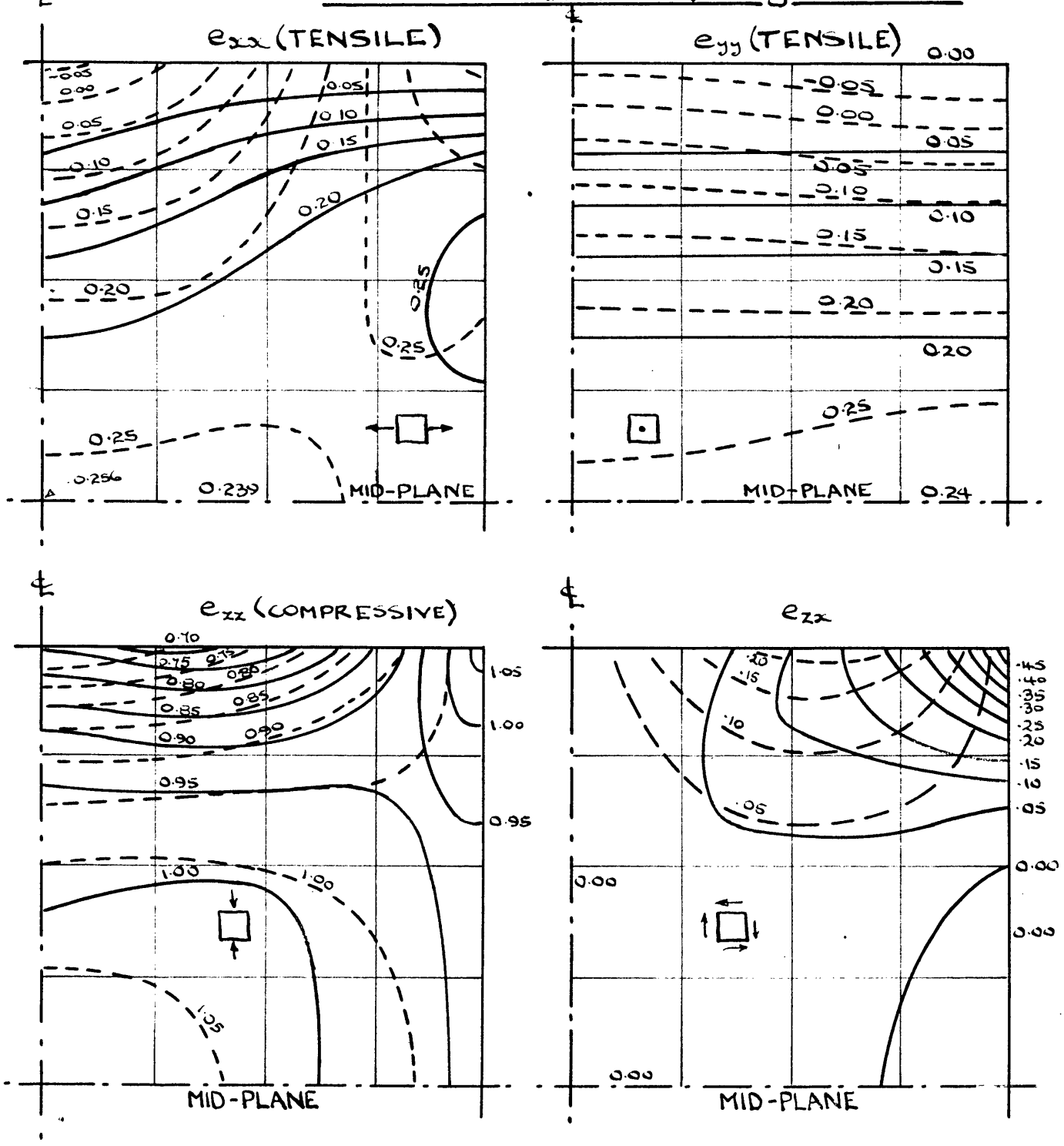

e_{xy} IS ZERO EVERYWHERE

e_{yz} IS ZERO EVERYWHERE IN THE COMPLEMENTARY SYSTEM OF STATES AND HAS A MAXIMUM (NUMERICAL) VALUE OF -0.029 IN THE ASSOCIATED SYSTEM

ASSOCIATED STATES STRESS CONTOURS IN FULL LINES
COMPLEMENTARY " " " "BROKEN "

FIG. 4.10

STRAINS ON SURFACE PLANE $y=1$ $\sigma=1/4$

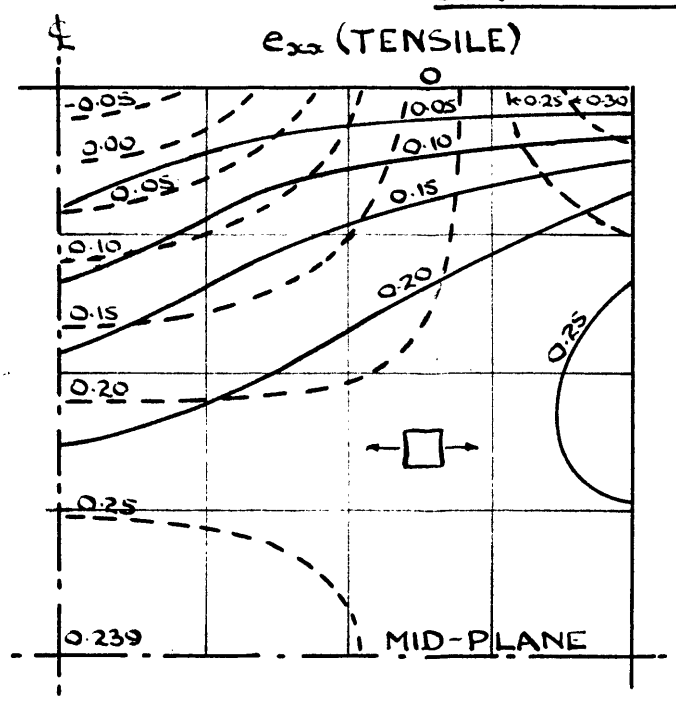

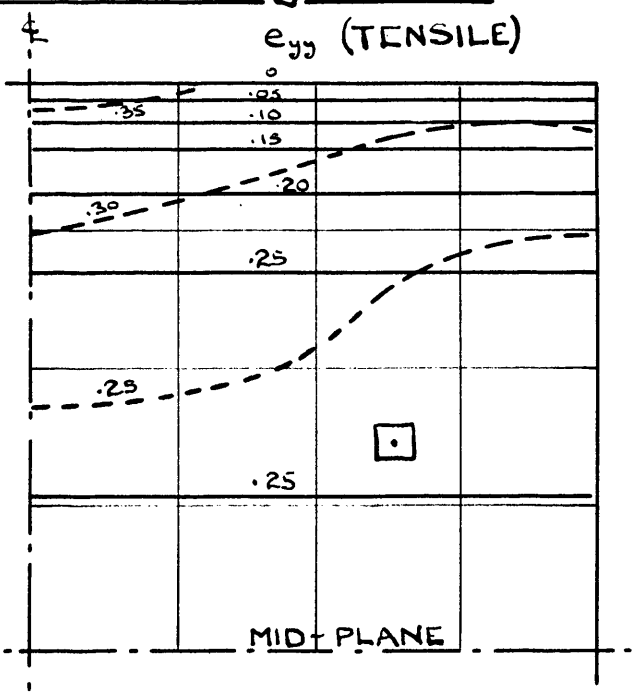

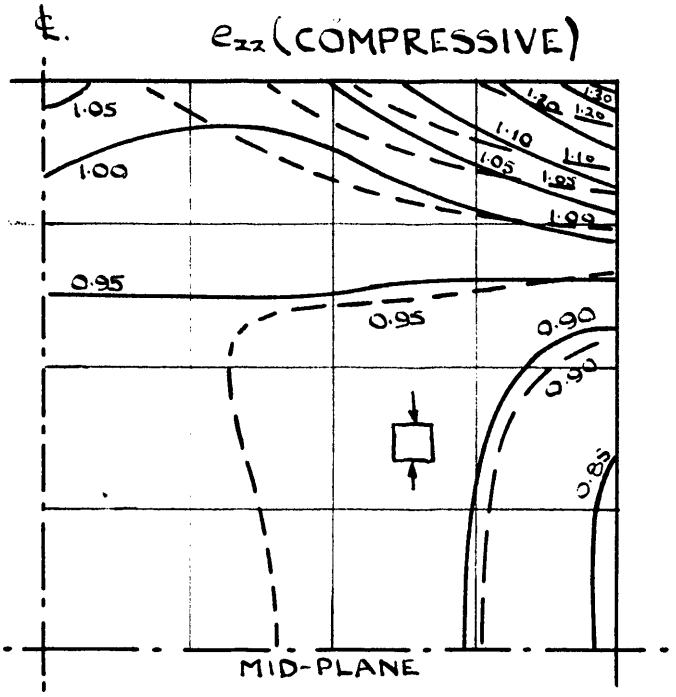

e_{zx} - AS FOR PLANE $y=0$

e_{xy} - ZERO EVERYWHERE

e_{yz} - AS FOR e_{zx} IN PLANE $y=0$ WHEN $x=+1$

ASSOCIATED STATES STRESS CONTOURS IN FULL LINES

COMPLEMENTARY " " " " BROKEN "

FIGURE 4.11

The shear strains e_{zx} do not show such good agreement. This is because the incompatability at the corner has very great influence. Also on the outer surface the shear stresses and hence the strains are zero in the system of complementary states but the associated states are not subject to this condition. It is interesting to note, however, that there is good agreement between the shear strains of the associated states and the strains of Markland's solution on the upper surface, see figure 4.12.

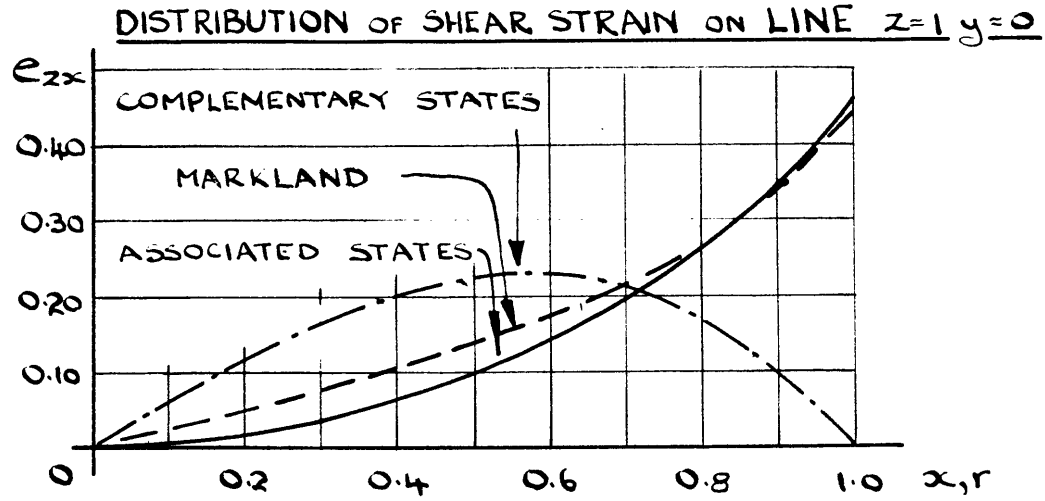

FIGURE 4.12

The preceding remarks on figure 4.10 apply also to figure 4.11 depicting the strains on the outer surface. Consider the two sets of tensile strains e_{xx} and e_{yy}. As before there is good agreement between the two methods of calculation except in the plane $z = 1$. Here we must believe the strains due to the associated states rather than those due to the complementary states because the former

set/

set conforms with the no slip condition whilst the latter does not. This being so it appears that the maximum tensile strain for an average end load of unity is approximately 0.25/**E** which is the value obtained when there is no friction present. Thus on the basis of the maximum tensile strain theory we would expect the end friction to have no effect! In this case the points at which we would expect failure to occur are remote from the ends and furthermore the two methods of calculation are substantially in agreement as to the magnitude and position of these 'high spots'. It must be that on passing the elastic limit the stress is redistributed to such an extent that failure is delayed considerably when there is end friction. If failure can be ascribed to the tensile strain then the curve of e_{xx} and e_{yy} explain the type of failure sketched in figure4.9. The tensile strain normal to the surface increases as the surface is moved explained the tendency to flake off (see e_{xx} in figures 4.10 and 4.11). Now a flaking tendency on one surface becomes a cracking tendency on a plane at right angles to it. This explains the formation of cracks 'A' (figure 4.9) at the corners.

CONCLUSION

From the academic viewpoint the analysis given in this chapter is very interesting. This work is, as far as the author is aware, the first application of the Prager-Synge technique/

technique to the solution of a three dimensional stress problem. The comparison between the stress distribution on the axial plane of the cube with that derived by Markland for the axial plane of a cylinder is very instructive especially as Markland's solution is obtained by an entirely different approach. Nevertheless, to an extent the work of this section has failed to achieve its object. It appears from the above that the increase in strength which results from plate friction cannot be explained by study of the elastic distribution of stresses and any of the recognised theories of failure for a brittle material. Possibly in a cube or cylinder test plastic yield starts at a lower mean stress than it does in a beam or a column of the same material, there may even be a formation of minute hair cracks at a comparatively low load, but the distribution of stresses and strains beyond this stage must be such that the frictional restraint at the ends is able to give effective support to the material. This support enables the material of the restrained specimen to withstand a greater stress than it can in beam or column form where such restraint is absent. So much could have been said without undertaking the work of this section. This does not, however, mean that the labour has been in vain. It had to be done in order to see if anything could be learnt. Furthermore there is one positive result:

We have seen that if Young's modulus is required under elastic conditions then it is sufficient in practice to measure the overall movement of the two ends in order to determine the strains. This is despite the fact that the stress distribution is very complex and that the main stress (p_{zz}) varies considerably from the mean value. The fixing of strain gauge to a small gauge length at the centre of a cylinder (the usual method) is an unnecessary refinement.

The results also show that any attempt to suggest that the distribution of stress in a beam at failure may be obtained by 'scaling down' a stress-strain curve from a cube test to be quite unjustified. By 'scaling down' is meant the reducing of the stress ordinates in order to obtain the right value for the total compressive force in a beam. If this is done the slope in the elastic range will be wrong because it was substantially correct before scaling down. Secondly the stress system is so complex, even under elastic conditions, that the material will be subjected to stresses quite different to those existing in a beam.

APPENDIX 4.1

The object of this appendix is to amplify a little the description of the calculations as given in the printed paper. Appendix 4.2 places on record the basic numerical quantities involved. It will be recalled that the problem is split into two components. The first of these represents a state of simple compression in which lateral expansion is unhindered. In the second state a shear movement is applied at the ends of the specimen just sufficient to counteract the expansion due to the first component of the problem.

The boundary conditions on the second component are; $u_x = -\sigma$ ax and $u_y = -\sigma$ ay at the ends u_z being zero there, whilse the surface tractions are zero on the sides of the specimen.

The stress states are now selected. We will deal first with the associated states. S* must satisfy the boundary conditions on displacement and also the compatability equations

$$e_{xx} = \frac{\partial u}{\partial x} \quad \text{etc.}$$

and $$e_{xy} = \tfrac{1}{2}\left(\frac{\partial u}{\partial y} + \frac{\partial u}{\partial x}\right) \text{ etc.}$$

S_1', S_2' etc. must also satisfy the compatability equations but their displacements must vanish at all points on the boundary/

boundary where they are prescribed, in this example the displacements must vanish at the ends of the specimen.

The easiest way to select the above states is to choose functions for u_x, u_y and u_z which accord with the boundary conditions in the required manner. The strains are then obtained from the compatability equations and these stresses form the strains by applying

$$p_{xx} = \frac{E}{(1+\sigma)(1-2\sigma)}\left\{(1-\sigma)e_{xx}+\sigma(e_{yy}-e_{zz})\right\} \text{ etc.}$$

and $$p_{xy} = \frac{E}{1+\sigma}\,.e_{xy} \text{ etc.}$$

Note that the displacements of S* depend on the value of Poisson's ratio, σ , but those of S_1' etc. do not. These calculations are best set out in the table drawn up below.

	u_x	u_y	u_z	e_{xx}	e_{yy}	e_{zz}	e_{xy}	e_{yz}	e_{zx}	p_x	p_{yy}	p_{zz}	p_{xy}	p_{yz}	p_{zx}
S_1'															
S_2'															
S_3'															
S_4'															
S_5'															
S^*															

The entries in the columns u_x, u_y and u_z are as in Table I of the printed paper (p. 146) except that the S* entries are varied with σ .

This being done a table of scalar products is made. The scalar product of two states is defined as

$$(S.S') = \int e_{ij} p_{ij}' \, dv$$

on being expanded in Cartesian co-ordinates this becomes

$$(S.S') = \iiint \left\{ \begin{matrix} e_{xx}p_{xx}' + e_{yy}p_{yy}' + e_{zz}p_{zz}' \\ +2e_{xy}p_{xy}' + 2e_{yz}p_{yz}' + 2e_{zx}p_{zx}' \end{matrix} \right\} dxdydz$$

Tables of scalar products are given in Appendix 4.2

The next step is to orthonormalise the series of states. The reason for this step may be illustrated as follows:

Let us suppose that only a crude approximation is required so that S_1' alone is considered. The resultant stress system will be

$$S^* + A_1 . S_1'$$

where A_1 has to be determined. The resultant strain energy will be

$$U = \tfrac{1}{2} (S^* + A_1 . S_1')^2$$

$$\frac{dU}{dA_1} = (S_1'.S^*) + A_1 (S_1'.S_1'). = 0 \text{ for min.}$$

so that $$A_1 = - (S_1'.S^*)/(S_1'.S_1').$$

Thus the best stress system which can be obtained using only S* and S' is

$$\underset{\sim}{S^*} - \left\{ (S_1'.S^*)/(S_1'.S_1') \right\} \; S_1'$$

Which can be written

$$S^* - (I_1'.S^*) I_1'$$

where $$I_1' = S_1/(S_1'.S_1')^{\frac{1}{2}}$$

It is immediately clear that $(I_1'.I_1') = 1$ so that I_1' is said to be normalised. The strain energy is given by

$$2U = (S^* - (I_1'.S^*)I_1')^2$$
$$= (S^*.S^*) - 2(I_1'.S^*)(I_1'.S^*) + (I_1'.S^*)^2(I_1'.I_1')$$
$$= (S^*.S^*) - (I_1'.S^*)^2$$

Let us now seek to improve the result by adding S_2' to the system. Let it be assumed that we can form

$$a.S_1' + b.S_2' = I_2'$$

such that $(I_2'.I_2') = 1$

and $(I_1'.I_2') = 0$

This being done I_2' will be normalised and orthogonal to I_1'. In general if we have n independent states S we can form n orthonormal states I such that

$$I_iI_k = 1 \text{ for } i = k$$
$$\text{and} = 0 \text{ for } i \neq k$$

Various methods for doing this exist the one used by the author is due to Peach (33).

The resultant stress system will now be

$$S^* + B_1I_1' + B_2I_2'.$$
$$2U = (S^* + B_1I_1' + B_2I_2')^2$$
$$\frac{\partial U}{\partial B_1} = (S^* + B_1I_1' + B_2I_2')I_1'$$
$$= S^*.I_1' + B_1 = 0 \text{ for minimum}$$

and $$\frac{\partial U}{\partial B_2} = S^*.I_2' + B_2 = o \text{ for minimum.}$$

Thus $B_1 = -(S^*.I_1')$ and $B_2 = -(2^*I_2')$. giving the stress system for minimum strain energy to be

$$S^* - (S^*.I_1')\ I_1' - (S^*.I_2')\ I_2'$$

and $2U = (S^*.S^*) - (S^*.I_1')^2 - (S^*.I_2')^2$

Thus in order to allow for the effect of S_2 we add

$-(S2.I_2')I_2$ to the stress system already found

and $-(S^*.I_2)^2$ to the strain energy already derived.

In general

$$S = S^* - \sum_{p=1}^{p=m} (S^*I_p')I_p'$$

and $$2U = (S^*.S^*) - \sum_{p=1}^{p=m} (S^*.I_n')^2$$

The intermediate step of orthonormalisation is not essential but it is a very convenient one which gives S and U relatively simple forms where they would otherwise be very unwiedly. It also enables the numerical work to be done in a very compact form.

The preceding work shows how the upper bound to the strain energy is fixed. The lower bound is determined by the complementary states which are selected as follows:-

The states S''_1, S''_2 etc. must satisfy the equilibrium equations

$$\frac{\partial p_{xx}}{\partial x} + \frac{\partial p_{xy}}{\partial y} + \frac{\partial p_{xz}}{\partial z} = 0 \quad \text{etc.}$$

and the boundary conditions on stress. In this case these simply/

simply state that the surface tractions must be zero on the sides of the cube. Calculations relative to these states are quite independent of those already described for the associated states except that the same S* is used for convenience. The calculations are, however, parallel to those of the associated states as is the derivation of the appropriate stress system and strain energy. In this case however the aim is to maximise the strain energy whereas before it was minimised.

APPENDIX 4.2. - Calculations for the cube problem.

$\sigma = \frac{1}{4}$. Associated States.

Scalar products ($S_i' . S_k'$).

	S_1'	S_2'	S_3'	S_4'	S_5'	S^*
S_1'	2.13333	-0.05541	2.13333	-0.05541	1.42222	-0.07111
S_2'		0.48904	-0.02771	0.41054	0	-0.02955
S_3'			2.59971	-0.04618	1.88860	-0.03556
S_4'				0.40720	-0.01847	-0.01178
S_5'					1.47517	0
S^*						0.06032

Coefficient of S_1', S_2' etc. in I_1', I_2' etc.

	$S_1'x$	$S_2'x$	$S_3'x$	$S_4'x$	$S_5'x$
I_1'	0.68465				
I_2'	0.03720	1.43208			
I_3'	-1.46894	-0.08334	1.46678		
I_4'	-0.10436	-3.37368	0.12096	4.01284	
I_5'	1.35188	0.00375	-4.06622	-0.09641	4.06789

Strain energy.		Coefficients of S_i' in resultant system				
	$(I_i' . S^*)$	$S^{*2} - \sum (I_i . S^*)^2$	$S_1'x$	$S_2'x$	$S_3'x$	$S_4'x$	$S_5'x$
S_1'	-0.04869	0.05795	0.0333				
S_2'	-0.04497	0.05593	0.0350	0.0644			
S_3'	0.05477	0.05293	0.1155	0.0690	-0.0803		
S_4'	0.05557	0.04984	0.1213	0.2564	-0.0871	-0.2230	
S_5'	0.04947	0.04739	0.0544	0.2563	0.1141	-0.2182	-0.2012

Note that the entries in any row represent the final state at that stage. For example if only states S_1, S_2 and S_3 are used then the strain energy is represented by 0.05293 and the stress system is $S^* + 0.1155 S_1 + 0.0690 S_2 - 0.0803 S_3$.

$\sigma = \frac{1}{4}$. Complementary States.

Scalar Products ($S_i" . S_k"$)

	$S_1"$	$S_2"$	$S_3"$	$S_4"$	S^*
$S_1"$	2.38600	0.26667	0.02032	-0.02748	-0.26667
$S_2"$		1.00000	0.66667	0	0
$S_3"$			0.62222	-0.05689	0
$S_4"$				0.59443	0

Coefficients of $S_1"$, $S_2"$ etc. in $I_1"$, $I_2"$ etc.

	$S_1"x$	$S_2"x$	$S_3"x$	$S_4"x$
$I_1"$	0.64739			
$I_2"$	-0.11347	1.01524		
$I_3"$	0.16642	-1.67540	2.44654	
$I_4"$	0.04727	-0.32223	0.46444	1.32055

Strain energy — Coefficients of $S_i"$ in resultant system

	$(I_i" . S^*)$	$\sum (I"_i . S^*)^2$	$S_1"x$	$S_2"x$	$S_3"x$	$S_4"x$
$S_1"$	-0.17264	0.02980	-0.1118			
$S_2"$	0.03026	0.03072	-0.1152	0.0307		
$S_3"$	-0.04438	0.03269	-0.1226	0.1051	-0.1086	
$S_4"$	-0.01260	0.03285	-0.1232	0.1091	-0.1144	-0.0166

$\sigma = 1/3$. Associated States.

Scalar Products ($S_i' . S_k'$)

	S_1'	S_2'	S_3'	S_4'	S_5'	S^*
S_1'	2.66667	-0.10390	2.66667	-0.10390	1.77778	-0.17778
S_2'		0.54053	-0.07792	0.46693	-0.03463	-0.01097
S_3'			3.21501	-0.10390	2.32612	-0.13333
S_4'				0.47748	-0.06061	0.01126
S_5'					1.79779	-0.05926
S^*						0.11905

Coefficients of S_1', S_2' etc. in I_1', I_2' etc.

	$S_1'x$	$S_2'x$	$S_3'x$	$S_4'x$	$S_5'x$
I_1'	0.61237				
I_2'	0.05319	1.36529			
I_3'	-1.35454	-0.06546	1.35199		
I_4'	-0.13201	-3.19806	0.15149	3.69801	
I_5'	1.31330	-0.00922	-3.94924	-0.06322	3.94967

Strain Energy

	$(I_i' . S^*)$	$S^{*2} - \sum (I_i . S^*)^2$
S_1'	-0.10887	0.10720
S_2'	-0.02443	0.10660
S_3'	0.06126	0.10285
S_4'	0.07996	0.09645
S_5'	0.05842	0.09304

σ = 1/3. Complementary States.

Scalar Products

	$S_1"$	$S_2"$	$S_3"$	$S_4"$	S*
$S_1"$	2.40225	0.35556	0.06265	-0.03664	-0.35556
$S_2"$		1.00000	0.66667	0	0
$S_3"$			0.62222	-0.07585	0
$S_4"$				0.59443	0

Coefficients of $S_1"$, $S_2"$ etc. in $I_1"$, $I_2"$ etc.

	$S_1"x$	$S_2"x$	$S_3"x$	$S_4"x$
$I_1"$	0.64520			
$I_2"$	-0.15206	1.02740		
$I_3"$	0.18898	-1.71133	2.46621	
$I_4"$	0.07074	-0.45281	0.64149	1.34085

Strain Energy

Coefficients of $S_i"$ in resultant system.

	$(I_i".S*)$	$\sum(I_i".S*)^2$	$S_1"x$	$S_2"x$	$S_3"x$	$S_4"x$
$S_1"$	-0.22940	0.05263	-0.1480			
$S_2"$	0.05407	0.05555	-0.1562	0.0555		
$S_3"$	-0.06719	0.06006	-0.1689	0.1705	-0.1657	
$S_4"$	-0.02515	0.06070	-0.1707	0.1819	-0.1818	-0.0337

σ = 1/6. Associated States

Scalar Products ($S_i' . S_k'$).

	S_1'	S_2'	S_3'	S_4'	S_5'	S^*
S_1'	1.90476	-0.02969	1.90476	-0.02969	1.26984	-0.02540
S_2'		0.47709	0	0.39298	0.01979	-0.02553
S_3'			2.34096	-0.01484	1.70604	0
S_4'				0.38159	0.00495	-0.01583
S_5'					1.34350	0.01693
S^*						0.02608

Coefficients of S_1', S_2' etc. in I_1', I_2' etc.

	S_1'	$S_2'x$	$S_3'x$	$S_4'x$	$S_5'x$
I_1'	0.72457				
I_2'	0.02257	1.44848			
I_3'	-1.51880	-0.09450	1.51733		
I_4'	-0.08073	-3.43529	0.09209	4.16443	
I_5'	1.35057	0.01605	-4.06287	-0.12222	4.06592

Strain Energy

	$(I_i' . S^*)$	$S^{*2} - \sum (I' S^*)^2$
S_1'	-0.01840	0.02574
S_2'	-0.04190	0.02398
S_3'	0.04127	0.02229
S_4'	0.03413	0.02112
S_5'	0.03602	0.01982

σ = 1/6. Complementary States.

Scalar Products $(S_i".S_k")$

	$S_1"$	$S_2"$	$S_3"$	$S_4"$	S*
$S_1"$	2.36974	0.17778	-0.02201	-0.01832	-0.17778
$S_2"$		1.00000	0.66667	0	0
$S_3"$			0.62222	-0.03793	0
$S_4"$				0.59443	0

Coefficients of $S_1"$, $S_2"$ etc. in $I_1"$, $I_2"$ etc.

	$S_1"x$	$S_2"x$	$S_3"x$	$S_4"x$
$I_1"$	0.64961			
$I_2"$	-0.07553	1.00674		
$I_3"$	0.14606	-1.64606	2.43014	
$I_4"$	0.02835	-0.20588	0.30126	1.30712

Strain energy. Coefficients of $S_i"$ in resultant system

	$(I_i".S^*)$	$\sum(I_i.S^*)^2$	$S_1"x$	$S_2"x$	$S_3"x$	$S_4"x$
$S_1"$	-0.11549	0.01334	-0.0750			
$S_2"$	0.01343	0.01352	-0.0755	0.0135		
$S_3"$	-0.02597	0.01419	-0.0798	0.0563	-0.0631	
$S_4"$	-0.00504	0.01422	-0.0800	0.0573	-0.0646	-0.0066

PART V GENERAL SUMMARY

In part II of this thesis the author introduced his method of determining the distribution of stress in a concrete beam when it is tested to destruction under a pure bending moment. This method is based upon an approach fundamentally different to others which attempt to measure the stresses directly. In contrast the author states certain assumptions and from these derives a way of inferring the stresses from strain readings. It is assumed that creep has no influence on the stress distribution and that the formation of tensile cracks also has no effect.

These two assumptions are considered in detail. It seems that for a test completed in a few hours creep will not invalidate the author's analysis except at very high stresses. Since the calculations are calculated step by step the lower stress portion of the resultant stress strain curve is unaffected by any inaccuracies in the higher stress part. It appears that due allowance may be made for creep at higher stresses when more information is available on this phenomenon but that this will be possible only if the creep laws conform with the possibility envisaged by the author of creep rate being proportional to the instantaneous strain. If this is not the case the problem will be exceedingly complex.

The assumptions that the distribution of stress is unaffected by the finite spacing of tensile cracks is investigated in Part III. It is shown that provided the cracks are spaced closer than one half the beam depth the errors in the stiffness of uncracked blocks below the neutral axis will be very small. With wider crack spacing, up to full beam depth, the errors will still be small provided that the cracking does not penetrate more than 60% of the depth and provided that the cracks do not bifurcate. In practice this means that no doubts need be felt on this score if the author's analysis is used for reinforced or pre-stressed beams using properly bonded reinforcement but that errors will be introduced if it is applied to non-bonded beams which generally find with deep widely spaced cracks.

The results of tests on a number of pre-stressed beams are analysed in Part II. Here a few interesting points emerged. It was shown that apart from determining the distribution of stress in the compressed zone of a beam the author's analysis provides a very useful means of determining the steel force and hence of deducing the amount of slip between steel and concrete. It is demonstrated with a number of examples that the stress strain curve obtained is often independent of the positioning of the strain gauges along the zone of constant bending moment.

That is to say resultant stress strain curve is the same for sections A, B and C.

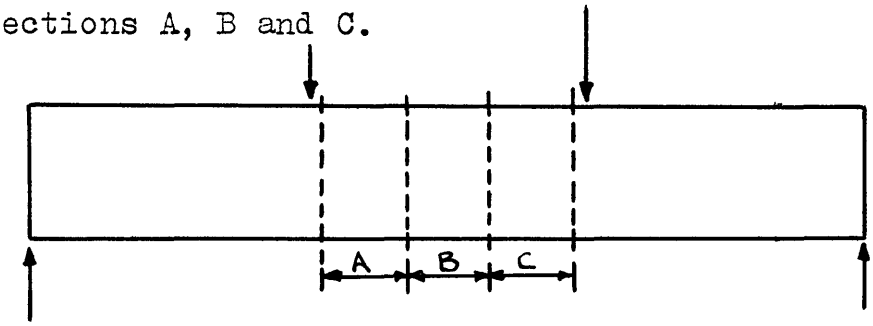

This is not very surprising since they are all of the same concrete. Nevertheless it is very rare for failure to occur right the way along the top of a beam. It is almost invariably localised as shown in figures 2.23, 2.24 etc. If the same stress-strain curve is obtained for sections A, B and C whilst failure is in section A it means not that there is local weakness at A but that the cracking and local slip of the steel have conspired to cause A to be more severely stressed. This point leads us back to consider again the effect of creep. If the material of section A is more highly stressed than that of B or C then one would expect higher creep in section A. This should cause the stress-strain curve recorded for A to differ from those recorded for B and C. It does not differ thus demonstrating that creep does not have a very great effect.

These tests also show that it is possible for local steel strains in a crack to be higher than the average concrete strains whereas it is natural to assume that they should equal or, as a result of slip, be less than the concrete strains.

Part IV analyses the stresses in a cube compressed between rough plates. This work shows that although the distribution of stress is very complex the overall strain is affected but little. This means that in a cube or cylinder test carried out for the purpose of determining Young's modulus it is sufficient to take the overall movement of the loading plates as a measure of the strains and that to attach a strain gauge is an unnecessary refinement. The fact that the stress distribution is so complex shows that it would be unjustifiable to attempt to determine the full 'plastic' stress strain curve by this method. We saw that it does not appear possible to reconcile this stress distribution and any of the accepted criteria of failure with the fact that concrete in a cube is stronger than concrete in a column or beam.

The general purpose of this thesis has been to examine the means of determining the stress distribution in the compression zone of a concrete beam under a bending moment. A method of doing this has been evolved and the limits within which the method can be expected to give valuable results have been defined.

It has been taken as axiomatic that it is desirable to know this stress distribution. That the problem is an interesting one from the academic viewpoint need not be argued.

That its solution provides information of value to the practicing engineer can be debated. It can be pointed out that Whitney has evolved a satisfactory plastic theory for the determination of the ultimate bending moment of an ordinary reinforced concrete beam using simply the stress-strain curve derived from a cylinder test. At the time of writing some authorities believe that Whitney's theory covers also the failure of pre-stressed concrete. If this is so is it necessary to go to all this trouble to determine the actual distribution of stress in a concrete beam? The author believes that it is because he does not agree with these authorities but finds the theory of A.L.L. Baker more acceptable. If this theory is to be fully developed for the use of the designer then many beams will have to be tested in order to determine the factors used in the theory. These factors depend on the shape of the concrete stress-strain curve. Professor Baker himself believes that it is desirable to know the true stress distribution and, as mentioned earlier has designed the bending simulation machine with the object of solving this problem.

A full discussion of this controversy is outside the scope of this thesis and it is mentioned here only to indicate how the information gained as a result of application of the author's method of analysis is applied in the realm of practical engineering.

The method may with profit be applied in the analysis of test data even when the main objective is not the derivation of the stress-strain curve. For example it may be suspected in a given case that the discontinuity in the slope of a deflection curve is due to slip of the steel; application of the author's method will show whether or not this explanation is acceptable. It must be emphasized that at present many beams are tested to destruction and sufficient information is booked to enable this analysis to be applied. The only data required are the strains in the concrete and these must be noted if the depth of the neutral axis is to be determined.

That no additional preparations need be made over and above those already made greatly commends the method as does the fact that beams commercially made can be tested as supplied by the maker without the need to make special modifications for the purpose of test. Extra time is, of course, taken up in making the necessary calculations but this labour is small compared with that which must be spent in any case in the testing of a beam.

References

1. A. HOOL & C. JOHNSON - 'Concrete Engineers' Handbook', McGraw-Hill, (1918).

2. G. MAGNEL - 'Prestressed Concrete', Conc. Pubs. (1948).

3. L.A. HERR and L.E. VANDEGRIFT - 'Studies of compressive stress distribution in simply reinforced concrete near the point of failure, Ohio State University, Engineering Experiment Station, Bulletin No.144 (1951).

4. A.L.L. BAKER - 'A plastic theory for the design of reinforced and pre-stressed concrete', Mag. of Conc. Res. No.2, (1949)

5. G.E. MONFORE - 'An analysis of the stress distributions in and near stress gages embedded in elastic solids', U.S. Dept. of the Interior, Bureau of Reclamation, Struct. Res. Lab. Report No. SP-26.

6. C.S. WHITNEY - 'Plastic theory of reinforced concrete design' - Proc. Amer. Soc. Civ. Eng., 66, (1940).

7. J.M. PRENTIS - 'The distribution of concrete stress in reinforced and pre-stressed concrete beams when tested to destruction by a pure bending moment', Mag. of Conc. Res., No.5, (1951).

8. L. BOLTZMAN - 'Zur Theorie der elastische Nachwirkung', Pogg. Ann. Phys., 7, (1876).

9. J.M. PRENTIS - M.Sc.(Eng.) Thesis. University of London 1946.

10. D. McHENDRY - 'A new aspect of creep in concrete and its application to design'. A.S.T.M. Reprint No.64, (1943).

11. A.D. ROSS - 'The case for a high modular ratio' Conc. and Const. Eng., Oct., (1946).

12. J.R. SHANK - 'Plastic flow of concrete at high overload' - J. Amer. Conc. Inst., 20, (1949).

13. W.H. GLANVILLE - 'The creep or flow of concrete under load' Building Research Station Technical Paper No.12 (1930).

14. R.H. EVANS - 'The plastic theories for the ultimate strength of reinforced concrete beams', J. Inst. C.E. 21, (1943) 98-121.

15. Y.C. LAO - Ph.D. Thesis. University of London (1950).

16. R.D. BINNS and H.S. MYGIND - 'The use of electrical resistance strain gauges, and the effect of aggregate size on gauge lengths in connection with the testing of concrete', Mag. of Conc. Res., No.1 (1949).

17. K. HAJNAL-KONYI - 'Tests on concrete beams reinforced with 12 gauge wires of an ultimate strength of 120 tons per square inch', Mag. of Conc. Res. No.9 (1952).

18. M.M. FROCHT - 'Photo elasticity', vol. II, Wiley, (1948).

19. L. FOX and R.V. SOUTHWELL - 'Biharmonic analysis as applied to the extension and flexure of flat elastic plates' - Phil. Trans. Roy. Soc, 239A, (1945), 419-460.

20. J.D. McINTOSH - 'Methods of graphing several variables', Mag. of Conc. Res. No.3, (1949).

21. R. JONES - 'The non-destructive testing of concrete', Mag. of Conc. Res., No.2, (1949).

22. L.N.G. FILON - 'On the elastic equilibrium of circular cylinders under certain practical systems of load', Phil. Trans. Roy. Soc., 198 A, (1902).

23. F. EDELMAN - 'Compression of a short cylinder between rough end blocks', Quart. of Applied Math., 7, (1949), 334.

24. W. PRAGER and J.L. SYNGE - 'Approximations in elasticity based on the concept of a function space', Quart. of Applied Math., 5, (1947), 241.

25. E. MARKLAND - 'An investigation of a circular cylinder compressed between rigid end plates', a paper read at a conference on stress analysis, University of Nottingham, (1954).

26. G. PICKETT - 'Application of the Fourier methods to the solution of certain boundary problems in the theory of elasticity', J. Applied Mech., 11, (1944), 176.

27. E. d'APPOLONIA and N.M. NEWMARK - Proc. 1st. U.S. Nat. Cong. Applied Mechs., (1951), 217.

28. J.M. PRENTIS - 'On the compression of a cube between rigid rough plates', Quart. J. Mech. and Applied Maths., 5, (1952), 253-256.

29. A. and L. FOPPL - 'Drang und Zwang', Munich, (1920).

30. H.J. GREENBURG and R. TRUELL - 'On a problem in plane strain(, Quart. of Applied Math., 5 (1947), 241.

31. D.R. HARTREE - 'Numerical Analysis', Oxford, (1952).

32. H.J. COWAN - 'The strength of plain, reinforced and prestressed concrete under the action of combined stresses ...', Mag. of Conc. Res., No.14, (1953).

33. M.O. PEACH - 'Simplified technique for constructing orthonormal functions', Bull. Amer. Math. Soc., 50, (1944), 556.

SLENDER REINFORCED CONCRETE COLUMNS

BY

J. M. PRENTIS, M.Sc.

AND

Professor A. D. ROSS, Ph.D., A.M.Inst.C.E.

Reprinted from

"CONCRETE & CONSTRUCTIONAL ENGINEERING,"

September, 1948

Slender Reinforced Concrete Columns.

By J. M. PRENTIS, M.Sc., and Professor A. D. ROSS, Ph.D., A.M.Inst.C.E.

INSUFFICIENT is known about the strength of slender reinforced concrete columns, although codes give coefficients by which the safe load on a short column should be multiplied to determine the reduced working load on a slender column of the same lateral dimensions. The instability of slender columns and the effect of creep of the concrete are considered in this article.

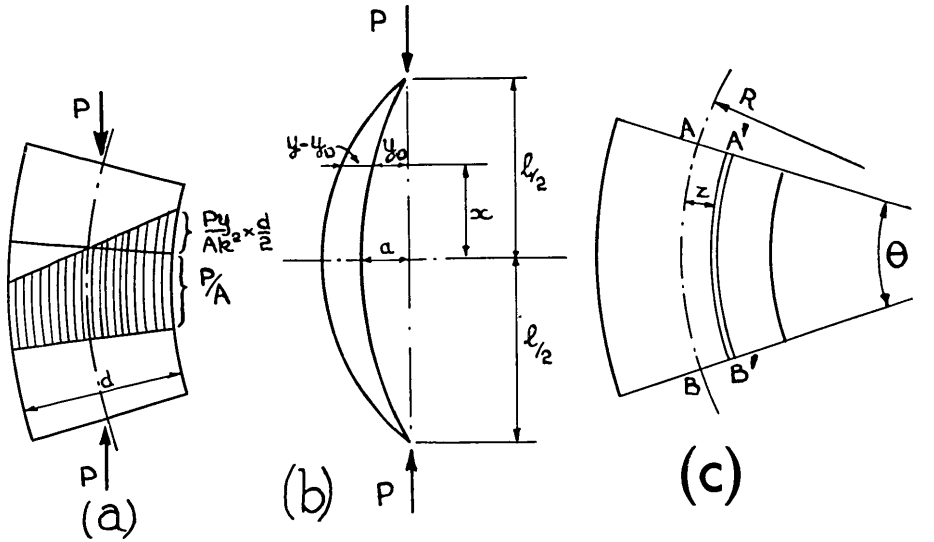

Fig. 1.

A straight concentrically-loaded homogeneous column fails in compression if the length is short compared with the lateral dimensions, and by instability if the column is slender. The load at failure of an ideal slender column hinged at both ends is given by Euler's formula,

$$P_e = \pi^2 E A \left(\frac{k}{l}\right)^2 \quad . \quad . \quad . \quad . \quad . \quad (1)$$

where E is the modulus of elasticity of the material, A is the cross-sectional area of the column, k is the radius of gyration of the section, and l is the distance between the hinges. In practice the conditions of an ideal column are not attained, but it is possible to allow for variations by assuming either an eccentricity of the load or a curvature of the centre-line of the column. An analysis [1] based on an assumed cosine curve shows that the load at failure depends on the yield stress p_y of the material, and for a column hinged at both ends the load at failure is

$$P = \frac{p_y A + (1+\eta)P_e}{2} - \sqrt{\left[\frac{p_y A + (1+\eta)P_e}{2}\right]^2 - p_y A P_e} \quad . \quad . \quad (2)$$

*

where η is a coefficient depending on the curvature of the centre-line. For a material like concrete having no definite yield point, it is not correct to assume an equivalent yield stress, because the continual change of slope of the stress-strain curve is due to creep during the test. If a correction is made for creep [2] the relation between stress and elastic strain is linear within the range of working stresses. In the absence of corrected stress-strain curves for instantaneous loading up to the limit of proportionality and thence to failure, the yield stress must be given an arbitrary value, such as 0·8 of the crushing stress, as is assumed in the following. The numerical value assumed does not affect the theoretical deductions. If the strength of concrete in a column is assumed to be two-thirds of the crushing strength u of 6-in. cubes the assumed yield stress p_y is $0{\cdot}533u$.

Since concrete deforms continually under sustained load, it is evident that strain due to bending increases with time. If an initially curved member is subjected to an end load, the stresses are a combination of the direct stress and the bending stress caused by the eccentricity of the load due to curvature. The bending moment increases the curvature and the bending stress is therefore increased. Unless the column is overloaded equilibrium is reached, and the resultant distribution of stress is as shown in *Fig.* 1(*a*). If the material creeps under the stress and if, as is the case with concrete, the rate of creep increases with increase in stress, the curvature and the bending stress also increase. The stress is greatest on the concave side where the creep is greater than on the convex side, that is the curvature increases.

If the effect of creep is too great the material becomes overstressed and collapses. In all cases the conditions of stress deteriorate and a reduction of the original load-factor results. These effects are assessed in the following.

Calculation of the Effects of Creep.

Fig. 1(*b*) shows a column of uniform cross-section with a centre-line conforming to the equation $y_0 = a \cos \frac{\pi x}{l}$. It can be shown [1] that on the application of an end load P the equation to the centre-line becomes

$$y = \frac{aP_e}{P_e - P} \cos \frac{\pi x}{l} \quad . \quad . \quad . \quad . \quad . \quad (3)$$

Consider an elementary length of a member [*Fig.* 1(*c*)] bent to a radius R and subtending to an angle θ. From the geometry of the figure,

$$\frac{\mathrm{AB} - \mathrm{A'B'}}{\mathrm{AB}} = \frac{z}{R} \quad . \quad . \quad . \quad . \quad . \quad (4)$$

If it is assumed that the rate of creep is proportional to the instantaneous stress, that is, $\frac{\partial c}{\partial t} = f\frac{\partial \phi(t)}{\partial t}$, where $\phi(t)$ is the creep in time t under unit stress, and if $p = \frac{P}{A}$, then

$$-\frac{1}{\mathrm{AB}} \cdot \frac{\partial(\mathrm{AB})}{\partial t} = p\frac{\partial \phi(t)}{\partial t} + \frac{1}{E} \cdot \frac{\partial p}{\partial t} \cdot \quad . \quad . \quad . \quad (5)$$

Also,

$$-\frac{1}{A'B'}\cdot\frac{\partial A'B'}{\partial t}=(p+f)\frac{\partial\phi(t)}{\partial t}+\frac{1}{E}\cdot\frac{\partial(p+f)}{\partial t}. \quad . \quad . \quad . \quad (6)$$

where $f=\frac{Py}{Ak^2}z$.

By differentiating (4) with respect to t and assuming AB = A'B' for a large radius of curvature, and substituting from (5) and (6),

$$\frac{1}{E}\cdot\frac{\partial f}{\partial t}+f\frac{\partial\phi(t)}{\partial t}=-\frac{z}{R^2}\cdot\frac{\partial R}{\partial t} \quad . \quad . \quad . \quad . \quad (7)$$

Substituting $f=\frac{Py}{Ak^2}z$, and $\frac{\partial^3 y}{\partial x^2\,\partial t}=\frac{1}{R^2}\cdot\frac{\partial R}{\partial t}$,

$$\frac{p}{Ek^2}\cdot\frac{dy}{\partial t}+\frac{py}{k^2}\cdot\frac{\partial\phi(t)}{\partial t}+\frac{\partial^3 y}{\partial x^2\,\partial t}=0.$$

If $p_e=\frac{P_e}{A}=\pi^2E\left(\frac{k}{l}\right)^2$, the solution of this equation is

$$y=\frac{ap_e}{p_e-p}e^{\frac{pE\phi(t)}{p_e-p}}\cdot\cos\frac{\pi x}{l} \quad . \quad . \quad . \quad . \quad (8)$$

Comparison of (8) and (3) shows that the effect of creep is to multiply the lateral deflection (and hence the bending stresses) by the factor $\sigma=e^{\frac{pE\phi(t)}{p_e-p}}$. To determine the load which causes failure in any time t, it is therefore necessary to replace η in (2) by $\sigma\eta$. The resultant equation is not easy to solve because σ is a function of p, the stress to be determined, but the solution can be obtained by successive approximations.

Effective Modulus.

In the foregoing it is assumed that the rate of creep is proportional to the instantaneous stress, but a simpler method is to replace E by an effective modulus, $E_e=\frac{E}{1+E\phi(t)}$, when calculating P_e. This gives a smaller failing load because it is assumed that all the creep has occurred under a stress equal to the final stress in the material, since it is assumed that the final strain in any fibre is $\frac{f}{E_e}=\frac{f}{E}+f\phi(t)$. In a column the stress in the concave side increases to f during the period of loading; hence at any given moment the stress is less than f. Therefore the total strain obtained is too high. On the other hand, if the stress is increasing, the rate of creep $\frac{\partial c}{\partial t}$ must be greater than the assumed rate $f\frac{\partial\phi t}{\partial t}$. Therefore the deflection given by (8) is slightly too low and the failing load is slightly too high. Thus the true result is expected to lie between the results obtained by the two theories.

Fig. 2 shows a comparison between the loads required to cause failure as calculated by the two theories when the load has been applied for an infinite time.

To demonstrate the effect of creep the loads calculated from (2) to produce immediate failure are also given. The ratio of P to P_y is plotted against $\frac{l}{k}$, the curves being therefore applicable to all columns. A discontinuity in the curves occurs at $\frac{P}{P_y} = 0{\cdot}5$ due to the stress on the convex side [*Fig.* 1(*a*)] becoming tensile. If the concrete is assumed to possess no tensile strength, failure of a plain column must occur when the tensile stress due to bending exceeds the direct compressive stress.

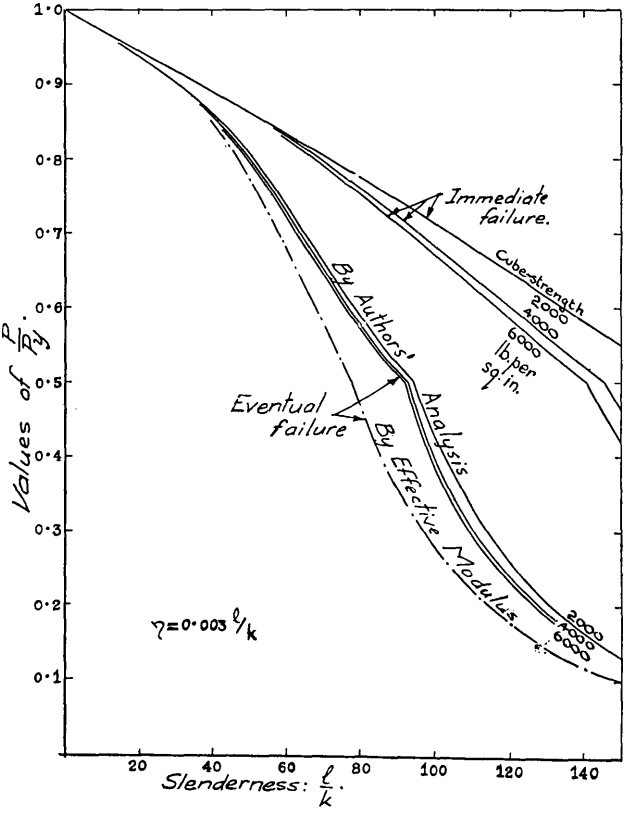

Fig. 2.

There is little experimental verification of the preceding theories for homogeneous columns. When the analytical results are compared with the results obtained on a phenolic plastic material,[3] which exhibits characteristics of creep very similar to those of concrete but on a greatly reduced time-scale, close agreement is shown, the results of tests being between those of the two theories.

Short Reinforced Concrete Columns.

If a short reinforced concrete column is loaded concentrically so rapidly that creep does not occur, it behaves elastically when subjected to small loads. If

the load is increased the steel is eventually stressed beyond the limit of proportionality and thereafter the concrete takes a greater share of the increased load. When eventually the steel yields it can only sustain its yield stress, so that further increase of load is borne entirely by the concrete. When the concrete becomes overstressed there is total collapse. Thus, disregarding the effects of lateral reinforcement, the strength of a short reinforced concrete column is

$$P_y = 0{\cdot}67uA_c + p_{ys}A_s \quad . \quad . \quad . \quad . \quad (9)$$

where A_s and A_c are the areas of the reinforcement and concrete respectively and p_{ys} is the yield stress of the steel.

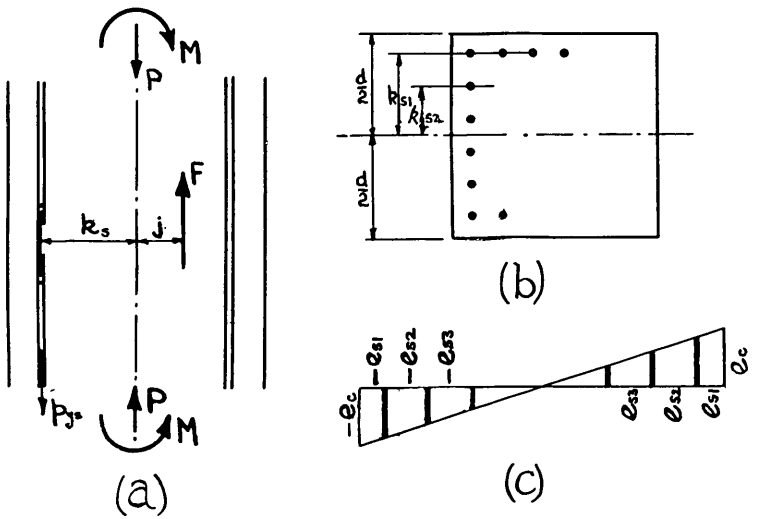

Fig. 3.

When the load is applied eccentrically, or when a concentric load is combined with a bending moment, it is common to permit a higher compressive stress in the concrete than for direct load alone. There is no reason to suppose that concrete is capable of withstanding a greater stress due to bending than due to direct load, but this assumption allows a linear variation of strain to be assumed when in reality the variation is otherwise.

One plastic theory [4] shows that the load P applied at an eccentricity e causing failure due to compression of a member of breadth b and effective depth d is

$$\frac{A_s p_{ys}}{\frac{e}{k_s} + 1} + \frac{bdu_c}{\frac{3de}{(0{\cdot}5d + k_s)^2} + 1{\cdot}178},$$

where $2k_s$ is the distance between the compressive and tensile reinforcement and u_c is the strength of concrete cylinders. If P is plotted to a base of Pe (or M) the result is a straight line passing through $P = P_y$ for $M = 0$, and through $M_0 = M = b(0{\cdot}5d + k_s)^2 . \frac{u_c}{3} + p_{ys}A_s k_s$ for $P = 0$. The relation of the load to the moment to cause failure due to compression is, therefore, given by

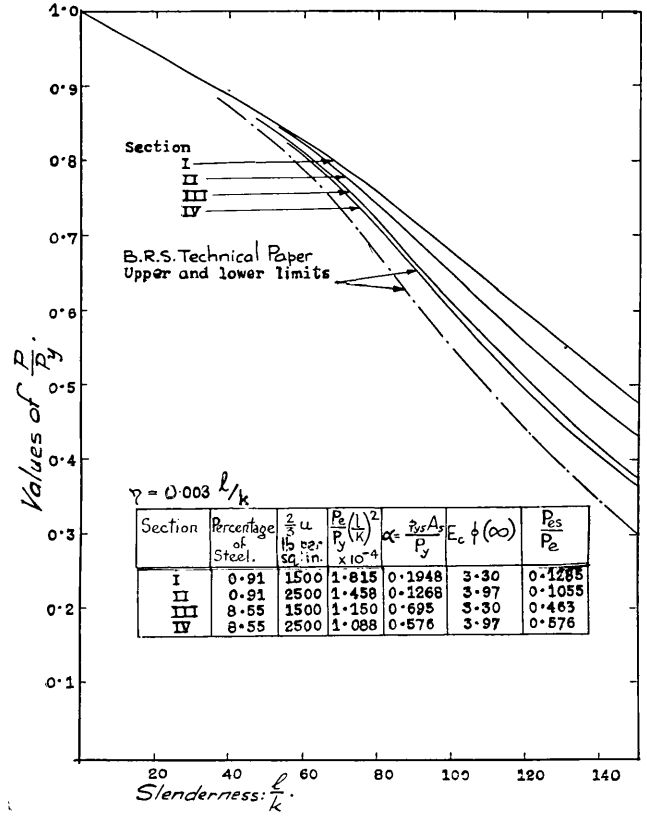

Section	Percentage of Steel.	$\frac{2}{3}u$ lb per sq. in.	$\frac{P_e}{P_y}\left(\frac{L}{K}\right)^2$ x 10^{-4}	$\alpha = \frac{f_{ys}A_s}{P_y}$	$E_c\,\phi(\infty)$	$\frac{P_{es}}{P_e}$
I	0·91	1500	1·815	0·1948	3·30	0·1285
II	0·91	2500	1·458	0·1268	3·97	0·1055
III	8·55	1500	1·150	0·695	3·30	0·463
IV	8·55	2500	1·088	0·576	3·97	0·576

Fig. 4.

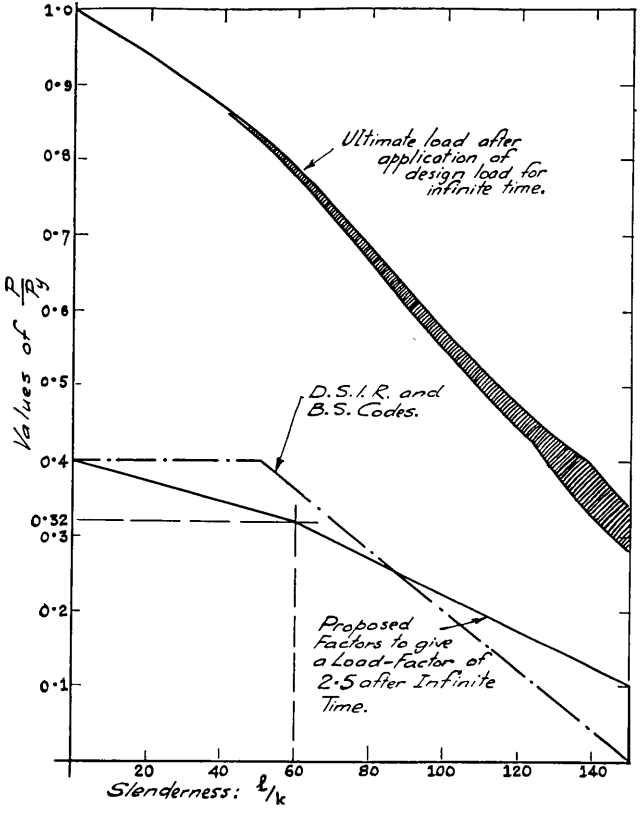

Fig. 5.

$$M = (P_y - P)\frac{M_0}{P_y} \quad . \quad . \quad . \quad . \quad . \quad (10)$$

An expression relating P and M for failure due to insufficient tensile strength can be derived by considering the section in *Fig.* 3 when tensile failure is imminent. Replace the forces on the compression side by F. By equating the internal and external forces and the moments of these forces about the centre-line, and by combining the resultant expressions,

$$\frac{M}{k_s} = P + \alpha P_y \quad . \quad . \quad . \quad . \quad . \quad (11)$$

in which $\alpha P_y = p_{ys} A_s$, and k_s is assumed to be approximately equal to j. Comparing this equation with the results of tests, there is so close an agreement that the use of this simple equation in place of more elaborate expressions seems to be justified.

Slender Reinforced Concrete Columns.

Tests over short periods [5] show that (2) is applicable to slender reinforced concrete columns if $p_y A = P_y$ is the load at failure in compression of a short column of the same cross-section as the slender column and if $\eta = 0{\cdot}003\frac{l}{k}$. Formula (2) can be obtained from the elastic theory, but an inconsistency is thereby introduced because P_y is calculated from a plastic theory of failure. The formula can, however, be obtained by using a plastic theory of failure as expressed in (10) and (11).

If the failure is by tension

$$P = -\frac{\alpha P_y - (1-\eta)P_e}{2} + \sqrt{\left[\frac{\alpha P_y - (1-\eta)P_e}{2}\right]^2 + \alpha P_y P_e}. \quad . \quad (12)$$

in the derivation of which the elastic theory is used to determine the lateral deflections and the plastic theory is used as a criterion of failure. The justification for this anomaly is that there is, as yet, no satisfactory theory for the distribution of moments and forces in a reinforced concrete member when the deformations cease to be elastic.

The Strength of Slender Reinforced Concrete Columns when Loaded Instantaneously to Failure.

In *Fig.* 4 formula (2) is applied to four representative columns assuming $\eta = 0{\cdot}003\frac{l}{k}$. The selected limiting values for the strength of the concrete and the percentage of reinforcement are also given. Values of P_e are obtained from (1) in which E is the value for concrete and $A = A_c + mA_s$, the modular ratio m being applicable to zero time ; P_y is calculated from (9). Curves published elsewhere [5] are also plotted and give lower reduction-factors than those given by the writers. This is because the curves are based on a modular ratio of $\frac{40{,}000}{u}$, which corresponds approximately to the effective modulus at one day, an allowance therefore being made for the creep that occurs during the first day under load. By using

the modulus at zero time the effect of creep at this stage is excluded. Formula (12) is not applicable to the values of $\frac{l}{k}$ in *Fig.* 4; thus the curves exhibit no discontinuity. This does not imply that slender reinforced concrete columns of these dimensions collapse without tensile cracks appearing, but that a state of instability is attained before the cracks occur.

The Effect of Creep in a Slender Reinforced Concrete Column.

The analysis of the effects of creep on the deformation of a slender homogeneous column can be extended to a reinforced concrete column [*Fig.* 3(*b*)]. If the stress in the concrete at a distance z from the centre-line is f_{cz}, then (7) is true if f is replaced by f_{cz}. The derivation of (7) is unaffected by the presence of reinforcement. If the extreme fibre stress is f_c and the variation of strain is linear [*Fig.* 3(*c*)], substitution gives

$$\frac{2}{dE_c}\cdot\frac{\partial f_c}{\partial t}+\frac{2f_c}{d}\cdot\frac{\partial\phi(t)}{\partial t}=-\frac{1}{R^2}\cdot\frac{\partial R}{\partial t} \quad . \quad . \quad . \quad . \quad (13)$$

The strains on the concrete and steel at any point at distance z from the centre-line are equal, that is $e_{cz}=e_{sz}$. Thus $\frac{\partial e_{cz}}{\partial t}=\frac{\partial e_{sz}}{\partial t}$.

Hence
$$\frac{1}{E_s}\cdot\frac{\partial f_{sz}}{\partial t}=\frac{1}{E_c}\cdot\frac{\partial f_{cz}}{\partial t}+f_{cz}\frac{\partial}{\partial t}\phi(t),$$

or
$$\frac{1}{E_sk_s}\frac{\partial f_s}{\partial t}=\left\{\frac{1}{E_c}\frac{\partial f_c}{\partial t}+f_c\frac{\partial}{\partial t}\phi(t)\right\}\frac{2}{d} \quad . \quad . \quad . \quad . \quad (14)$$

where f_s is the stress in the steel at a distance k_s from the centre-line. From (13) and (14) $\frac{1}{E_sk_s}\cdot\frac{\partial f_s}{\partial t}+\frac{1}{R^2}\cdot\frac{\partial R}{\partial t}=0$. By integration, the constant being determined from f_s and R at zero time,

$$-\left(\frac{f_s}{E_sk_s}-\frac{1}{R}\right)=\frac{a.P_e}{\Phi_cE_c}\cos\left(\frac{\pi x}{l}\right) \quad . \quad . \quad . \quad . \quad (15)$$

where $\Phi_c=I_c+\frac{E_s}{E_c}I_s$; I_c and I_s are the second moments of the area of the steel and concrete. The bending moment to which the section is subjected is

$$M=\frac{2}{d}f_cI_c+\frac{1}{k_s}f_sI_s \quad . \quad . \quad . \quad . \quad . \quad (16)$$

Combining (15) and (16) and substituting $\frac{1}{R}=-\frac{\partial^2y}{\partial x^2}$ gives

$$\frac{2}{d}f_c=\frac{1}{I_c}\left\{Py+E_sI_s\left(\frac{\partial^2y}{\partial x^2}+\frac{a.P_e}{\Phi_cE_c}\cos\frac{\pi x}{l}\right)\right\} \quad . \quad . \quad . \quad (17)$$

Substituting (17) and the differential of (17) in (13), the resultant expression can be integrated to give

$$y=\frac{a.P_e}{P_e-P}\left\{e^{\frac{P-P_{es}}{P_e-P}E_c\phi(t)}\left(1+\frac{P_{es}}{P_e}\cdot\frac{P_e-P}{P-P_{es}}\right)-\frac{P_{es}}{P_e}\cdot\frac{P_e-P}{P-P_{es}}\right\}\cos\frac{\pi_x}{l}.$$

As in a slender plain-concrete column, the effect of creep upon the lateral deflection is to multiply the deflection by a factor σ which for a slender reinforced concrete column is given by

$$\left\{e^{\frac{P-P_{es}}{P_e-P}E_e\phi(t)}\left(1+\frac{P_{es}}{P_e}.\frac{P_e-P}{P-P_{es}}\right)-\frac{P_{es}}{P_e}.\frac{P_e-P}{P-P_{es}}\right\} \quad . \quad . \quad (18)$$

where $$P_{es}=\frac{\pi^2E_sI_s}{l^2}.$$

To be able to apply this analysis to an actual column, the proportion contributed by the reinforcement to the total Euler-load, and the characteristics of the creep of the concrete as defined by $\phi(t)$, must be known. As the ultimate strength of a column is the strength when the full effect of creep takes place, it is the strain due to creep when t is infinite that is required. The appropriate constants for the columns previously considered are given in the table in *Fig.* 4.

By assuming a value for $\frac{P}{P_y}$, σ can be obtained from (18). By replacing η by $\sigma\eta$, (2) can be solved for $\frac{P}{P_y}$; comparison of this value with the assumed value shows the validity of the assumption. A more accurate value can be obtained by continued approximations. If the results of calculations carried out in this manner are plotted, curves are obtained similar to those in *Fig.* 2, giving the theoretical load causing failure after the passage of infinite time. Such curves cannot be used in design since a load-factor is not introduced, but by a slight modification of the calculation a load can be obtained such that the load-factor never falls below a specified value. As an example, suppose that the load-factor required is 2·5. Solve (18) for $\frac{1}{2{\cdot}5}\times\frac{P}{P_y}$ instead of for $\frac{P}{P_y}$. With the value of σ so obtained, $\frac{P}{P_y}$ is determined from (2). In this way the ultimate load at infinite time is obtained for a column which has been maintained continuously under a load equal to 40 per cent. of that ultimate load, and with this load the load-factor approaches 2·5 but is never less. In *Fig.* 5 the curves are plotted for the four columns given in *Fig.* 4 for a load-factor of 2·5. The curves are so close together that the diagram is more clearly shown as an envelope within which it is expected that columns of the more common designs will lie. Because the envelope is so narrow, which is remarkable when the wide range of columns represented is considered, it is possible to plot a mean curve which may be used in practice without serious error. The ordinates of the mean curve have been reduced to 40 per cent. of their value to give, in the lower part of *Fig.* 6, a curve of reduction-coefficients for permissible loads. For comparison the reduction factors recommended in the D.S.I.R. Code (1934) and the British Standard Code CP114 (1948) are also given. The most important difference occurs for the more common values of $\frac{l}{k}$, that is up to 80, and this is due to the assumption in the code that no buckling factor need be applied for columns

for which $\frac{l}{k}$ is less than 50. Experiments seem to show, however, that the bending effects are sensible in all columns except those that are very squat.

Conclusions.

Creep has an adverse effect upon the strength of slender reinforced concrete columns and current methods of design make little allowance for this fact. The strength of a slender column subject to creep is a function of time. Only pin-ended columns are considered, but it is convenient and justifiable to consider the simplest case when attempting to solve the complex problem of the instability of a non-homogeneous column one of the components of which is subject to creep.

No distinction between dead and live loads has been made, it being assumed that the load is continuously applied. To allow for transient loads it is necessary to predict the value of σ for the dead load only; the combined dead and live loads are considered in the determination of the load-factor. When the ratio of live load to dead load is small it is probable that little economy is lost by considering the total load as dead load thereby enabling a curve such as that in *Fig.* 5 to be used, although verification by tests on actual columns is desirable. For such tests it is necessary to maintain many columns under load for long periods before testing them to destruction. Although a load cannot be maintained for an infinite time, the load-factor at any time can be estimated so that if actual failing loads at that time agree with the calculated loads it is possible to estimate by extrapolation for longer periods.

REFERENCES.

(1) "The Analysis of Engineering Structures." A. J. S. Pippard and J. F. Baker.
(2) "The Creep or Flow of Concrete Under Load." W. H. Glanville. Building Research Technical Paper No. 12.
(3) "The Effects of Creep on Instability and Indeterminacy Investigated by Plastic Models." A. D. Ross. "Structural Engineer," August, 1946.
(4) "Eccentrically-loaded Reinforced Concrete Columns." C. S. Whitney. "Concrete and Constructional Engineering." November, 1938.
(5) "The Strength of Long Reinforced Concrete Columns in Short-Period Tests to Destruction." F. G. Thomas. Building Research Technical Paper No. 24.